SYNTHESIS AND CHARACTERIZATION OF SHAPE MEMORY POLY (EPSILON-CAPROLACTONE) POLYURETHANE-UREAS

A Dissertation
Presented to
The Academic Faculty

by

Hongfeng Ren

In Partial Fulfillment
of the Requirements for the Degree
Doctor of Philosophy in the
School of Polymer, Textile and Fiber Engineering

Georgia Institute of Technology
May 2012

SYNTHESIS AND CHARACTERIZATION OF SHAPE MEMORY POLY (EPSILON-CAPROLACTONE) POLYURETHANE-UREAS

Approved by:

Dr. Karl I. Jacob, Co-Advisor
School of Polymer, Textile & Fiber Engineering
Georgia Institute of Technology

Dr. Fred L. Cook, Co-Advisor
School of Polymer, Textile & Fiber Engineering
Georgia Institute of Technology

Dr. Anselm C. Griffin
School of Polymer, Textile & Fiber Engineering
Georgia Institute of Technology

Dr. Yonathan S. Thio
School of Polymer, Textile & Fiber Engineering
Georgia Institute of Technology

Dr. Kyriaki Kalaitzidou
School of Mechanic Engineering
Georgia Institute of Technology

Date Approved: December 14, 2011

To my parents, without whom none of this would have been even possible

and

to my wife, who always believes in me

ACKNOWLEDGEMENTS

It is a pleasure to thank the many people who made this thesis possible. I am deeply indebted to my advisor, Dr. Karl I. Jacob and my co-advisor Dr. Fred L. Cook, for their constant guidance, support, allowance of freedom during the entire course of this work. I would like to thank them for their trust in my abilities and their continuous efforts to bring the best out of me. The improvements that they have brought in me over the years will help me for the rest of my career. Their professional and personable attitude has guided me in a variety of ways and has made my stay at Georgia Institute of Technology a very rewarding and memorable experience.

I am thankful to my committee member including Dr. Anselm C. Griffin, Dr. Kyriaki Kalaitzidou and Dr. Yonathan S. Thio, for serving as my thesis reading committee and their part in guiding and supporting this work.

I am grateful to Dr. Rex Hjelm and Dr. Monika Hartl (LANSCE, Los Alamos National Laboratory) for providing SANS facilities and help with the experiments and insightful discussions. I am thankful to Dr. Kenneth A. Gall and his group members for their help during cyclic thermal test. Thanks also extend to Mr. Michael Buchanan for FT-IR measurements.

I thank my group members for their great help and cooperation and fellow graduate students for providing a stimulating and fun environment in which to learn and grow. Thanks also extend to all the staff and faculty of School of Polymer, Textile & Fiber Engineering for their assistance and help in many different ways.

Last, I wish to express my deepest appreciation to my family. I am eternally indebted to my parents, Chun'an Ren and Nanqin Shi, for their wholehearted and endless support over the years. I would also like to thank my wife, Yang Li, for her understanding, patience and encouragement when it was most required. To them I dedicate this dissertation.

TABLE OF CONTENTS

LIST OF TABLES

LIST OF FIGURES

LIST OF SYMBOLS AND ABBREVIATIONS

SME	Shape memory effect
SMAs	Shape memory alloys
SMPs	Shape memory polymers
MDI	Bis (4-isocyanatophenyl) methane
TDI	4-Diisocyanatotoluene
HDI	1, 6-Diisocyanatohexane
BDO	1, 4-Butanediol
BEBP	4, 4'-Bis (2-hydroxyethoxy) biphenyl
BHBP	4'4-Bis (2-hydroxyhexoxy) biphenyl
DMPA	2, 2-Bis (hydroxymethyl) propionic acid
PCL	Poly (ε-caprolactone)-diol
PTMG	Poly (tetramethylene glycol)
EG	Ethylene glycol
DHBP	4, 4'-Dihydroxy biphenyl
NMDA	N-Methyldiethanolamine
BIN	N, N-bis (2-Hydroxyethyl) isonicotinamide
PLA	Polylactide
BPE	4, 4-Bis (4-Hydroxyhexoxy)-isopropylane
ND	Napathoxy diethanol
BES	Bis (2-phenoxyethanol)-sulfone
PEA	Poly (ethylene adipate)
PBA	Poly (butylene adipate)
PHA	Poly (hexylene adipate)

PE	Polyethylene
PEO	Polyethylene oxide
PET	Polyethylene terephthalate
SMPUU	Shape memory polyurethane –urea
NMR	Nuclear magnetic resonance
DSC	Differential scanning calorimetry
FT-IR	Fourier transform infrared
GPC	Gel permeation chromatography
DMAc	N, N-Dimethylacetamide
BDA	1, 4-Butanediamine
EDA	Ethylenediamine
HDA	1, 6-Hexanediamine
PCLUU	Poly (epsilon-caprolactone) polyurethane –urea
DMA	Dynamic Mechanical Analysis
THF	Tetrahydrofuran
MDA	4, 4'-Methylenedianiline
HS	Hard segment
DMSO-d_6	Dimethyl sulfoxide-d_6
MPDA	2-Methyl-1, 5-pentanediamine
SEM	Scanning electron microscope
SANS	Small angle neutron scattering
LQD	Low-Q diffractometer
TOF	Time-of-flight
DDS	4, 4'-Diaminodiphenyl sulfone
ODA	4, 4'-Dianimodiphenyl ether

IPDI	Isophorone diisocyanate
POPA	Poly (Oxy 1, 3-propyleneoxyadipate)
TCE	1, 1, 2, 2-Tetrachloroethane
TGA	Thermogravimetric analysis
LC	Liquid crystal

SUMMARY

Shape memory polymers (SMPs) have attracted significant interest in recent times because of their potential applications in a number of areas, such as medical devices and textiles. However, there are some major drawbacks of SMPs, such as their relatively low moduli resulting in small recovery stresses, and their long response times compared with shape memory alloys (SMAs). A suitable recovery stress which comes from the elastic recovery stress generated in the deformation process is critical in some medical devices. To address some of these shortcomings, the work in this dissertation mainly focuses on the design and synthesis of linear shape memory polymers with higher recovery stress.

A series of segmented poly (epsilon-caprolactone) polyurethane-ureas (PCLUUs) were prepared from poly (epsilon-caprolactone) (PCL) diol, different dissociates and chain extenders. NMR and FT-IR were used to identify the structure of the synthesized shape memory polyurethane-ureas. Parameters such as soft segment content (molecular weight and content), chain extender and the rigidity of the main chain were investigated to understand the structure-property relationships of the shape memory polymer systems through DSC, DMA, physical property test, etc. Cyclic thermal mechanic tests were applied to measure the shape memory properties which showed that the recovery stress can be improved above 200% simply by modifying the chain extender. Meanwhile, the synthesis process was optimized to be similar to that of Spandex /LYCRA®. Continuous fibers form shape memory polyurethane-ureas were made from a wet spinning process, which indicated excellent spinnability of the polymer solution. Small angle neutron scattering (SANS) was used to study the morphology of the hard segment at different

temperatures and stretch rates and found that the monodisperse rigid cylinder model fit the SANS data quite well. From the cylinder model, the radius of the cylinder increased with increasing hard segment content. The SANS results revealed phase separation of hard and soft segments into nano scale domains.

The overall objectives of this dissertation were:

- To improve the recovery stress of linear shape memory polymers.
- To study the morphology and structure property relationships of shape memory polymers.

Chapter 1 reviews the literature on SMAs and SMPs, especially on linear SMPs. Chapter 2 is devoted to SMPUUs with the aliphatic amine 1, 4-Butanediamine (BDA) as chain extender. Chapter 3 reports the effects of different aliphatic diamines as the chain extenders. Chapter 4 covers the results for shape memory polyurethane-ureas with aromatic diamine 4, 4'-Methylenedianiline (MDA) as the chain extender. The effect of different diisocyanates is covered in Chapter 5. Chapter 6-7 show some synthesized polymer systems with unimproved recovery stress or even no shape memory properties. The overall conclusions of this work are reported in Chapter 8.

CHAPTER 1

INTRODUCTION

1.1. Concepts associated with shape memory materials

1.1.1. Shape memory materials

Shape memory materials are those that exhibit shape memory effects (SME). These materials can be deformed from an initial reference state, but they can go back to the original reference state though the application of an appropriate stimulus such as pH or temperature change, these materials are thus stimuli-responsive. If the original reference state can be recovered by a change in temperature, it is called a thermally induced shape memory effect. Other shape memory effects, such as pH induced shape memory effects, are observed when other external stimuli cause recovery of the permanent reference shape. Figure 1.1 shows a general approach to produce a shape memory effect:[1]

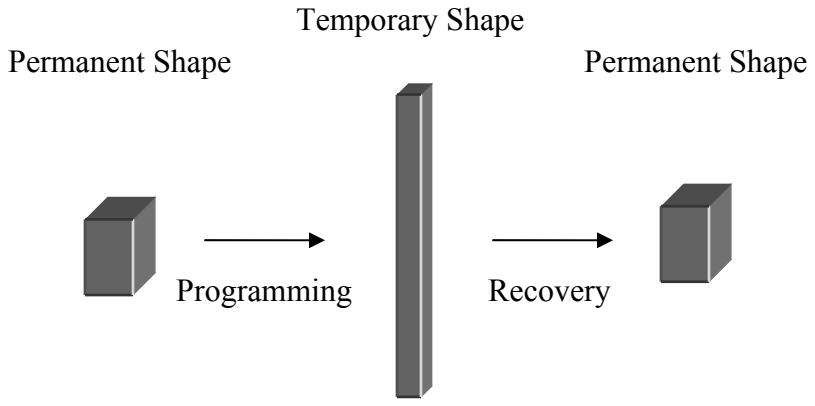

Figure 1.1. Schematic representation of processing of shape memory effect

A temporary shape can be fixed by the programming process and the permanent shape can be recovered by the external stimulus such as heat.

1.1.2. Shape memory alloys (SMAs)

The shape memory effect of metal alloys was first observed in samples of gold-cadmium in 1951 by Chang and Read which is based on the reversible martensitic transformation.[2] The concept of thermoelastic martensitic transformation, which explained the reversible transformation of martensite, was introduced in 1949 by Kurdjumov and Khandros, based on the experimental observations of the thermally reversible martensitic structure in CuZn and CuAl alloys.[3] Not until 1963, however, shape memory materials found applications, essentially through the discovery of NiTi ("Nitinol") by Buehler and coworkers at the U.S. Naval Ordnance Laboratory (NOL).[4] SMAs such as Nitinol usually exhibit two unique properties. The first is the shape memory effect, and the other is "super elasticity", which is the ability of a material to exhibit large recoverable strains while deformed within a range of temperature characteristic of a specific alloy. The two phases present in shape memory alloys are called martensite and austenite (Figure 1.2). The former one exists at lower temperatures and is the relatively soft and easily deformed phase of SMAs. Austenite is reached upon heating the sample above the phase transition temperature and recovery of the original shape is observed for deformation up to 8%.

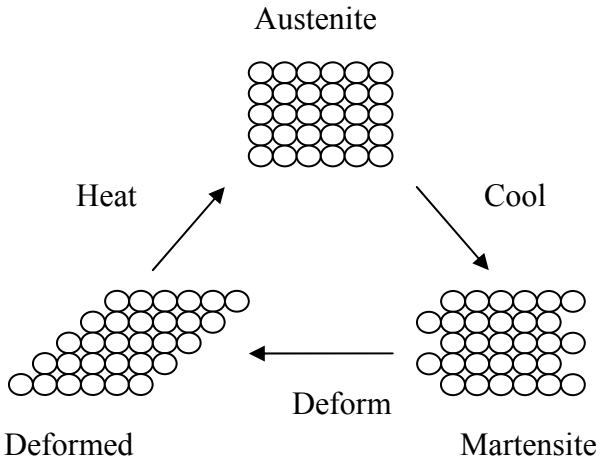

Figure 1.2. Schematic representation of the mechanism of shape memory effect for SMAs

1.1.3. Shape memory polymers(SMPs)

The first commercial shape memory polymer was developed by CDF Chimie/Nippon Zeon Company in the late 1970s under the trade name of Norsorex® for polynorbornene.[5] Differing from shape memory alloys, shape memory polymers use the glass transition or melting transition from a hard phase to soft phase as the responsible mechanism for the shape memory effect. A large number of temperature-induced shape memory polymers are based on physically or covalently cross linked polyurethanes. These elastic materials show at least two separated phases. The phase with the highest thermal transition serves as the physical cross link and is responsible for the permanent shape. A second phase acts as a molecular switch and is responsible to fix the temporary shape. After processing the material above the switching temperature, but below T_{perm}, the temporary shape will be frozen with cooling the polymer below the switching temperature. Heating up the material above T_{trans} again removes the physical cross-links induced in the switching phase and the material recovers its permanent shape because of

its entropy elasticity. The molecular mechanism of programming the temporary form and recovering the permanent shape is demonstrated schematically in Figure 1.3 for a linear multiblock copolymer, as an example of a T_m type thermoplastic shape-memory polymer.[1]

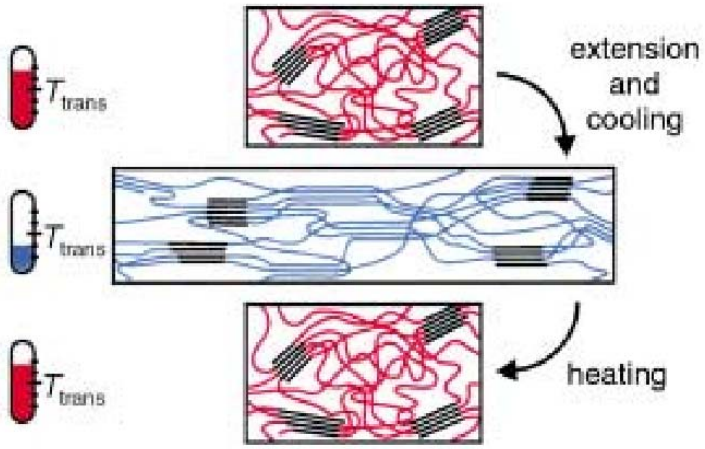

Figure 1.3. Schematic representation of the molecular mechanisms of thermally induced shape memory effect for a linear multiblock copolymer with $T_{trans}=T_m$[1]

1.1.4. Comparison of the properties of SMAs with SMPs

Compared with shape-memory alloys, polymeric shape memory materials possess the advantages of high elastic deformation (strain up to 200% for most of the materials), low cost, low density, and potential biocompatibility and biodegradability. SMPs also have a broad range of application temperatures that can be tailored, tunable stiffness, and are easily processed. Meanwhile, the main disadvantages of shape memory polymers reside in their lower recovery stress, their lower recovery speed/response time and their possibly lower achievable cycle life, although the latter has only rarely been investigated in the literature. These two materials (polymers and metal alloys) also possess distinct applications due to their intrinsic differences in mechanical, viscoelastic, and optical

properties. A comparison of the different characteristics of SMPs and SMAs are summarized in Table 1.1.[6]

Table 1.1. Comparison of the properties of shape memory alloys with shape memory polymers[6]

	SMPs	SMAs
Density/g.cm^{-3}	0.9-1.1	6-8
Extent of deformation (%)	Up to 800%	<8%
Young's modulus at T<T_{tran}/GPa	0.01-3	83 (NiTi)
Young's modulus at T>T_{tran}/GPa	(0.1-10)*10-3	28-41
Stress required for deformation/MPa	1-3	50-200
Stress generated during recovery/MPa	1-3	150-300
Recovery speeds	<1s-several min.	<1s
Thermal conductivity/W.m-1.K-1	0.15-0.30	18(NiTi)
Biodegradability	Can be	Not
Processing conditions	<200°C, low pressure	>1000°C, high pressure
cost	<$10 per lb	~$250 per lb

1.2. Preparation of shape memory polymers

1.2.1. The classes of shape memory polymers

Shape memory polymers can be categorized into different classes depending on their chemical architecture, the origin of their transformation temperature and their shape memory stimuli:

By chemical architecture:

Physically cross-linked shape memory polymers

Chemically cross-linked shape memory polymers

By transformation temperature:

Shape memory polymers based on melting temperature (T_m)

Shape memory polymers based on glass transition temperature (T_g)

By shape memory stimuli:

Thermally-induced shape memory polymers

Light-induced shape memory polymers

pH-induced shape memory polymers

Electrically-induced shape memory polymers

Most of SMPs are thermally-induced, while more interests have been taken in other inducing methods such as light and electrical field as shown in Figures 1.4[7] and 1.5.[8]

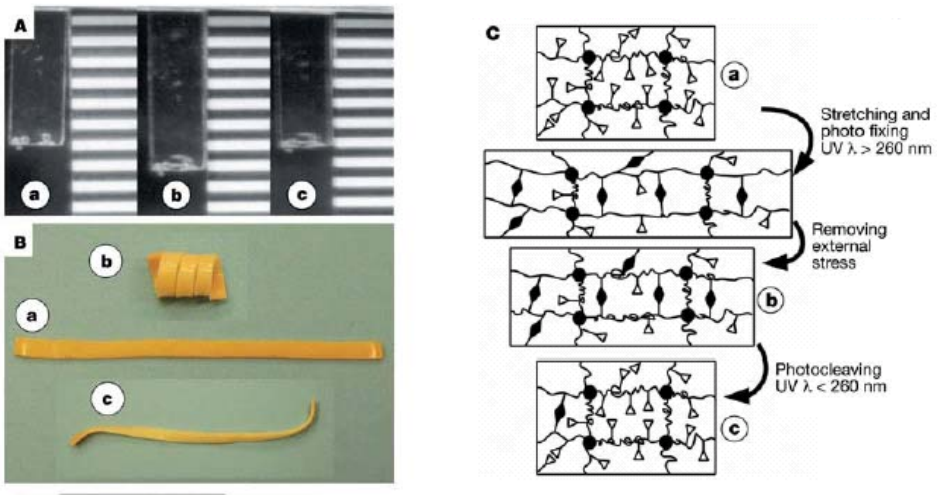

Figure 1.4. Shape memory effect of photo responsive polymers[7]

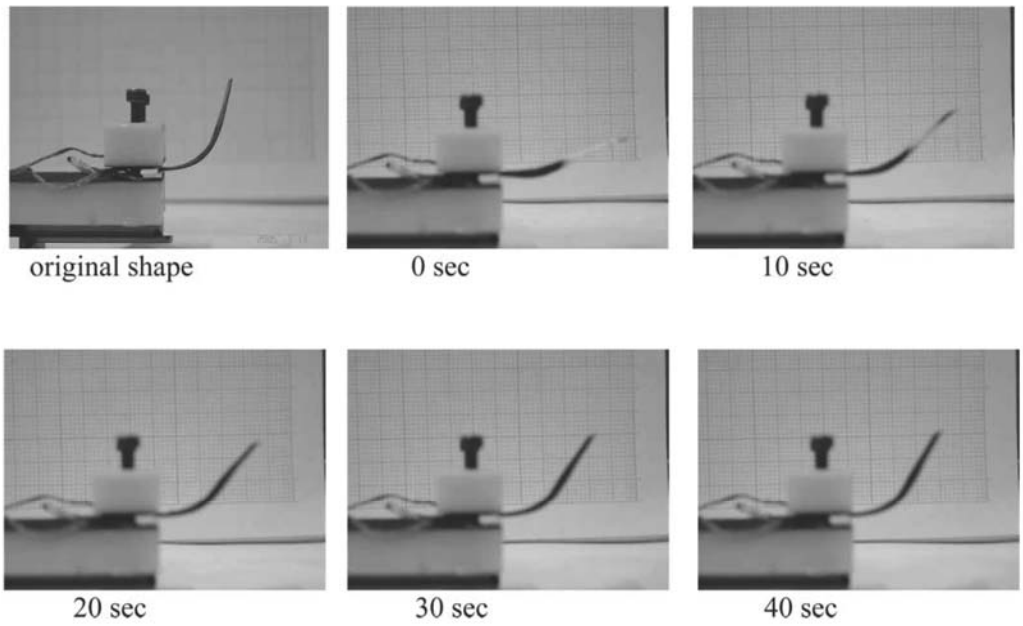

Figure 1.5. Electroactive shape memory behavior of Polyurethane-MWNT composites[8]

A large number of temperature-induced SMPs are based on physically or covalently cross linked polyurethanes.[9-16] Physically cross linked polyurethanes, which usually are linear copolymers, have drawn significant research interest because many of them are thermoplastic and can be processed by conventional processing techniques such as extrusion or injection molding.

1.2.2. Preparation of linear shape memory polyurethanes

The prepolymer method is widely used to synthesize the linear polyurethanes and the linear polyurethane-ureas. Thermoplastic polyurethane elastomers are produced at large industrial scale with this technique. In this process, isocyanate-terminated pre-polymers are synthesized by coupling of a difunctional polyol with an excess of a diisocyanate such as Bis (4-isocyanatophenyl) methane (MDI) and 4-Diisocyanatotoluene (2, 4-TDI) (Figure 1.6, first reaction step).

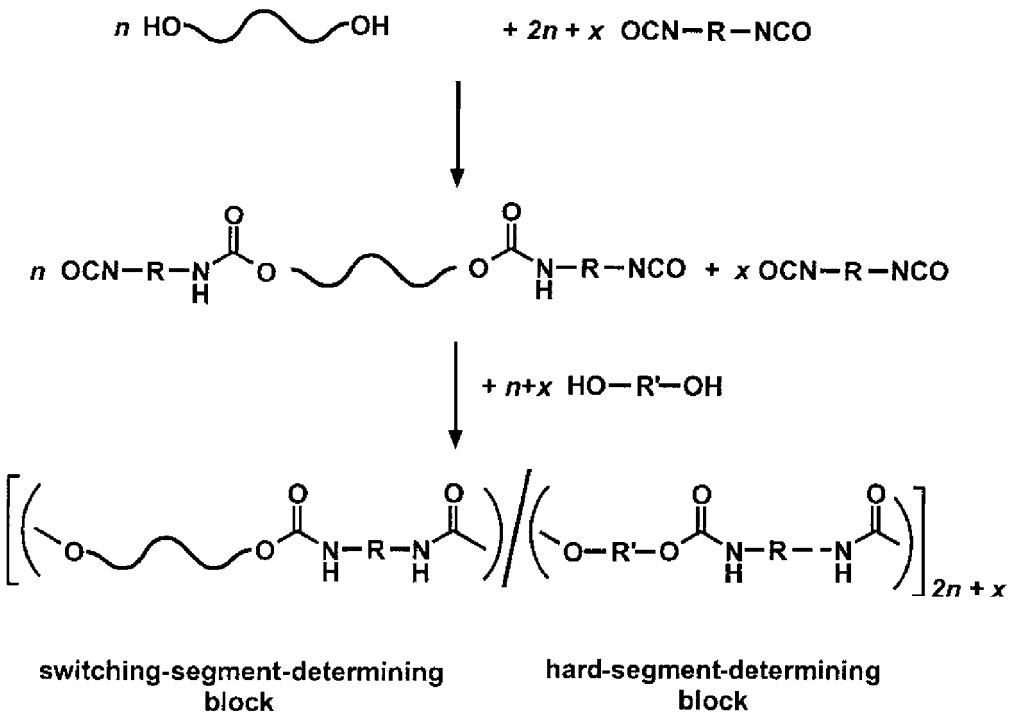

Figure 1.6. Prepolymer method for the synthesis of thermoplastic polyurethanes (R and R' are short chain groups with two free valences)[1]

Chain extenders such as low molecular weight diols and diamines are added to further couple the prepolymers. Linear polyurethane or polyurethane-urea block copolymers with phase separation are obtained in this way (Figure 1.6, second reaction step). Each polymer chain contains high polarity segments which are composed of urethane and urea bonds. Because of their high intermolecular interaction, "hard" segments are formed in those regions from preliminary observations. The hard-segment-forming phase is embedded in an amorphous elastic matrix. The amorphous matrix, with its low glass transition temperature, is called "soft" segment. For shape memory polyurethanes, this segment serves as a switching segment and traditionally it is modified to locate the thermal transition in a temperature range relevant for the respective application. Hard segment "clusters" with dimensions < 1 μm are formed by the phase

separation process and these clusters have higher T_g or T_m values than the ones of soft segment and act as multifunctional physical netpoints. These plastic domains act as reinforcing filler that can deflect mechanical energy by deformation. They thus simultaneously improve the cross-breaking strength and impact strength of the material.

1.2.3. Chemical composition of linear shape memory polyurethanes

The linear shape memory polyurethanes are composed of three components: polyol, isocyanate and chain extender. Various shape memory polyurethane compositions and their shape recovery stresses are presented in Table 1.2. The most widely used isocyanates are Bis (4-isocyanatophenyl) methane (MDI), 2, 4-Diisocyanatotoluene (2, 4-TDI) and 1, 6-Diisocyanatohexane (HDI) which are also quite popular in polyurethane industry. Combined with different chain extenders such as 1, 4-Butanediol (BDO), 4, 4'-Bis (2-hydroxyethoxy) biphenyl (BEBP) or 2, 2-Bis (hydroxymethyl) propionic acid (DMPA), the hard segment is formed and the highest thermal transition, T_{perm}, is determined at the same time. Poly (ε-caprolactone)-diol (PCL), poly (tetramethylene glycol) (PTMG) and plyesters such as poly (ethylene adipate) (PEA) are used as polyol which forms the soft segment. The transition temperature, T_{trans}, is usually determined by the melting temperature or the glass transition temperature of the polyol.

Table 1.2. Overview of linear polyurethanes with thermally induced shape memory effects

Hard segment	Soft segment	Shape recovery stress(MPa)[a]	references
MDI/BDO	PCL	~2.7/~2.3	17-19
MDI/BEBP or BHBP	PCL	~4.2/~3.5	20
TDI/EG	PCL	~/~	21
MDI/BDO,DMPA	PCL	~0.9/~	22, 23
HDI/DHBP	PCL	~4.6/~2.9[b]	24
MDI/BDO, NMDA or BIN	PCL	~0.9/~0.6[c]	25
HDI/BDO	PLA	~/~	26
HDI/BDA	PLA	~/~	27
MDI/BDO	PTMG	~/~	28-31
MDI/BDO,BES/BPE/ND	PTMG	~/~	32
MDI/BDO	PTMG	~3.0/~2.0[d]	33
PDI/BDO	PTMG	~8.0/~5.0[d]	33
MDI/BDO	PEA	~3.9/~4.2[e]	34, 35
MDI/BDO	PBA	~/~	36
MDI/BDO	PHA	~/~	37

Note: a) the shape memory recovery stress is usually measured with 100% strain and 30% hard segment with molecular weight 4000, first and second circle at 65°C; b) 20% hard segment; c) 25% hard segment with Mw 10000, NMDA 2%; d) Molecular weight 2000, measured at 20°C above T_g; e) 69% hard segment with Mw 600, measured at 20°C above T_g.

1.2.4. Other linear shape memory polymers

Other linear shape memory polymers such as Polyethylene(PE) grafted with Nylon-6[38] and PEO-PET copolymers[39, 40] have also been investigated. For PE grafted with Nylon-6, a reactive blending process is used to couple the PE block with the Nylon-6 block by adding maleic anhydride and dicumyl peroxide. The transition temperature of the shape memory PE grafted with Nylon-6 is introduced by the melting point of the PE crystallites, which is around 120°C. The Nylon-6 blocks work as hard segments and form stable physical net points. PEO-PET copolymers were synthesized by condensation reaction. This process is quite similar to the one for producing PET except there is another monomer (PEO) involved. The PEO blocks act as molecular switches and the switching temperature of PEO-PET copolymers is given by the melting temperature of PEO which ranges from 45°C to 65°C for PEO of 2,000 to 10,000 g/mol.

1.3. Characterization of shape memory properties in polymers

1.3.1. Measurements of shape memory properties

Shape memory properties of SMPs can be measured by different testing methods such as bending tests, shrinkage determination tests and cyclic thermo mechanical tests. The cyclic thermo mechanical test is the unique one to measure the recovery stress which involves a tensile tester and a constant temperature chamber. The typical test procedures are shown in Fig. 1.7. At Step 1, an SMP sample is heated to a high temperature, T_{high}, above the switching temperature, T_{trans}, and is extended to a designed strain (ε_m). At Step 2, the sample is maintained with constant strain ε_m, and is cooled to a low temperature, T_{low}, below the switching temperature, T_{trans}, to fix the temporary shape. At

Step 3, the clamps of the tensile tester go back to their original position. At the beginning of the unloading process, the elastic recovery stress of the sample is reduced and turns into zero at strain ε_u, and the sample will bend with further unloading. At Step 4, the sample is reheated to T_{high} and then recovers to the permanent shape with a residual strain ε_p. After that, the cycle begins again.

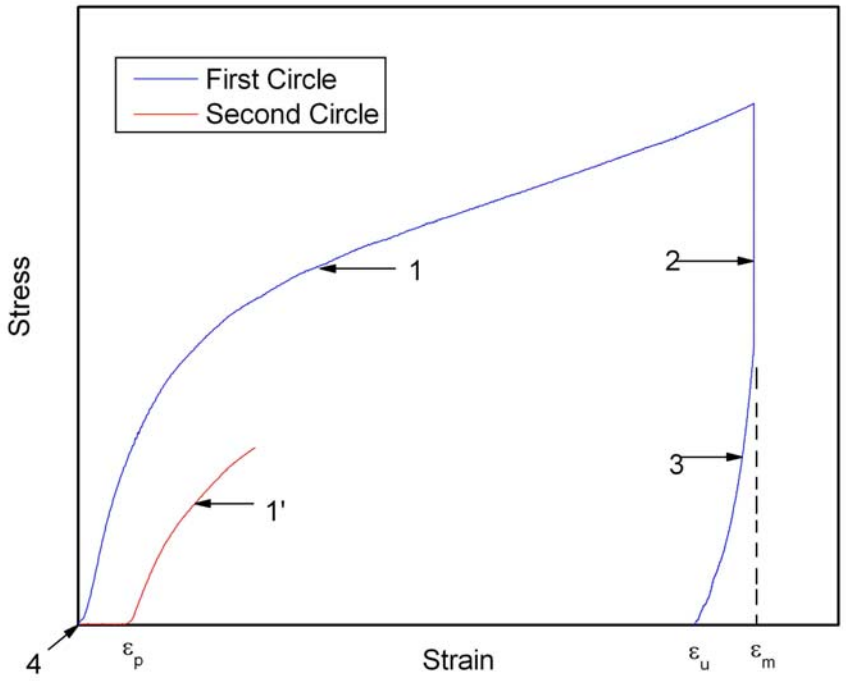

Figure 1.7. Diagram of stress-strain SME testing

1.3.2. Parameters for characterization

A set of parameters is introduced to characterize the shape memory properties of polymers. The objective using these parameters is to be able to characterize the shape memory nature of synthesized polymers and distinguish them from other properties of the materials.

Switching/Transformation Temperature, T_{trans}

The Switching/Transformation Temperature describes the temperature at which the SMP recovers its permanent shape which is either the glass transition temperature (T_g) or the melting point(T_m) of the soft segment.

Shape fixity, R_f

Shape fixity characterizes the ability of a SMP to fix its temporary shape during the deformation step after subsequent cooling and unloading which is given by the ratio of the fixed deformation to the total deformation[41]:

$$R_f(N) = \frac{\varepsilon_u(N)}{\varepsilon_m} \times 100\%$$

where $\varepsilon_u(N)$ and ε_m denote the strain in the stress-free state after the retraction of the tensile stress in the N^{th} cycle and the maximum strain.

Shape Recovery, R_r

Shape recovery describes the ability of a SMP to recover its permanent shape upon reheating to the rubbery state. Several ways exist to express shape recovery.[42] The first approach defines shape recovery as the ratio of the deformation recovered by the sample in a given cycle to the deformation taking place with the sample in the previous cycle:[43]

$$R_r(N) = \left[\frac{\varepsilon_m - \varepsilon_p(N)}{\varepsilon_m - \varepsilon_p(N-1)} \right] \times 100\%$$

where $R_r(N)$ and $\varepsilon_p(N)$ denote the strain recovery and the residual strain of N^{th} cycle, respectively. Another approach defines shape recovery as the ratio of the deformation

recovered after N passed cycles to the original shape of the sample, which is usually also described as the total strain recovery rate $R_{r,tot}(N)$:[17]

$$R_{r,tot}(N) = \left[\frac{\varepsilon_m - \varepsilon_p(N)}{\varepsilon_m} \right] \times 100\%$$

Recovery speed, V_r

Recovery speed is the speed which a SMP recovers from a temporary shape to its original shape when heated:

$$V_r = \frac{dR_r}{dT} \times \frac{dT}{dt}$$

where V_r is the shape recovery speed, dR_r/dT is the ratio of shape recovery to temperature and dT/dt is the heating rate. In reality, video cameras are used to qualitatively study the shape recovery speed[44] and a hot stage microscope is also useful to measure this parameter with the following formula[19, 40]:

$$V_r = \frac{0.8 R_f \varepsilon_2 (\frac{dT}{dt})}{T_{90} - T_{10}}$$

where T_{90} and T_{10} are the temperatures corresponding to the shape recovery $0.9R_f$ and $0.1R_f$ on the recovery curve, respectively.

Recovery stress, σ_r

Recovery stress derives from the elastic recovery stress generated in the deformation process. When the deformed and fixed SMPs are reheated above T_{trans}, the energy stored in SMPs will be released as shape recovery stress. For thermoplastic SMPs, a dilemma exists to characterize recovery stress because of the viscoelasticity property of

polymers. Owing to the limitations of equipment and efficiency of heat transfer, it is difficult to heat a SMP to a certain temperature in a very short time. As a result, stress relaxation is inevitable and the stress generated in deformation will be partially lost. In a cyclic test, the maximum stress value recorded in the heating process is considered as the effective shape recovery stress at a given strain, e.g., 100%. Since no established standard procedure to measure the shape recovery stress currently exists because of the complicated behavior of SMPs, it is occasionally difficult to compare the recovery stress with different testing methods and different transformation temperatures.

1.4. Applications of shape memory polymers

Important potential applications exist for SMPs in almost every area of daily life, such as self repairing auto bodies, kitchen utensils such as spoons, switches and sensors, etc. Shape memory polymers have tremendous applications in medical devices and the textile industry.

1.4.1. Smart fabrics

Unlike SMAs, SMPs are relatively inexpensive, easier to process, and have light weight, thus making them ideal candidates for textile and clothing applications, while SMAs cannot be used in textiles in any way. Two kinds of properties of SMPs can be used to design smart textiles. The first one is physical properties that will change significantly above and below T_{tran} such as water vapor permeability and air permeability. Mitsubishi Heavy Industry has designed several smart sportswear items with the shape memory polyurethane Diaplex®[45]. The principle of these smart fabrics is described in Figure 1.5. Below an activation point, which is the transformation temperature of SMPs, moisture permeability in such a film is quite low so more heat can be retained inside.

Above an activation point, water vapor is actively expelled to the outside air. As a result, these smart fabrics are always comfortable to wear in all climates.

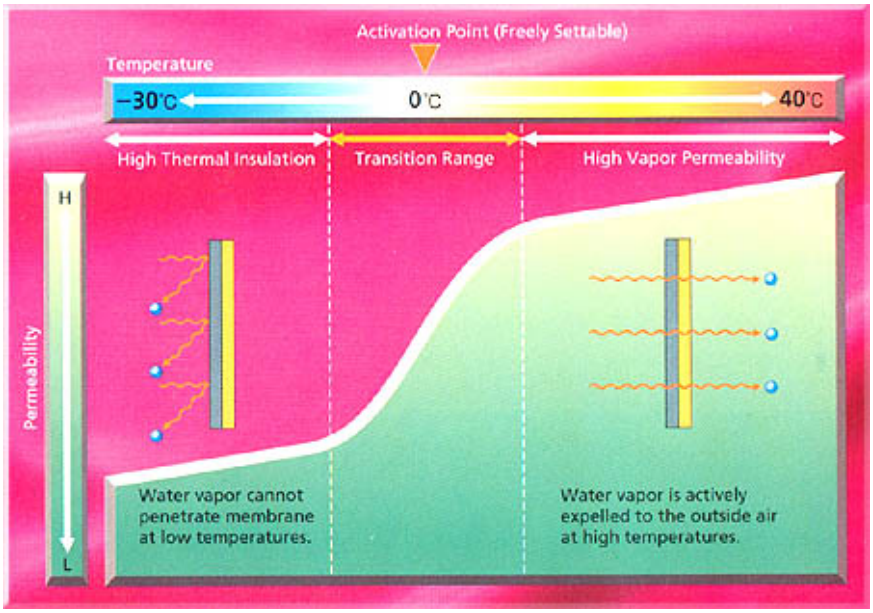

Figure 1.8. Schematic representation of the smart property of Diaplex®

The second one is the shape memory properties. One idea is to fabricate a smart fiber exhibiting a cross-section of crescent shape in hot weather, but will automatically close the opening to form a hollow fiber when the temperature is cool, trapping air and becoming an insulator. This smart fiber can mimic the advantages of the Invista's polyester products, CoolMax® and Thermolite®, which are also suitable for all climates.[46]

1.4.2. Biomedical applications

The biomedical applications of SMPs are mostly focused on medical devices such as surgical sutures[47], stents[48-50], drug delivery[50-52] and aneurysm coils[53] with shape memory properties. Lendlein and Langer[47] reported a shape memory polyurethane which can be used as a smart surgical suture to apply optimum force in endoscopic surgery. A

second surgery to remove the implant can be avoided with this technique since this shape memory polymer is biodegradable. Figure 1.9 - 1.12 show some examples of shape memory polymer devices.

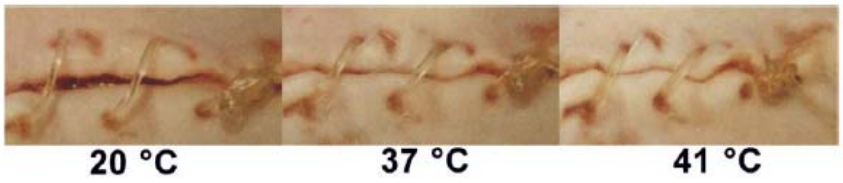

Figure 1.9. Smart surgical suture to apply optimum force[47]

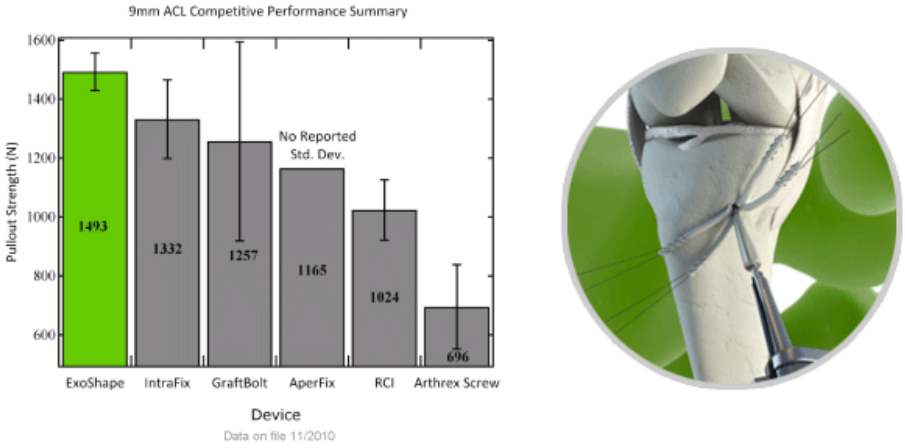

Figure 1.10. EXOSHAPE™ CL Interference Fixation Device with shape memory polymers

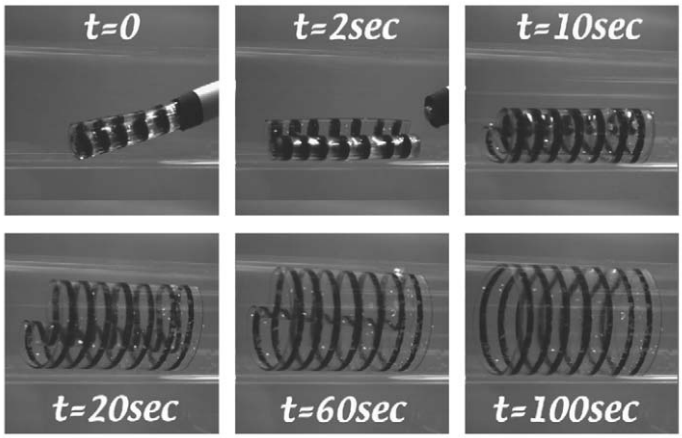

Figure 1.11. Recovery of a crosslinked SMP stent

CHAPTER 2

SHAPE MEMORY POLYURETHANE-UREAS WITH ALIPHATIC AMINE 1, 4-BUTANEDIAMINE AS CHAIN EXTENDER

2.1. Synthesis of Shape memory polyurethane-ureas (SMPUUs) with aliphatic amine 1, 4-Butanediamine (BDA) as chain extender

2.1.1. Prepolymer method for the synthesis of SMPUUs

The prepolymer method is widely used to synthesize the linear polyurethane and polyurethane-urea shape memory polymers. Although the process appears simple, some issues are critical. The monomers and solvents are carefully purified and dried because diisocyanates such as MDI and TDI are very sensitive to the moisture and can react with even trace amounts of water as illustrated in Figure 2.1.[54]

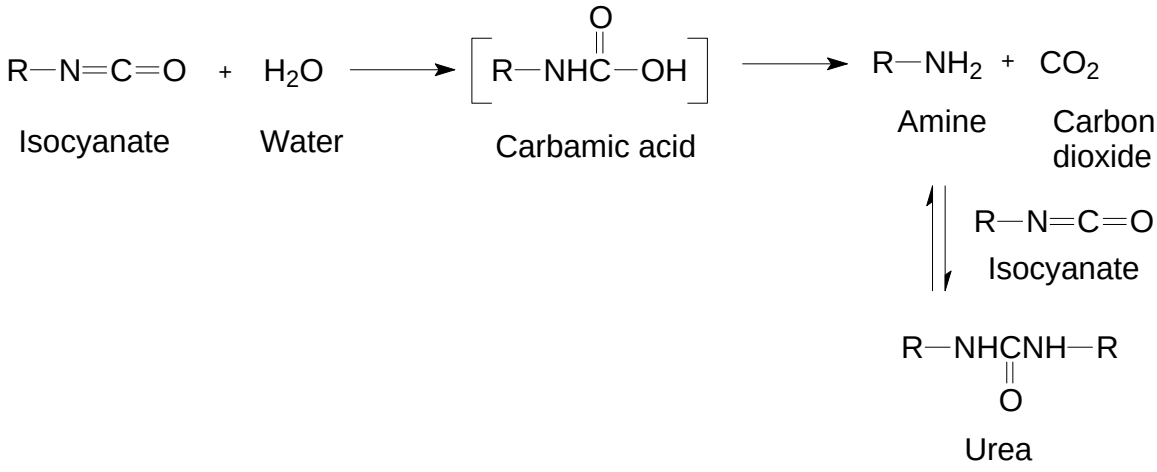

Figure 2.1. Isocyanate reacts with water

Water has a very low molecular weight, so even though the weight percent of water may be small, the molar proportion of water may be high and considerable amounts of urea are produced. As a result, the ratio of diisocyanate and diol/diamine in the

polymer will change and the molecular weight of the polymer will decrease according to the principles of polymerization.

Experimentally, all flasks and utensils were thoroughly desiccated before use under high temperature (100°C) and N_2 purging. PCL diols having molecular weights of 4000 (Perstorp, CAPA2402), 8000 (Perstorp, CAPA2803), and 10000 (Sigma-Aldrich) were dried under vacuum at 80°C for 12 hours before use. MDI (Alfa Aesar, 98%) was melted at 45°C and the supernatant liquid without MDI dimer or impurities was used to synthesize the polyurethane-ureas. N, N-Dimethylacetamide (DMAc, Sigma-Aldrich) was dried and distilled over calcium hydride (CaH_2, Sigma-Aldrich) at reduced pressure. 1, 4-Butanediamine (BDA, Alfa Aesar, 98%) and lithium chloride (LiCl, Alfa Aesar, 98%) were used as received.

2.1.2. Preparation of SMPUUs with BDA as chain extender

In a typical case, Poly (ε-caprolactone) polyurethane-ureas (PCLUUs) were prepared by a pre-polymer method: a preset amount of PCL and MDI were added in a 250 mL round-bottom, three-necked separable flask under a nitrogen environment. The reactant mixture was then mechanically stirred at 90°C for three hours to prepare a prepolymer with terminal isocyanate group. The prepolymer was then dissolved in dry DMAc and chain extended with BDA for another three hours. The final polymer concentration was about 20 wt% and the mole ratio of MDI/ (PCL+BDA) was kept at 1.01/1 to yield a linear polymer. The polymer solution was poured on a glass plate and dried at 80°C for 24 hours to prepare the test film. All of the samples were labeled as "PU-M-CL-n_1K-BDA-n_2%" which means polyurethane-urea with MDI and BDA as hard segment of n_2 wt% and the soft segment is PCL with molecular weight of n_1K.

2.2. Characterization of SMPUUs with BDA as chain extender

2.2.1. Structure verification

Nuclear magnetic resonance (NMR)

NMR is an invaluable and routine tool in organic structure determination and verification. Solution ^{1}H NMR spectra of SMPUUs were measured with a Varian Gemini 300 NMR spectrometer in 10 wt% solution in dimethyl sulfoxide-d_6 (DMSO-d_6). The NMR spectra of SMPUUs were quite similar except that some peaks were stronger with more hard segment content. Typical ^{1}H NMR spectra of SMPUUs with different hard segment contents are presented in Figure 2.2.

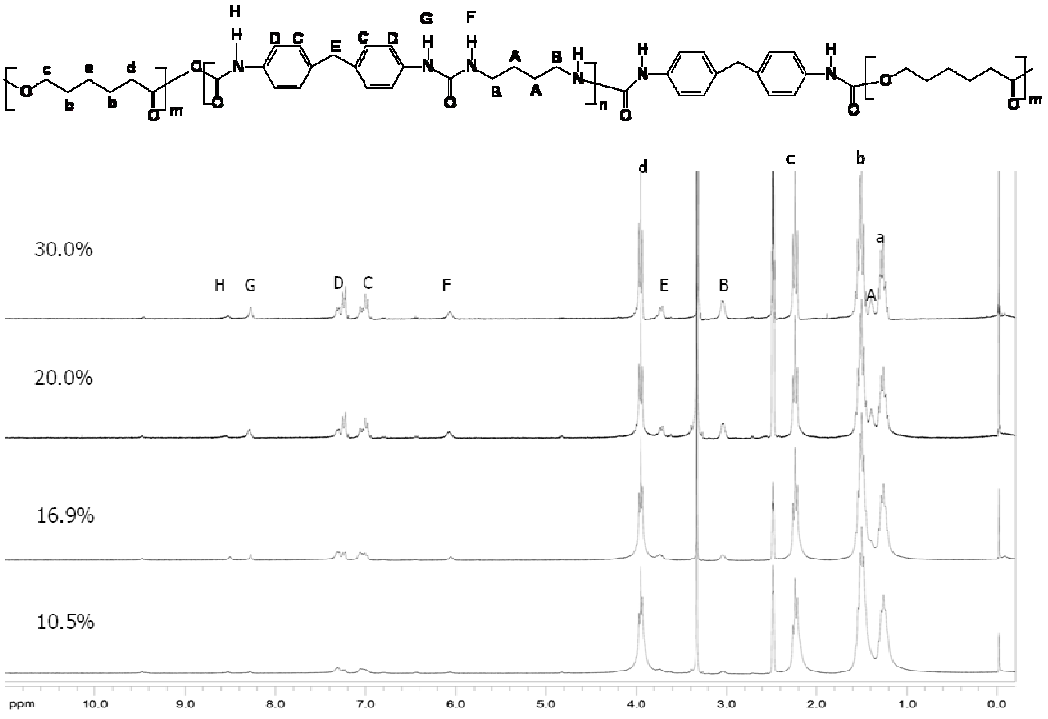

Figure 2.2. ^{1}H NMR spectra of PU-M-CL-8K-BDA with different hard segment contents

The assignments of the NMR chemical shift peaks identified in Figure 2.2 were as follows: chemical shifts at ~1.3 ppm (a), ~1.5 ppm (b), ~2.2 ppm (c), ~4.0 ppm (d) were

assigned to the protons of soft segment PCL; peaks at ~1.4 ppm (A) and ~3.0 ppm (B) were due to the protons of BDA; and peaks at ~7.0 ppm (C), ~7.3 ppm (D) and ~3.7 ppm (E) were from protons of MDI; peaks at ~ 6.0 ppm (F), ~8.3 ppm (G), and ~ 8.5ppm (H) were attributed to the NH group which is produced by the reaction.

Fourier transform infrared (FT-IR) spectra

Fourier transform infrared (FT-IR) spectroscopy is another complementary technique to elucidate the exact structure of chemicals. FT-IR spectra of SMPUUs were recorded between 4,000 and 600 cm^{-1} with a resolution of 4 cm^{-1} and 64 scans on a Magna 550 Fourier transform infrared spectrometer. FT-IR samples were in the form of thin films. Typical FT-IR absorption spectra of PCLUUs are presented in Figures 2.3 - 2.4.

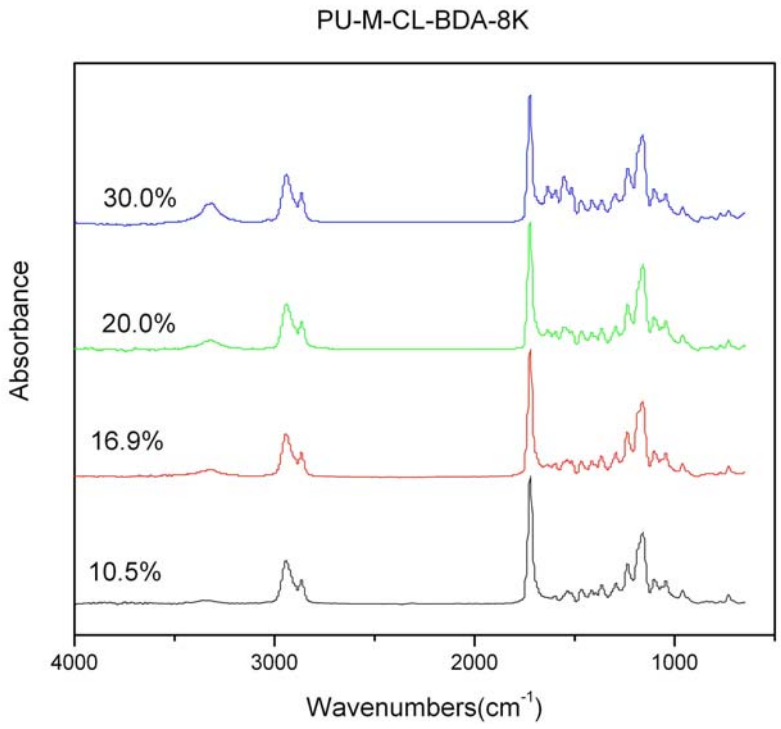

Figure 2.3. FT-IR spectra of PU-M-CL-8K-BDA with different hard segment contents

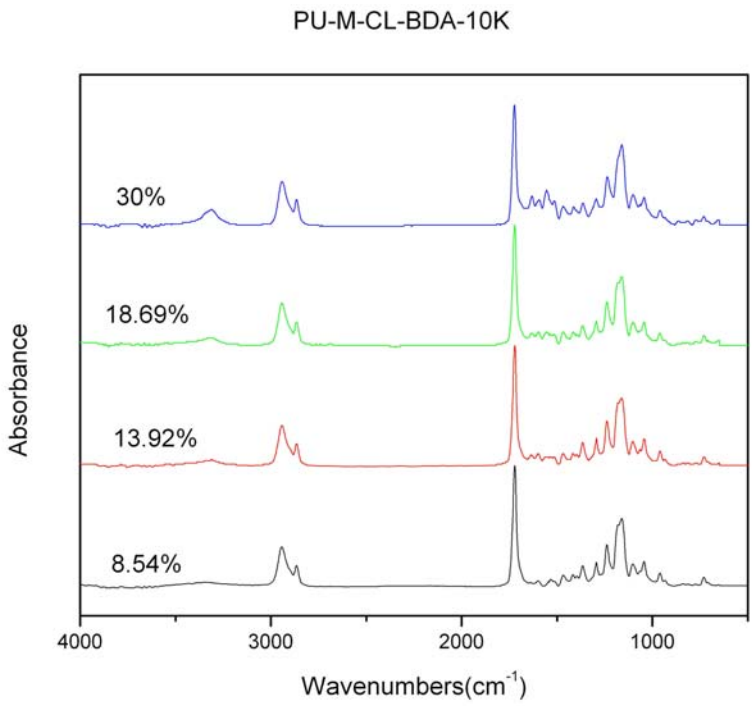

Figure 2.4. FT-IR spectra of PU-M-CL-10K-BDA with different hard segment contents

The assignment of the main peaks in FT-IR spectra are listed in Table 2.1. No significant difference was observed except that some absorption peaks were weaker due to lower hard segment content. The peak intensity at 3317 cm^{-1} for the bonded NH stretching increased with more hard segment content when normalized to the peak intensity of the carbonyl group at 1724 cm^{-1}, which indicated more hydrogen bonding was involved[55]. Based on the above analysis, the structures of synthesized PCLUUs were confirmed as designed.

Table 2.1. FT-IR Band Assignments for PCLUUs with BDA as chain extender

Freq(cm^{-1})	Intensity	Assignment	Domain
3317	medium	N-H stretching	hard
3032	very weak	Aromatic C-H stretching	hard
2941	strong	asymmetric CH2 stretching	soft
2864	medium	symmetric CH2 stretching	soft
1724	very strong	C=O stretching	soft
1599	medium	benzene C-C stretching	hard
1552	medium	amide II (C-N stretching + N-H bending)	hard
1514	medium	benzene C-C stretching	hard
1464	weak	CH2 bending	soft
1416	weak	benzene C-C stretching	hard
1294	medium	internal C-O stretching	soft
1236	strong	amide III (C-N stretching + N-H bending)	hard
1161	strong	CH in-plane bending	soft
1100	medium	C-O-C asymmetric stretching of Urethane	-

2.2.2. Properties of SMPUUs with BDA as chain extenders

Thermal properties

PCL is usually used as the soft segment component in the segmented polyurethane and polyester block polymers. Since the molecular weight of PCL incorporated into the segmented polyurethane will influence the shape fixity and shape recovery rate of SMPs, it is of great importance to understand the dependence of thermal behavior on the molecular weight of PCL before and after PCL is incorporated into the

segmented polyurethane-ureas. The thermal behaviors of pure PCL and its copolymers were investigated by differential scanning calorimetry (DSC, TA Instruments Model Q200). Typically the scan rate was 10°C/min and two cooling-heating cycles were conducted on each sample.

The thermographs of PCL prepolymers with different molecular weights and their copolymers are showed as Figure 2.5 - 2.8:

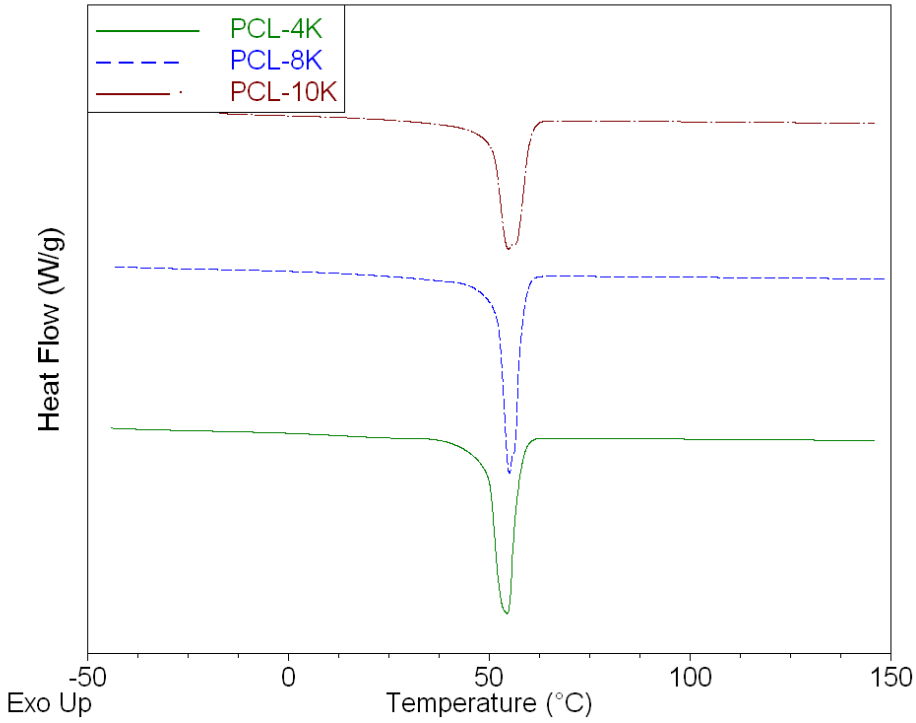

Figure 2.5. DSC curves of PCL prepolymers with different molecular weight

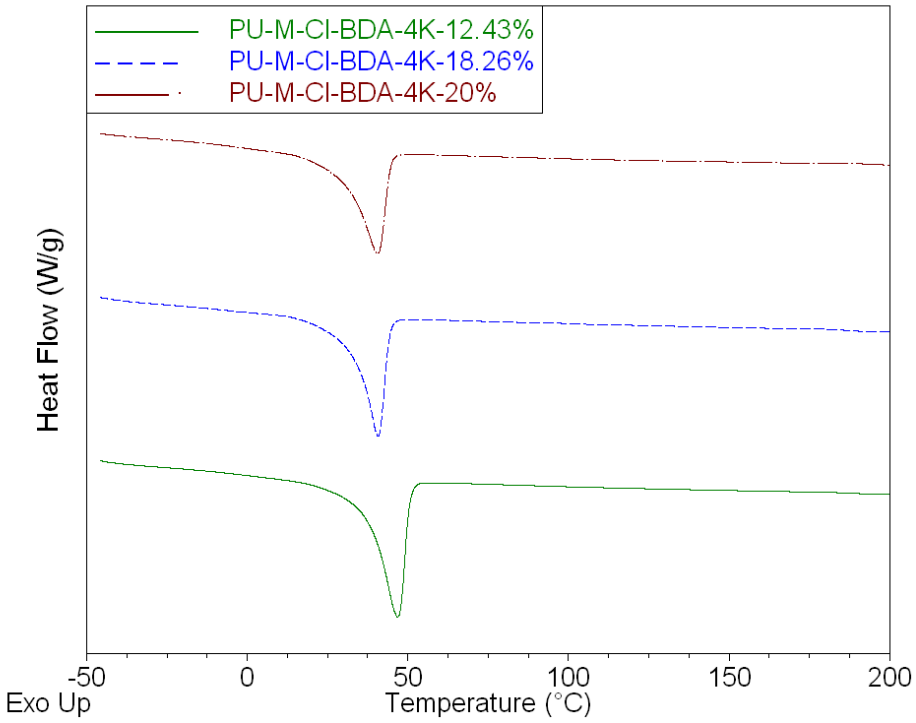

Figure 2.6. DSC curves of PU-M-CL-4K-BDA

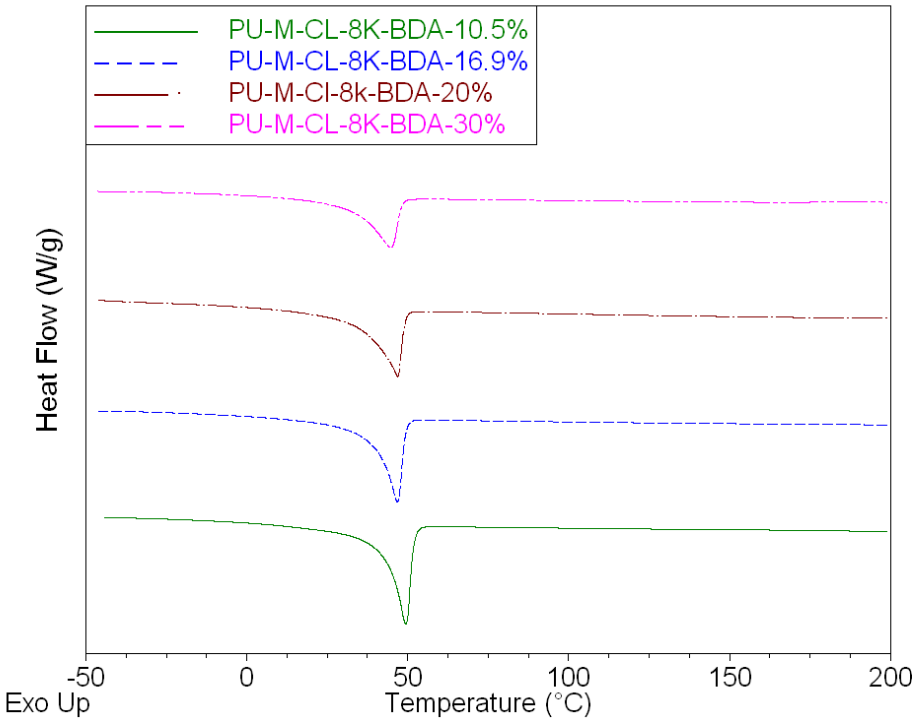

Figure 2.7. DSC curves of PU-M-CL-8K-BDA

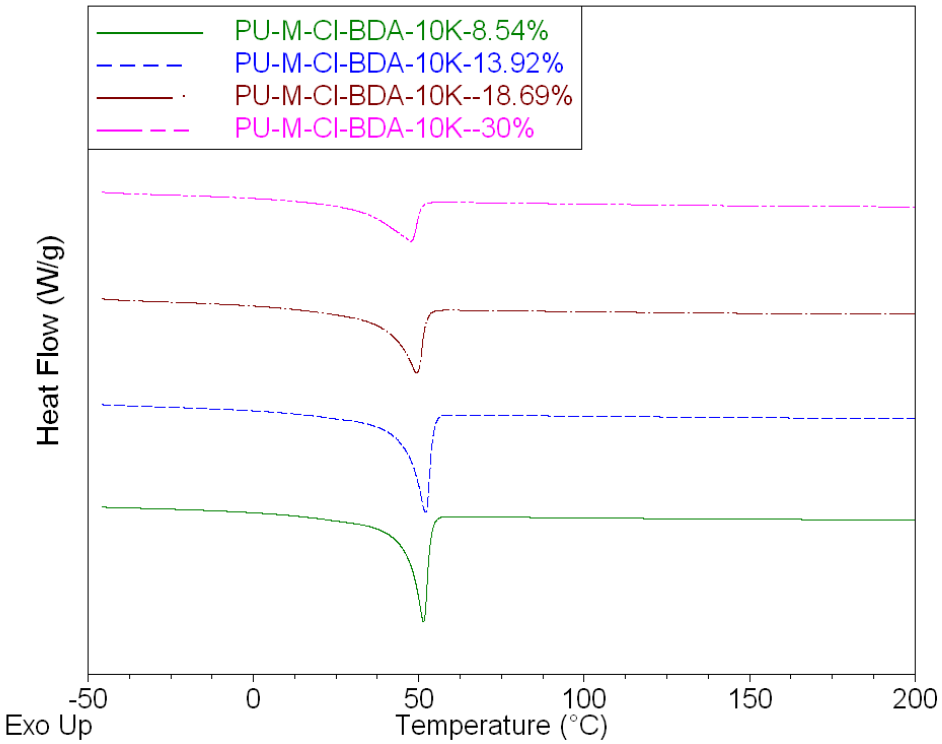

Figure 2.8. DSC curves of PU-M-CL-10K-BDA

All of them were crystallizable and the melting temperatures of the crystals are given in Table 2.2. The peak melting temperatures and heat of fusion were determined directly from DSC thermographs.

Table 2.2. DSC Results for PCL diols and Segmented PCLUUs

PCLUU with Hard segment (wt %)	T_m(°C)	ΔH_m (J/g)	X_c (%)
PCL-4K	54.5	86.1	60.6
PU-M-CL-4K-BDA-12.4%	46.9	44.2	35.5
PU-M-CL-4K-BDA-18.3%	40.7	34.9	30.1
PU-M-CL-4K-BDA-20%	40.5	34.1	30.0
PCL-8K	55.1	82.4	58.0
PU-M-CL-8K-BDA-10.5%	49.4	50.7	39.9
PU-M-CL-8K-BDA-16.9%	46.8	44.5	37.7
PU-M-CL-8K-BDA-20%	46.9	41.0	36.1
PU-M-CL-8K-BDA-30%	44.7	32.6	32.8
PCL-10K	55.7	74.4	52.4
PU-M-CL-10K-BDA-8.5%	51.4	52.9	40.7
PU-M-CL-10K-BDA-13.9%	52.0	49.9	40.8
PU-M-CL-10K-BDA-19.0%	49.4	42.6	37.0
PU-M-CL-10K-BDA-30%	47.6	33.0	33.2

The crystallinities of the PCL prepolymer and the PCL phase of PCLUUs were calculated according to the melting peak area of the DSC curve by assuming the perfect PCL crystal has a melting enthalpy of 142.0J/g.[56, 57] The melting points (T_m) of PCL prepolymers increased with increasing molecular weight (M_n) of PCL. The crystallinity of PCL prepolymer was in the range of 52-61% and dropped as PCL with higher M_n was introduced, due to the difficulty for the backbone chain to align as the chain gets longer.

As a result, the main chain with higher molecular weight was retarded to get the same crystal as the one with lower molecular weight.

The crystallization ability of PCL segments in segmented PCLUUs was significantly depressed due to the influence of hard segments. For the PCLUUs with the same molecular weight of PCL, the crystallinity of PCL usually decreased with increasing hard segment content, the same result as shown by the MDI/PCL/BDO system.[18] Crystallinities of the PCL segments of polyurethane-ureas were below 50%, indicating that the soft segments were only partially crystallized, which could be the reason that all of the PCLUUs exhibited lower T_m than the corresponding PCLs.

Tensile properties

SMPUU films to measure the mechanical properties were prepared by solvent casting on a glass plate. After standing at 80°C for 24 hours, films were further dried at 80°C under vacuum for another 24 hours. Tensile specimens with a length of 50.8 mm and a width of 12.7 mm were prepared to measure the mechanical properties and shape memory properties. The thickness of the specimens was in the range of 0.1~0.2 mm depending on the concentration and viscosity of the casting solution. Tensile tests were performed on the Instron Corporation tensile testing machine 5566 with the crosshead speed of 50 mm/min and a gauge length of 25.4 mm.

For each data point, three samples were tested, and the average value was calculated along with the standard deviation. The typical stress-strain curves of the PCLUU films are shown in Figure 2.9:

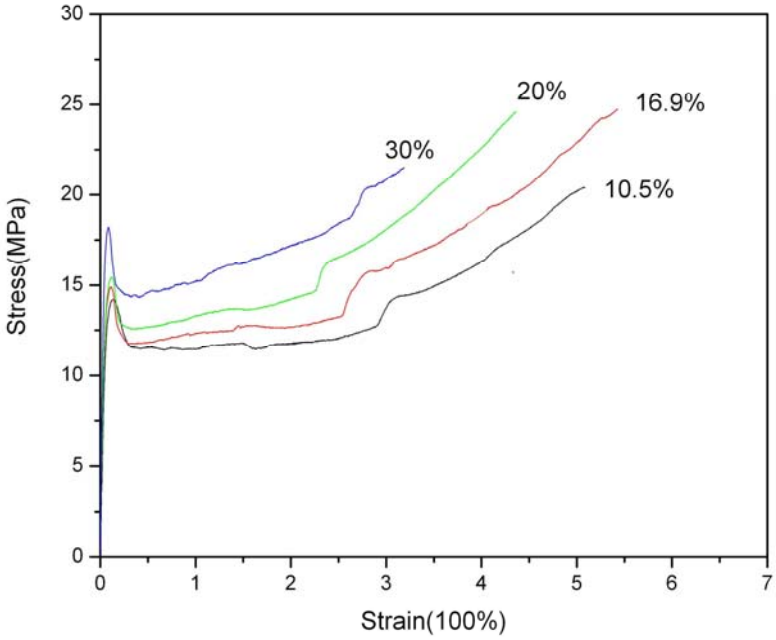

Figure 2.9. Tensile stress strain curves of PU-M-CL-BDA-8K

The tensile properties of all the PCLUU films with BDA as chain extender are listed in Table 2.3:

Table 2.3. Mechanical properties of PCLUUs with BDA as chain extender

PCLUU with Hard segment (wt %)	Tensile modulus (MPa)	Yield strength (MPa)	Tensile strength at 200% (MPa)	Intrinsic viscotiy (dL/g)
PU-M-CL-4K-BDA-12.4%	239.7±20.2	13.4±0.6	10.6±0.4	0.80
PU-M-CL-4K-BDA-18.3%	183.2±25.7	11.7±0.4	11.0±0.6	0.95
PU-M-CL-4K-BDA-20%	256.0±18.3	12.4±0.5	11.1±0.3	0.61
PU-M-CL-8K-BDA-10.5%	285.7±48.6	15.3±1.3	12.7±0.5	0.66
PU-M-CL-8K-BDA-16.9%	308.9±13.6	15.4±0.6	13.0±0.5	0.75
PU-M-CL-8K-BDA-20%	324.3±23.0	15.7±1.3	14.1±1.4	0.77
PU-M-CL-8K-BDA-30%	400.2±20.2	19.0±1.4	15.7±0.9	0.59
PU-M-CL-10K-BDA-8.5%	250.8±9.1	12.8±1.5	11.1±0.4	0.78
PU-M-CL-10K-BDA-13.9%	392.8±46.5	19.1±0.5	14.0±0.8	0.48
PU-M-CL-10K-BDA-19.0%	394.5±31.3	17.2±1.8	13.8±1.6	0.64
PU-M-CL-10K-BDA-30%	380.4±16.8	15.4±2.1	15.2±0.4	0.75

The mechanical properties of SMPUUs are greatly influenced by the molecular weight. The intrinsic viscosities of the polymers were measured using an Ubbelohde viscometer at 25°C in DMAc with 1 wt% of LiCl to indicate the molecular weight of SMPUUs which are also listed in Table 2.3. Most of the samples exhibited intrinsic viscosities above 0.50 dL/g, indicating high molecular weight of SMPUUs.

Gel Permeation Chromatography (GPC) is another popular tool to determine the molecular weight of polymers. Polyurethane-ureas synthesized in this study do not dissolve in traditional GPC solvents such as tetrahydrofuran (THF) or toluene. Matrix-assisted laser desorption/ionization (MALDI) time of flight mass spectroscopy may also not be suitable to measure the molecular weight of SMPUUs. Polymers with polydispersities greater than 1.2 are difficult to characterize with MALDI due to the signal intensity discrimination against higher mass oligomers[58-60], while condensation polymerization usually creates polymers with high polydispersity. As a result, only intrinsic viscosity data were used to determine the molecular weights. The tensile modulus for SMPUUs with BDA as chain extender was between 180 MPa to 400 MPa, while the tensile strength at 200% strain was between 11 MPa to 16 MPa.

Shape memory properties

The shape memory properties were investigated by cyclic tensile testing with an MTS Insight 2 fitted with a thermal chamber. The typical test procedures similar to that used with the MDI/PCL/BDO system[17] was: A SMP sample was heated to a high temperature (T_{high}=65°C) which was above the switching temperature (T_{trans}), and then stretched to a designed strain (ε_m=200%). The sample was maintained with constant strain ε_m for 20 minutes and then cooled to room temperature (below the switching temperature) to freeze in the temporary shape. Next, the clamps of the tensile tester were allowed to return to their original position to remove the strain. At the beginning of the unloading process, the elastic recovery stress of the sample was reduced and returned zero at strain ε_u, and the sample will bent with further unloading. Finally, the sample was reheated to T_{high}=65°C and then recovered to the permanent shape with a residual strain

ε_p. Subsequent loading and unloading cycles can be carried on the samples. In this study, four circles were tested since the difference after the fourth circle was negligible.

Figures 2.10 - 2.20 show the cyclic stress-strain behavior of SMPUUs:

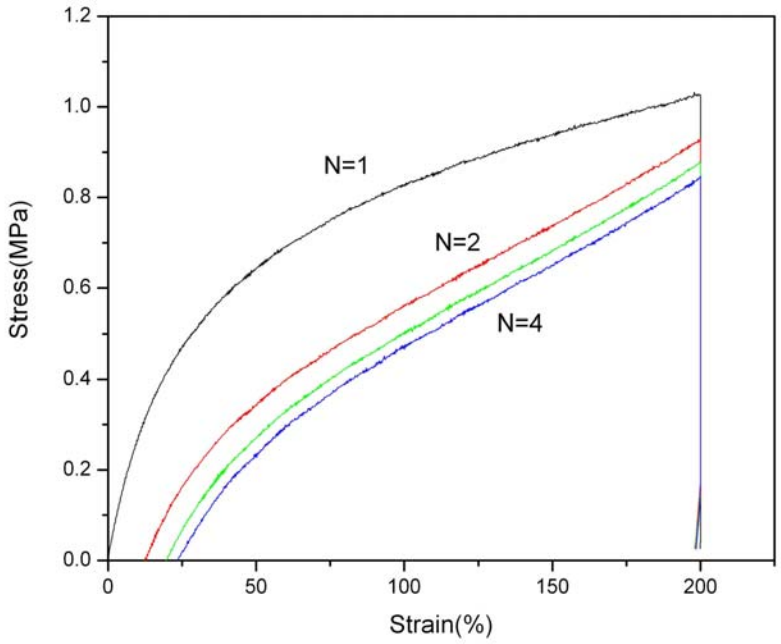

Figure 2.10. Cyclic tensile behavior of PU-M-CL-4K-BDA-12.4%

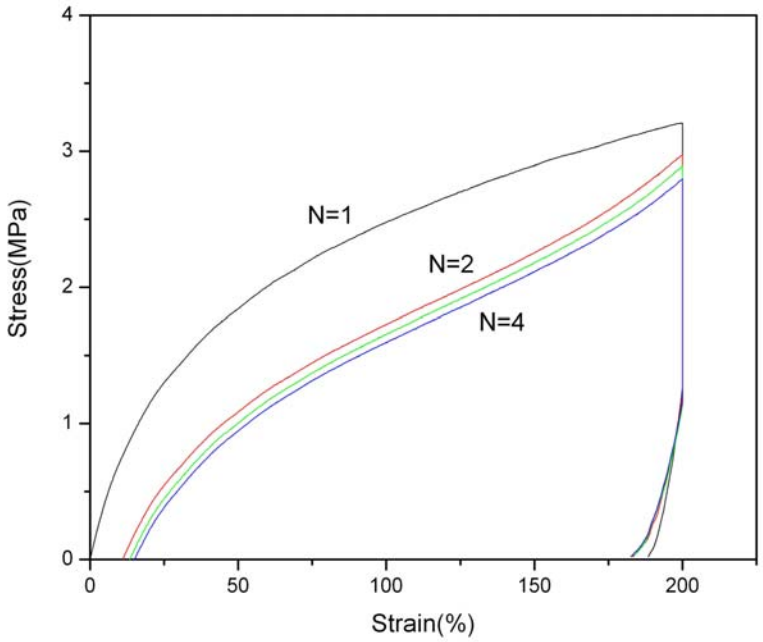

Figure 2.11. Cyclic tensile behavior of PU-M-CL-4K-BDA-18.3%

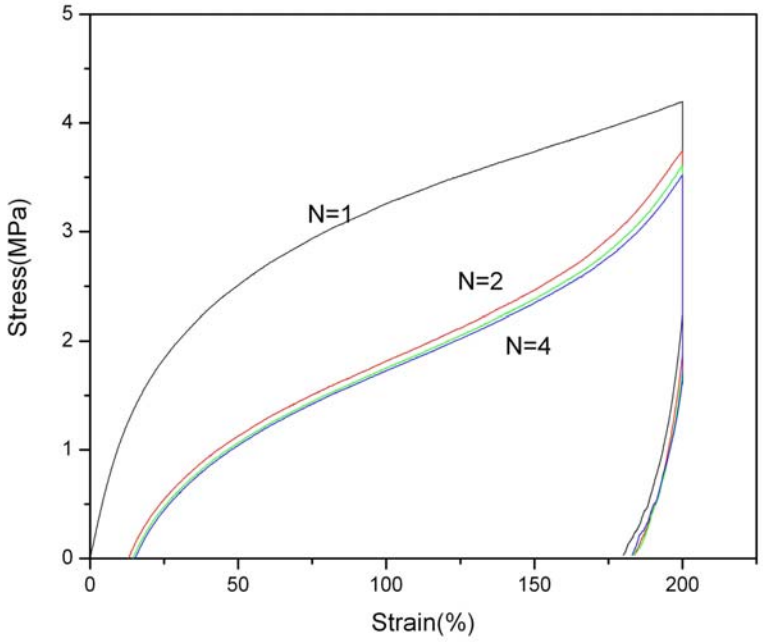

Figure 2.12. Cyclic tensile behavior of PU-M-CL-4K-BDA-20%

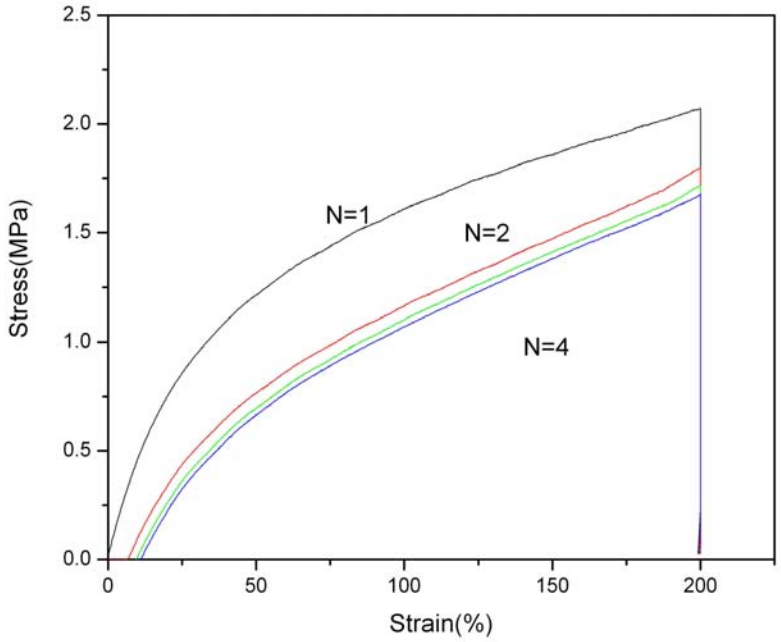

Figure 2.13. Cyclic tensile behavior of PU-M-CL-8K-BDA-10.5%

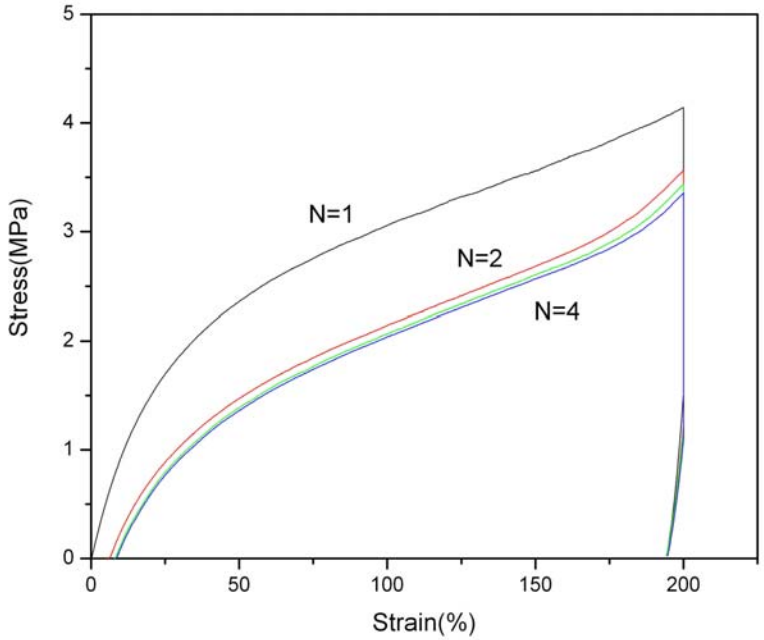

Figure 2.14. Cyclic tensile behavior of PU-M-CL-8K-BDA-16.9%

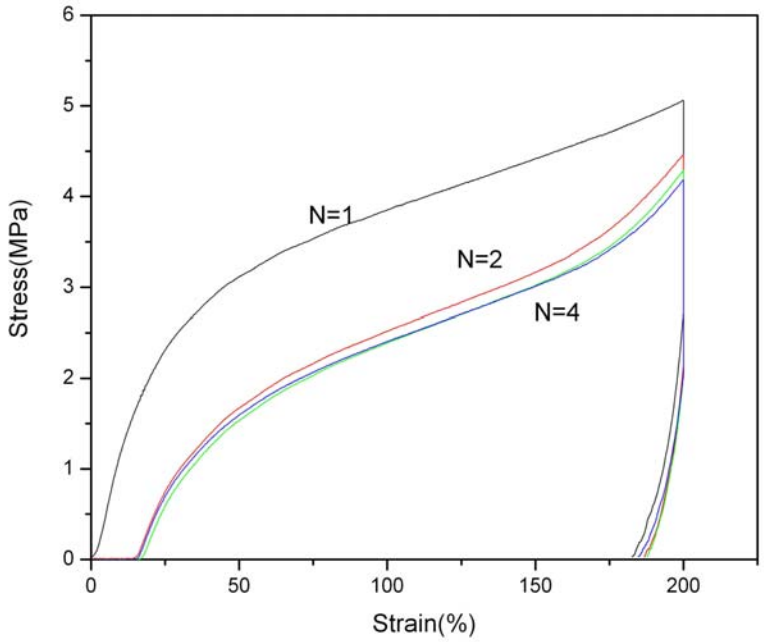

Figure 2.15. Cyclic tensile behavior of PU-M-CL-8K-BDA-20%

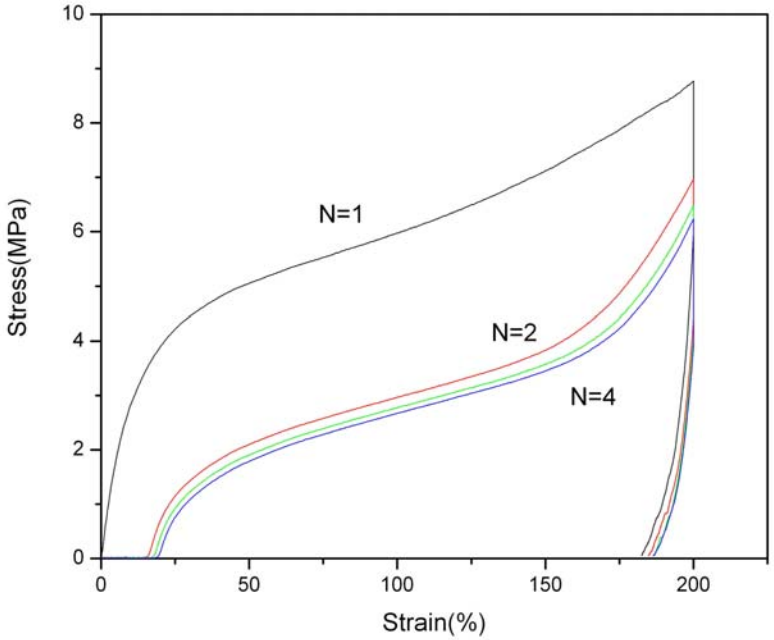

Figure 2.16. Cyclic tensile behavior of PU-M-CL-8K-BDA-30%

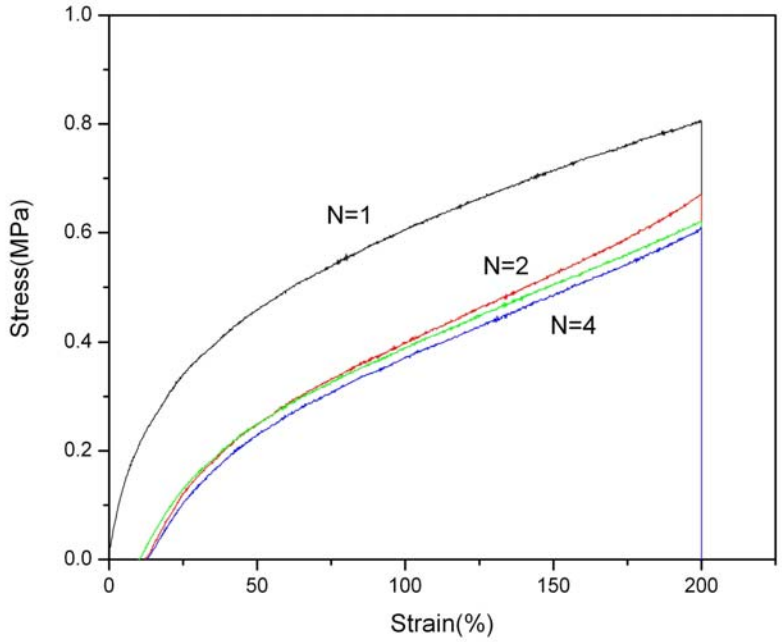

Figure 2.17. Cyclic tensile behavior of PU-M-CL-10K-BDA-8.5%

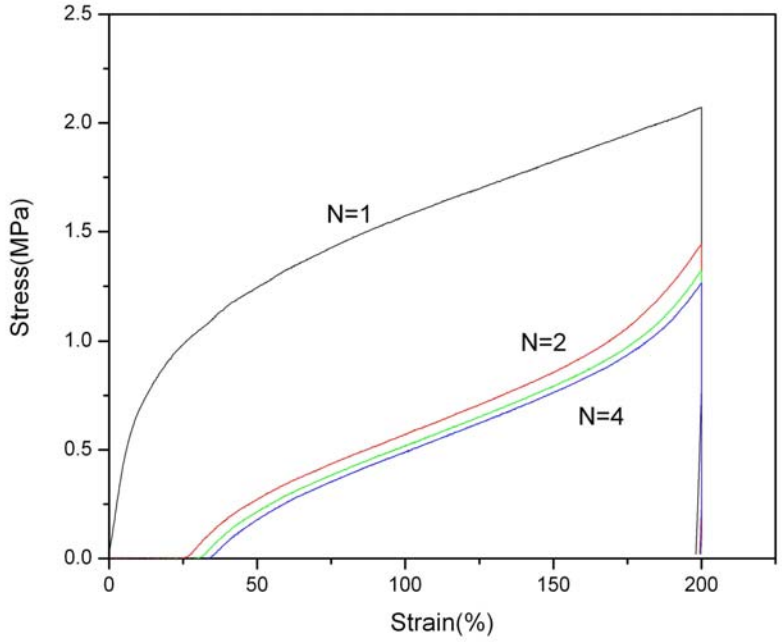

Figure 2.18. Cyclic tensile behavior of PU-M-CL-10K-BDA-13.9%

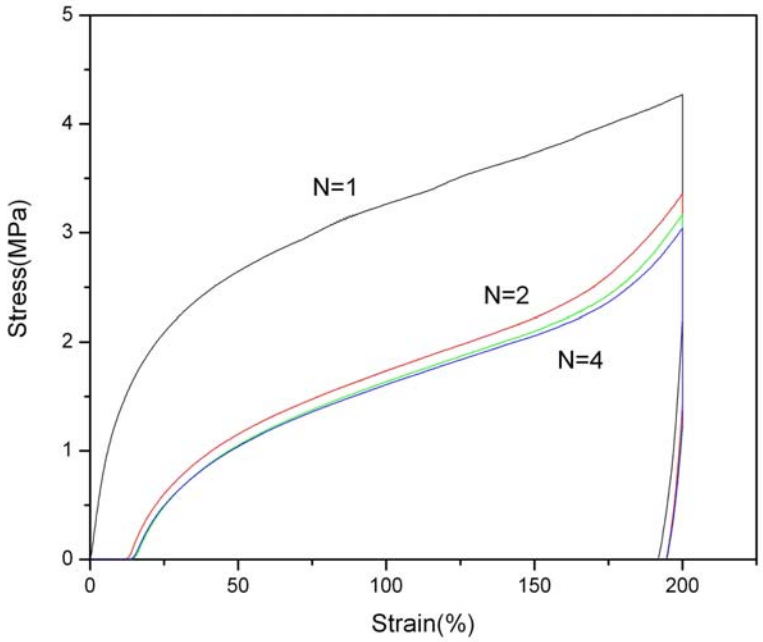

Figure 2.19. Cyclic tensile behavior of PU-M-CL-10K-BDA-18.7%

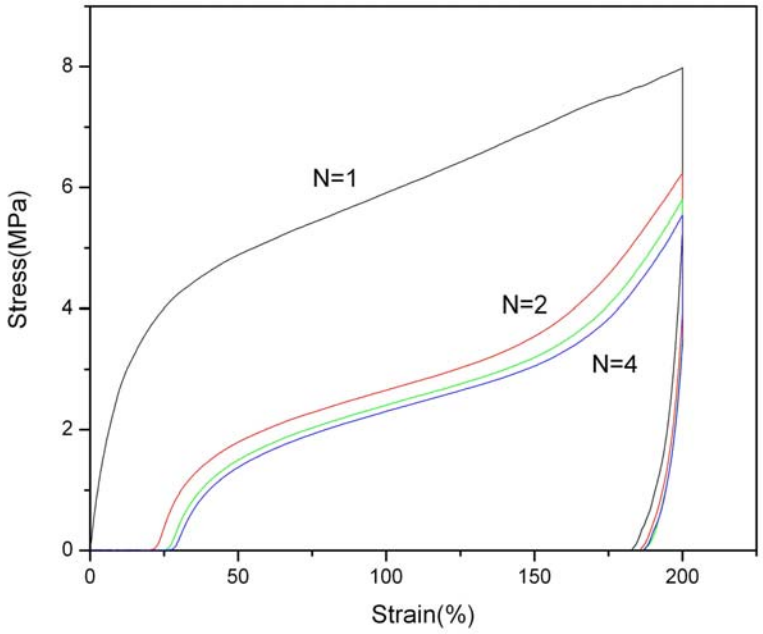

Figure 2.20. Cyclic tensile behavior of PU-M-CL-10K-BDA-30%

From the cyclic tensile behavior of SMPUUs, the typical cyclic dependence of strains was calculated according to as the MDI/PCL/BDO system (Figure 2.21):

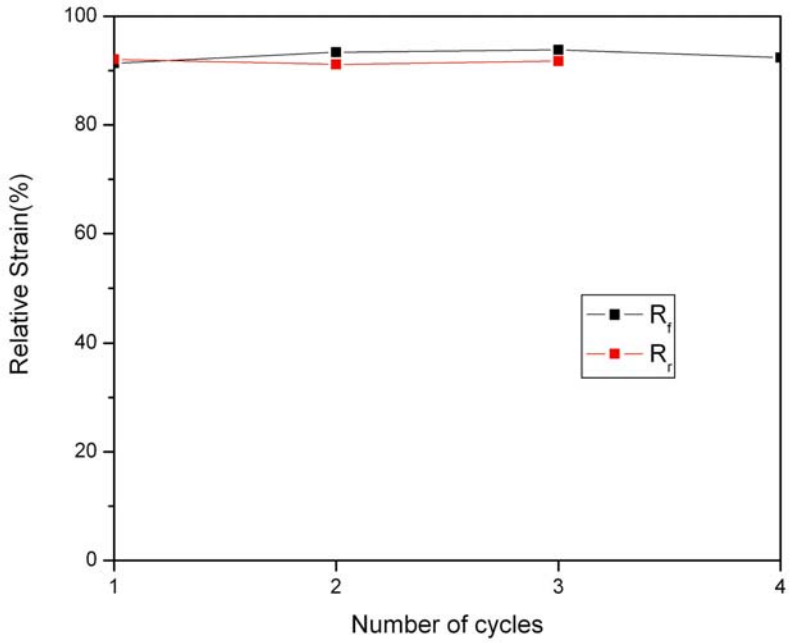

Figure 2.21. Cyclic dependence of strain of PU-M-CL-8K-BDA-20%

The shape recovery and fixity of MDI/PCL/BDA SMPUUs were similar to the MDI/PCL/BDO copolymer system.[17] Both properties for PU-M-CL-8K-BDA-20% were above 90% along with a small deviation which showed excellent shape memory properties after programming. This result indicates that the shape recovery and fixity were closely related to the crystallinity of the PCL phase of specimens cooled in the elongated state[20]. Meanwhile, the change of chain extender from BDO to BDA increased the recovery stress significantly, for example, PU-M-CL-8K-BDA-20% had a 5 MPa stress at 200% strain which was almost double of that in the PU-M-CL-8K-BDO-20% copolymer. This could be attributed to the influence of extra hydrogen bonding interactions involved in the MDI/PCL/BDA system as shown in Figure 2.22:

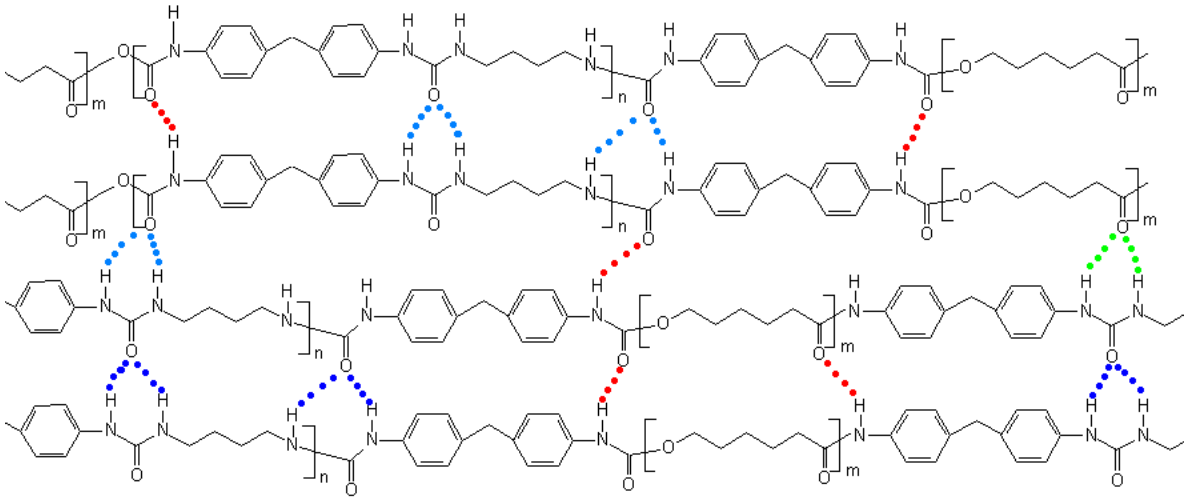

Figure 2.22. Hydrogen bonding in segmented polyurethane-urea copolymers

As illustrated, the bidentate hydrogen bonding of urea linkage (blue dashed lines) in which the oxygen of the urea carbonyl hydrogen bonds with two groups on a neighboring chain is much stronger than the monodentate hydrogen bonding of urethane linkage (red dashed lines), which is responsible for the improvement of the recovery stress. Due to the substantial level of hydrogen bonding, the SMPUUs degraded before melt processing becomes possible, indicating that this polymer could only be processed from solution as is Spandex®.

The recovery stress of the first cycle was greatly influenced by the content of the hard segment (HS) (Figure 2.23):

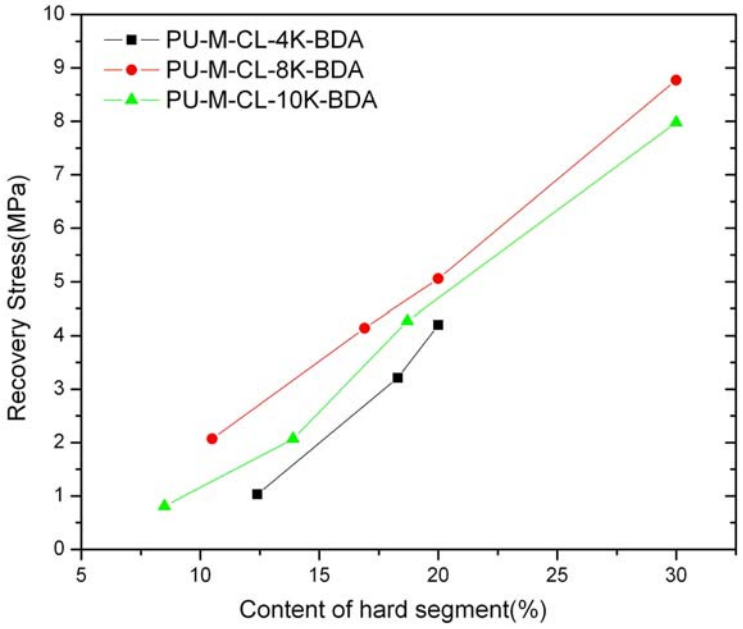

Figure 2.23. Recovery stress of first cycle with different M_n and HS at 200% strain

As hard segment content increases, more hydrogen bonds were formed between main chains, and the rigidity of the main chain increased.

Figure 2.24 shows the recovery stress influenced by chain extender. With the same molecular weight and content of soft segment, the MDI/PCL/BDA system improved the recovery stress to ~200% just because of the bidentate hydrogen bonding interactions of urea linkages.

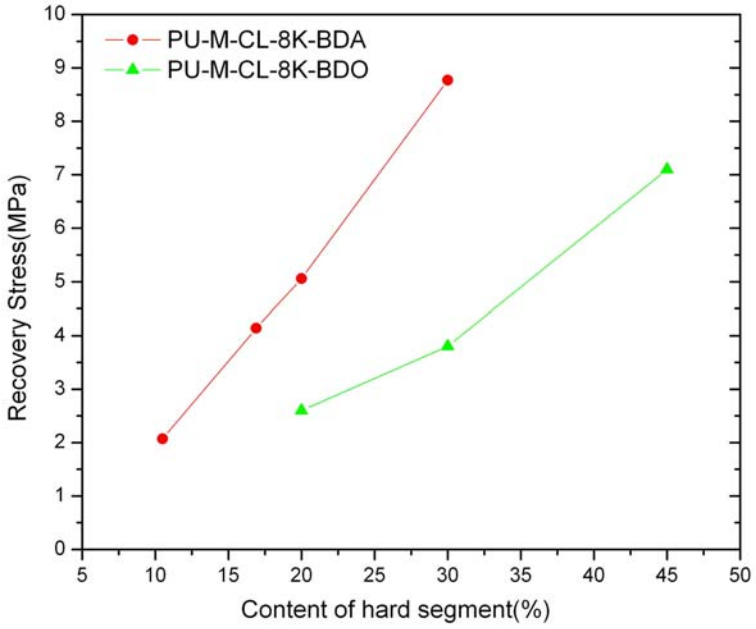

Figure 2.24. Influence of chain extender on the recovery stress

The bidentate hydrogen bonding interactions of urea linkages can also be studied with NMR. The inter molecular bidentate hydrogen bonding between the urea hard segments can be disrupted by the incorporation of a hydrogen bond inhibitor, LiCl.[61] Figure 2.25 shows the NMR spectra of PU-M-CL-4K-BDA-20% dissolved in DMSO-d_6 (b) and DMSO-d_6 + LiCl (a).

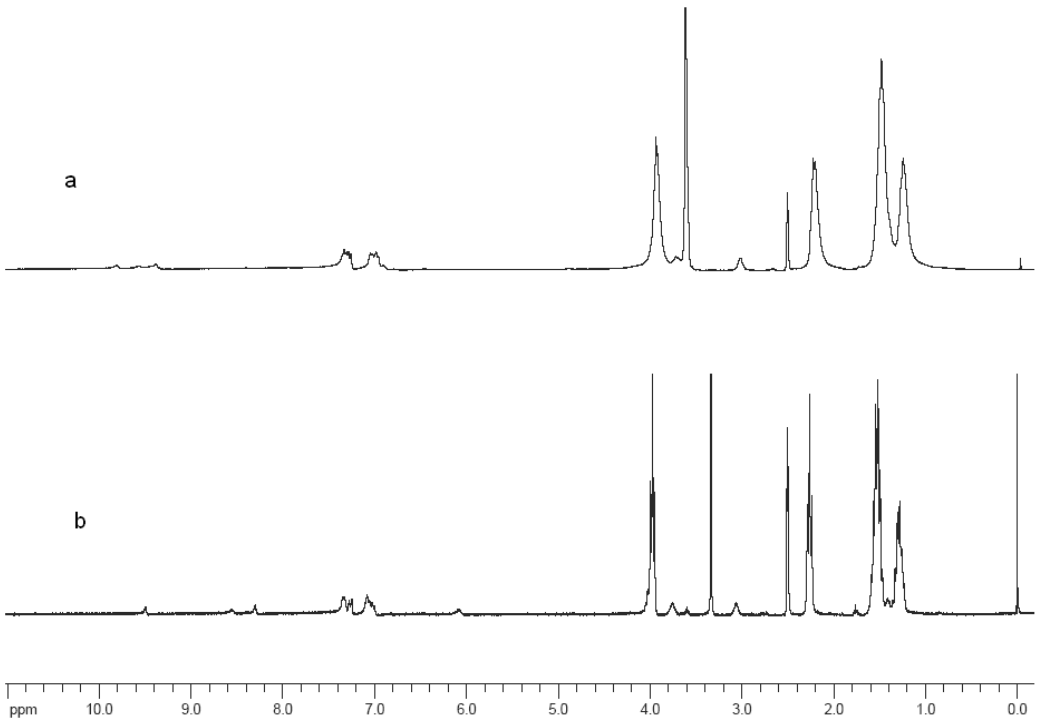

Figure 2.25. ^{1}H NMR spectra of PU-M-CL-4K-BDA-20% dissolved in solvent: (a) DMSO-d_6+LiCl and (b) pure DMSO-d_6

All of the peaks attributed to the NH group were shifted to a lower field because of the stronger magnetic anisotropic effect while the other peaks remained at the same positions.[62]

Thermal annealing of segmented polyurethane-ureas could lead to the rearrangement of hydrogen bonds[63]. As seen in Figure 2.26, the melting point increased from 45.8°C to 59.5°C with annealing temperature 100°C versus 200°C at first circle.

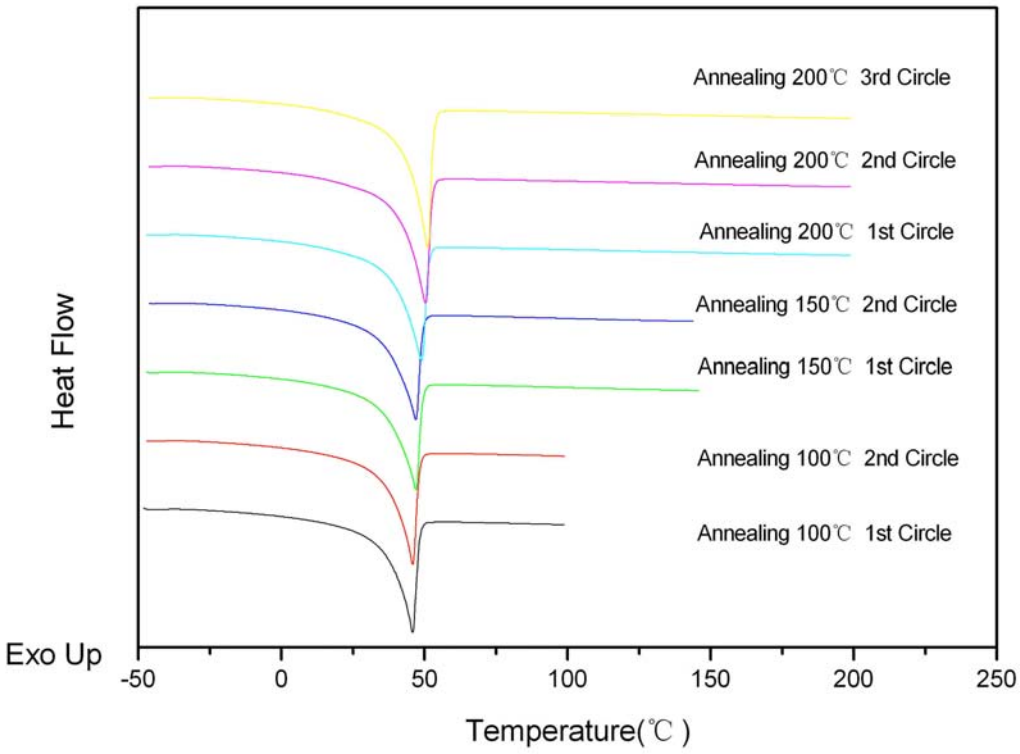

Figure 2.26. DSC curves of PU-M-CL-8K-BDA-20% at different annealing temperatures

On the other hand, the melting points at annealing temperature of 100°C and 150°C stayed the same within different circles while it increased at an annealing temperature of 200°C. The scission of the inter-urea hydrogen bonds apparently occurred around 200°C and affected the thermal property above this point. Moreover, an improvement of the micro phase separation was also indicated thermal annealing can be a promising method to program shape memory transition temperature for different applications.

Dynamic mechanical properties

The tensile storage moduli of synthesized polymers with different hard segment contents are shown in Figure 2.27:

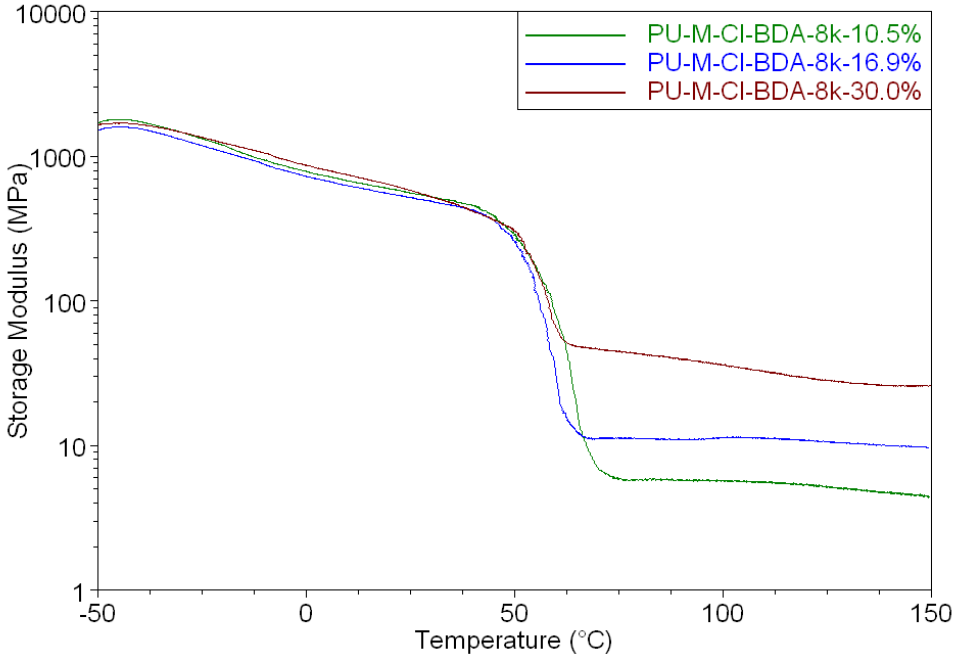

Figure 2.27. Tensile storage modulus of PU-M-CL-BDA-8K

The storage modulus slightly decreased below the melting temperature of PCL and a sharp drop was observed near the melting point. Unlike the MDI/PCL/BDO[17] and HDI/PCL/DHBP[24] systems, the storage modulus was much more stable above the melting point due to the bidentate hydrogen bonding of urea linkage, which indicated a more constant recovery stress at different temperatures. The effect of hard segment content was not obvious below the melting point, while the rubbery modulus increased with the increase of hard segment.

CHAPTER 3

SHAPE MEMORY POLYURETHANE-UREAS WITH DIFFERENT ALIPHATIC AMINES AS CHAIN EXTENDERS

3.1. Synthesis of shape memory polyurethane-ureas (SMPUUs) with aliphatic amines as chain extenders

SMPUUs with different aliphatic amines as chain extenders were synthesized with a prepolymer method similar to that described in the previous chapter. All flasks and utensils were thoroughly desiccated before use under high temperature (100°C) and N_2 purging. PCL diol having molecular weight of 4000 (Perstorp, CAPA2402) was dried under vacuum at 80°C for 12 hours before use. MDI (Alfa Aesar, 98%) was melted at 45°C and the supernatant liquid without MDI dimer or impurities was used to synthesize the polyurethane-ureas. N, N-Dimethylacetamide (DMAc, Sigma-Aldrich) was dried and distilled over Calcium hydride (CaH_2, Sigma-Aldrich) at reduced pressure. Ethylenediamine (EDA, Alfa Aesar,98%), 1,4-Butanediamine (BDA, Alfa Aesar,99%), 1,6-Hexanediamine (HDA, Alfa Aesar,98%), 2-Methyl-1,5-pentanediamine (MPDA, Alfa Aesar,98%) and Lithium chloride (LiCl, Alfa Aesar,98%) were used as received.

In a typical case, PCLUUs were prepared by a pre-polymer method described as follows: Specific amounts of PCL with molecular weight of 4000 and MDI were added in a 250 mL round-bottom, three-necked separable flask under a nitrogen environment. The reactant mixture was then mechanically stirred at 90°C for three hours to prepare a

prepolymer with terminal isocyanate groups. The prepolymer was then dissolved in dry DMAc and reacted with different chain extenders (Figure 3.1) for another three hours:

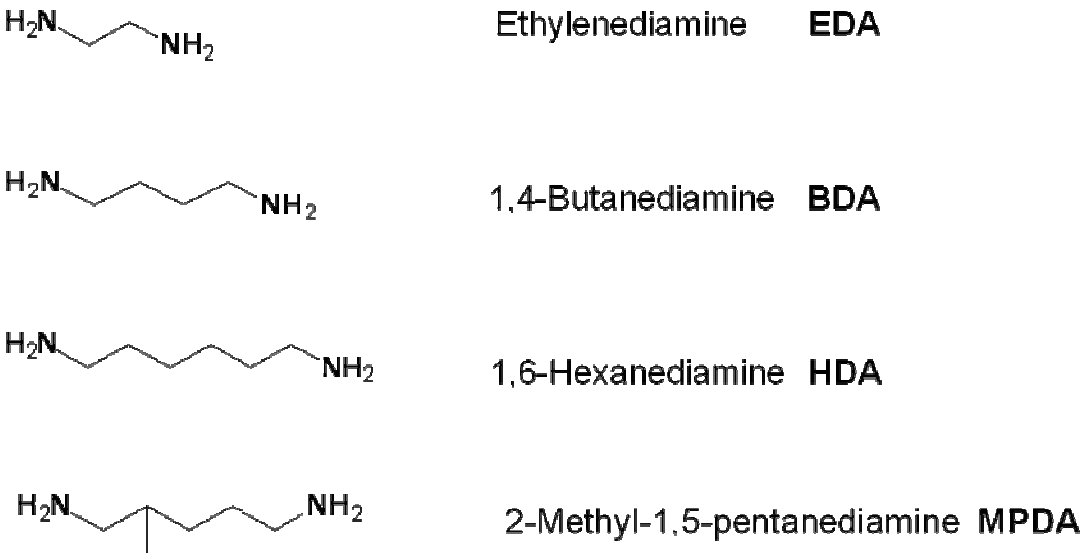

Figure 3.1. Aliphatic diamines as chain extenders

The final polymer concentration was ~ 20 wt% and the molar ratio of MDI/ (PCL+chain extender) was kept at 1.01 to yield a linear polymer. The polymer solution was poured onto a glass plate and dried at 80°C for 24 hours to prepare the test film.

In this chapter, four different aliphatic diamines were used as chain extenders. All of the synthesized samples were based on PCL with molecular weight of 4000 and had hard segment content (MDI+chain extender) of 20 wt%. These aliphatic diamines were carefully chosen to evaluate the effect of the structure of chain extenders. As a result, the influence of the chain extender's flexibility and the side chains were determined.

3.2. Characterization of SMPUUs with different aliphatic diamines as chain extender

3.2.1. Structure verification

Nuclear magnetic resonance (NMR)

The ^{1}H NMR spectra of shape memory PCLUUs are presented in Figure 3.2:

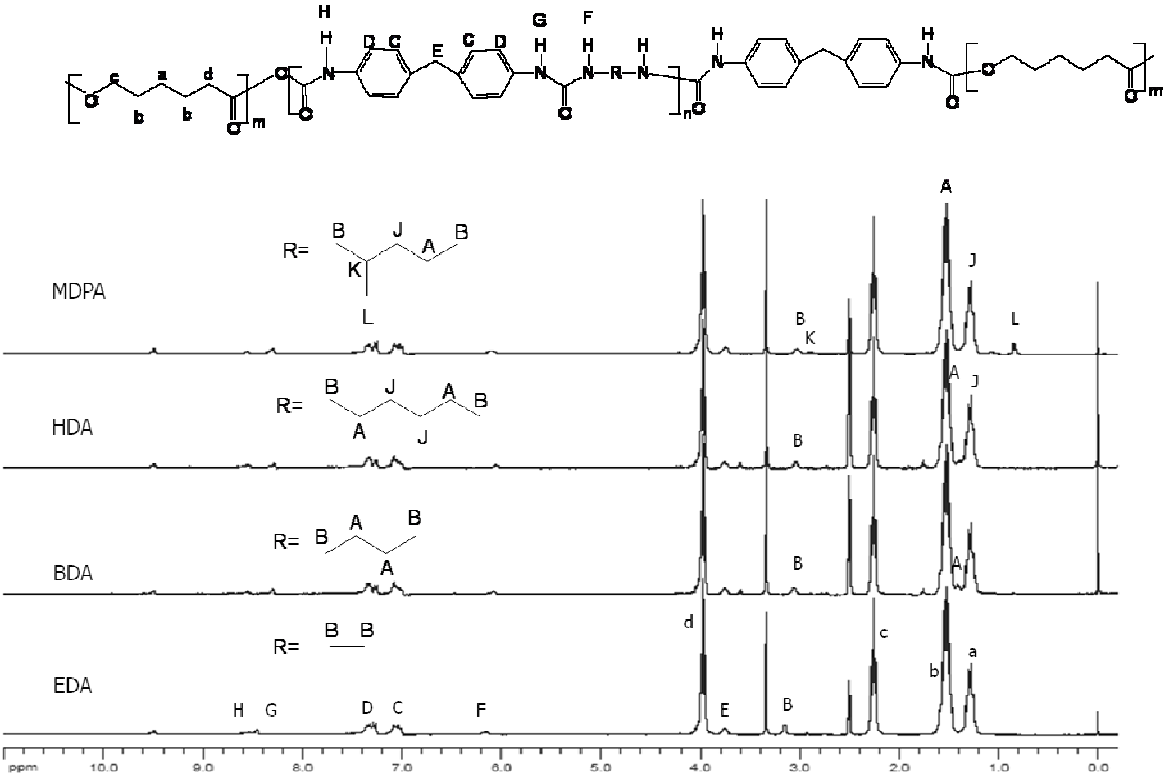

Figure 3.2. ^{1}H NMR spectra of PU-M-CL-4K with different aliphatic chain extenders

The assignment of the NMR chemical shift peaks identified in Figure 3.2 was as follows: chemical shifts at ~1.3 ppm (a), ~1.5 ppm (b), ~2.2 ppm (c), and ~4.0 ppm (d) were assigned to the protons of soft segment PCL; peaks at ~7.0 ppm (C), ~7.3 ppm (D), and ~3.7 ppm (E) were from the protons of MDI; peaks at ~ 6.0 ppm (F), ~8.3 ppm (G), and ~ 8.5ppm (H) were attributed to the NH group. Other peaks with different chain extenders are listed in the spectra.

Fourier transform infrared spectra (FT-IR)

Typical FT-IR absorption spectra of PCLUUs with different aliphatic chain extenders are presented in Figure 3.3:

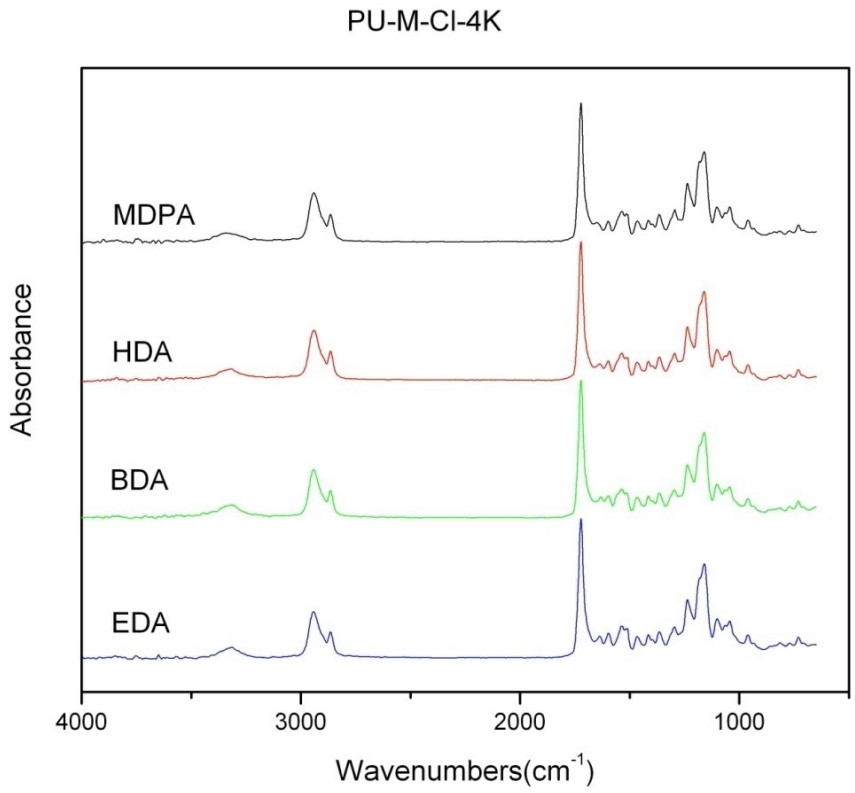

Figure 3.3. FT-IR spectra of PU-M-CL-4K with different aliphatic chain extenders

No significant difference was observed in these spectra and the assignments of the main peaks in FT-IR spectra were the same as Chapter 2 Table 2.1. Based on the above analysis, the structures of the synthesized PCLUUs were confirmed as designed.

3.2.2. Properties of SMPUUs with different aliphatic chain extenders

Thermal properties

The thermal behavior of pure PCL and its copolymers were investigated by DSC (Figure. 3.4):

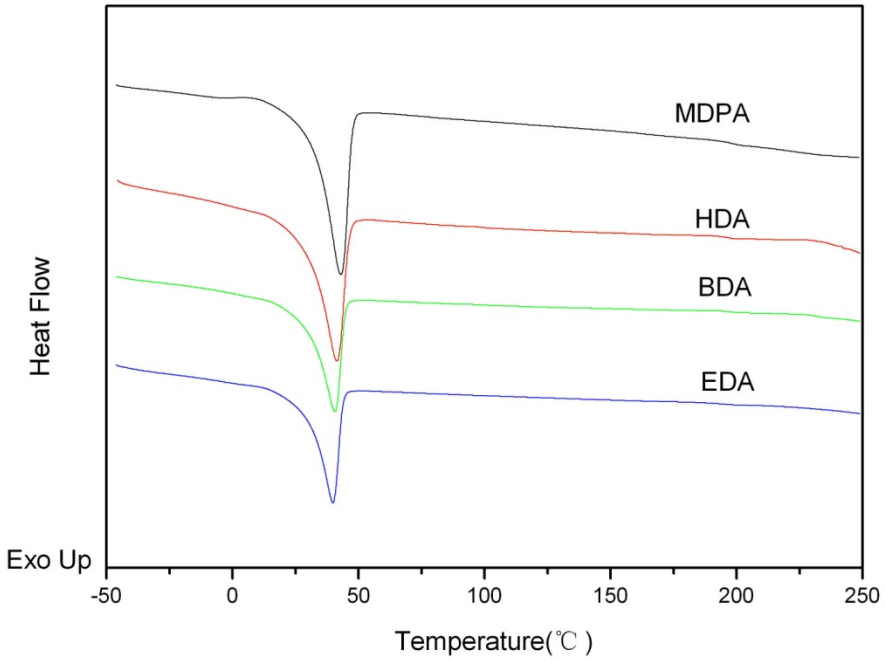

Figure 3.4. DSC curves of PU-M-CL-4K with different aliphatic chain extenders

The peak melting temperature and heat of fusion determined directly from DSC thermographs are summarized in Table 3.1:

Table 3.1. DSC results of PCL diols and segmented PCLUUs with different aliphatic diamines as chain extenders

PCLUU with different chain extender	T_m(°C)	ΔH_m(J/g)	X_c(%)
PCL-4K	54.5	86.1	60.6
PU-M-CL-4K-MDPA-20%	43.0	40.0	35.2
PU-M-CL-4K-HDA-20%	41.4	35.7	31.4
PU-M-CL-4K-BDA-20%	40.5	34.1	30.0
PU-M-CL-4K-EDA-20%	39.8	33.5	29.5

The crystallinities of the PCL prepolymer and the PCL phase of PCLUUs were calculated according to the melting peak area of the DSC curves by assuming the perfect PCL crystal had a melting enthalpy of 142.0 J/g.[56, 57]

The aliphatic chain extenders in the hard segment will influence the crystallization ability of the PCL soft segment. For the PCLUUs with PCL of 4000 molecular weight, the crystallinity of the PCL segment increased with improved flexibility of chain extenders. The more flexible chain extender facilitated crystallization. When a side chain is incorporated into the hard segment as chain extender MDPA, the hydrogen bonding in the segment polyurethane-ureas is hindered so that the crystalline inside can grow larger. MDPA is already used in commercial Spandex® to impart edge-curl resistance during fabric finishing, utilizing the same conecpt.[64]

Tensile properties

The tensile properties of all PCLUU films with different chain extenders are listed in Table 3.2:

Table 3.2. Mechanical properties of PCLUUs with different aliphatic diamines as chain extenders

PCLUU with different chain extender (wt %)	Tensile modulus (MPa)	Yield strength (MPa)	Tensile strength at 200% strain (MPa)	Intrinsic viscotiy (dL/g)
PU-M-CL-4K-MDPA-20%	370.8±24.1	15.9±0.8	13.4±0.5	0.72
PU-M-CL-4K-HDA-20%	351.4±9.1	14.8±0.6	13.6±0.5	0.62
PU-M-CL-4K-BDA-20%	256.0±18.3	12.4±0.5	11.1±0.3	0.61
PU-M-CL-4K-EDA-20%	349.3±14.0	16.1±0.9	13.8±0.2	0.63

The mechanical properties of PCLUUs were not affected by the chain extenders as much as recovery stress discussed later. The tensile modulus was between 250 MPa to 370 MPa, and the tensile strength at 200% strain was ~13 MPa. The mechanical properties were measured at standard room temperature, which is below the transition temperature of SMPUUs (~40°C). In this case, the bidentate hydrogen bonding between urea linkages was not the only factor that affected the mechanical properties. Other parameters such as molecular weight and soft segment also influenced them.

Shape memory properties

Figures 3.5 - 3.8 show the cyclic stress-strain behavior of SMPUUs with different aliphatic chain extenders:

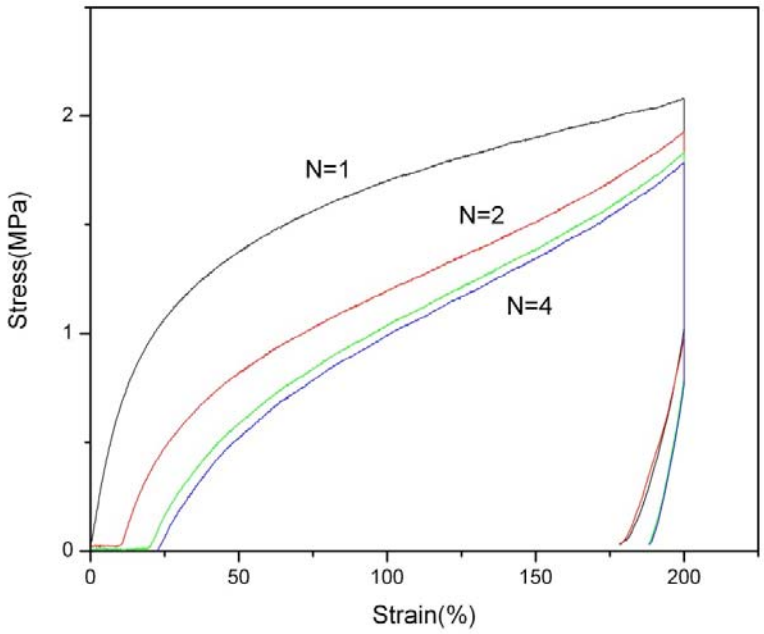

Figure 3.5. Cyclic tensile behavior of PU-M-CL-4K-MDPA-20%

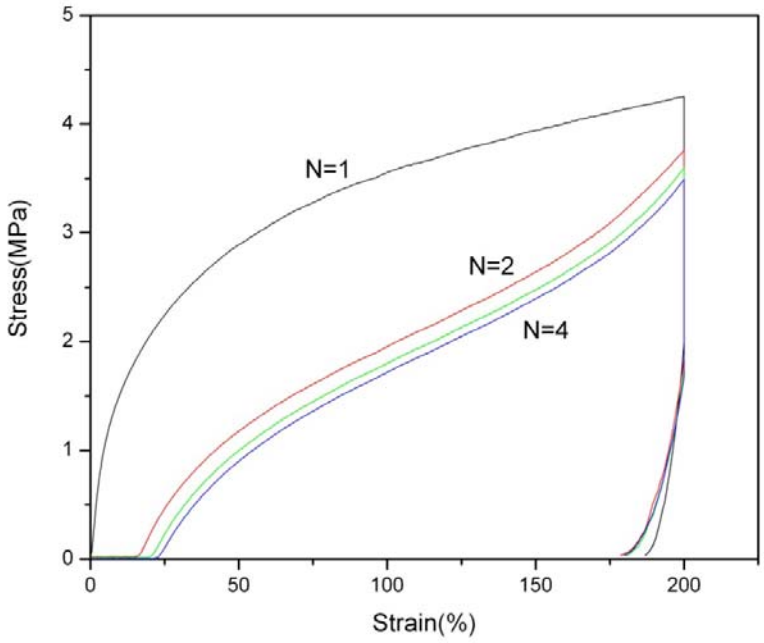

Figure 3.6. Cyclic tensile behavior of PU-M-CL-4K-HDA-20%

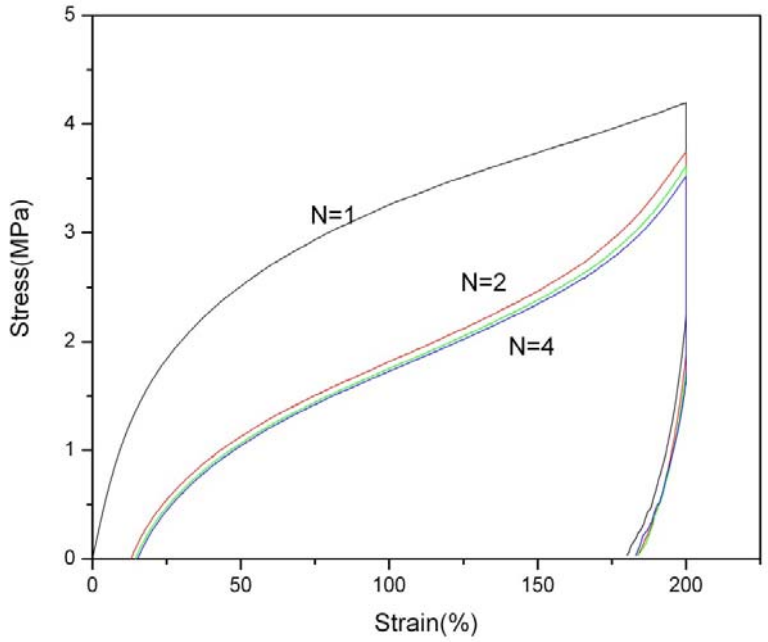

Figure 3.7. Cyclic tensile behavior of PU-M-CL-4K-BDA-20%

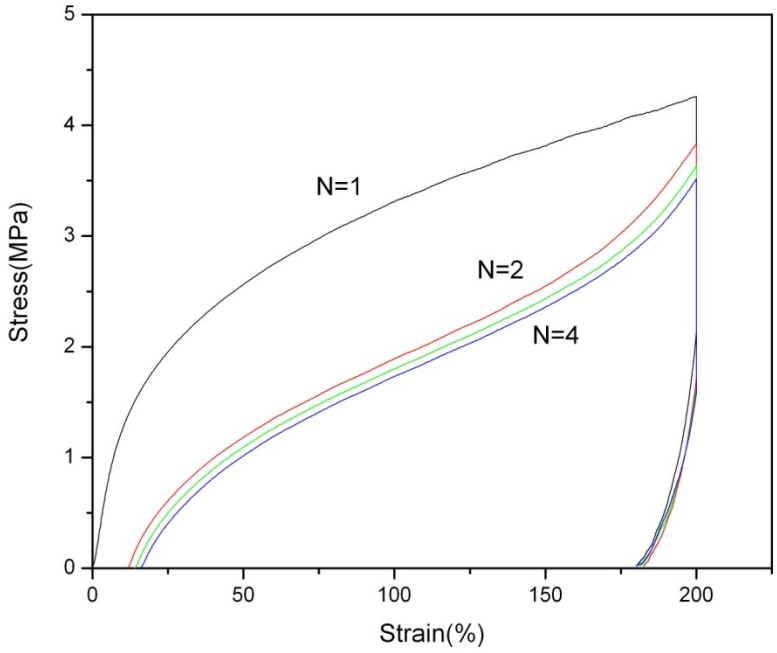

Figure 3.8. Cyclic tensile behavior of PU-M-CL-4K-EDA-20%

For linear aliphatic chain extenders such as EDA, BDA and HDA, no significant difference existed for the polymers' shape memory properties. The recovery stresses were around 4.3 MPa. However, for a chain extender with a side chain such as MDPA, the recovery stress dropped rapidly from 4.3 MPa to 2.1 MPa due to the hindrance of hydrogen bonding between the urea groups by the bulky methyl group. This result is consistent with the conclusion derived from the DSC data in Table 3.2. Other shape memory properties of these four polymers with different chain extenders such as fixity and recovery rate were quite similar, and thus will not be discussed in detail.

Dynamic mechanical properties

The tensile storage moduli of polymers with different aliphatic chain extenders are shown in Figure 3.9:

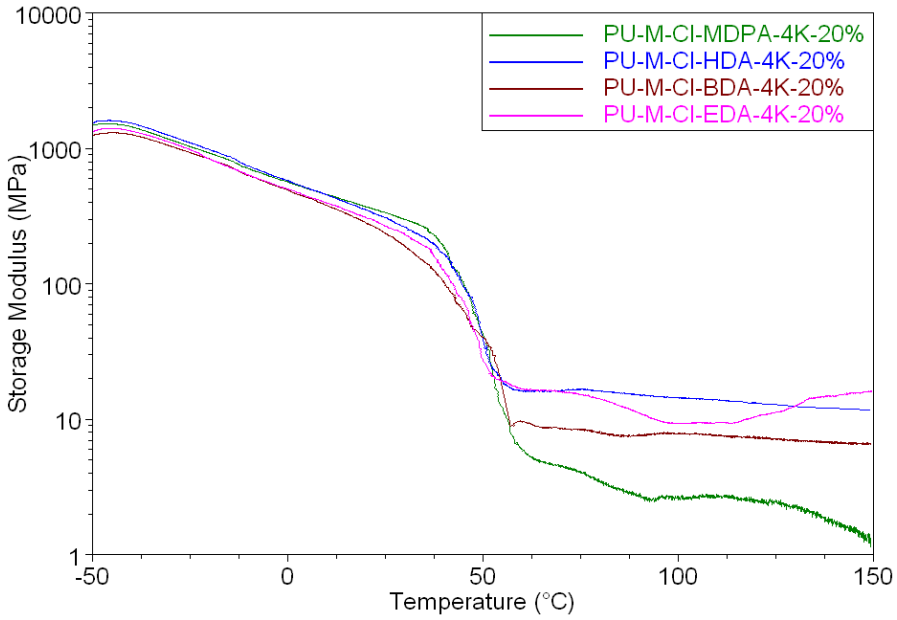

Figure 3.9. Tensile storage modulus of PU-M-CL-4K with different aliphatic chain extenders

The storage moduli slightly decreased below the melting temperature of PCL and a sharp drop was observed near the melting point. The storage moduli were much more stable above the melting point due to the bidentate hydrogen bonding of urea linkage with linear chain extenders which indicated a more constant recovery stress at different temperatures. With MDPA as chain extender, the side chain hindered the formation of the bidentate hydrogen bonding. As a result, the storage modulus decreased above the melting point of the soft segment as the MDI/PCL/BDO[17] and HDI/PCL/DHBP[24] systems.

SMPUU Fiber Spinning

In addition to films, SMPUU fibers were also spun in this study to verify the spinnability of SMPUU solution. Spandex® fibers can be produced in four different ways: melt extrusion, reaction spinning, solution dry spinning and solution wet spinning. All of these methods include the initial step of reacting monomers to produce a prepolymer. The formed prepolymer was then reacted further in various ways and spun into the fibers. All of these processes are the same in the synthesis of SMPUUs. For Spandex, the solution dry spinning method is used to produce over 94.5% of the world supply.[65] Because of the equipment limitation, only wet spinning was used in the research to test spinnability (Figure 3.10).

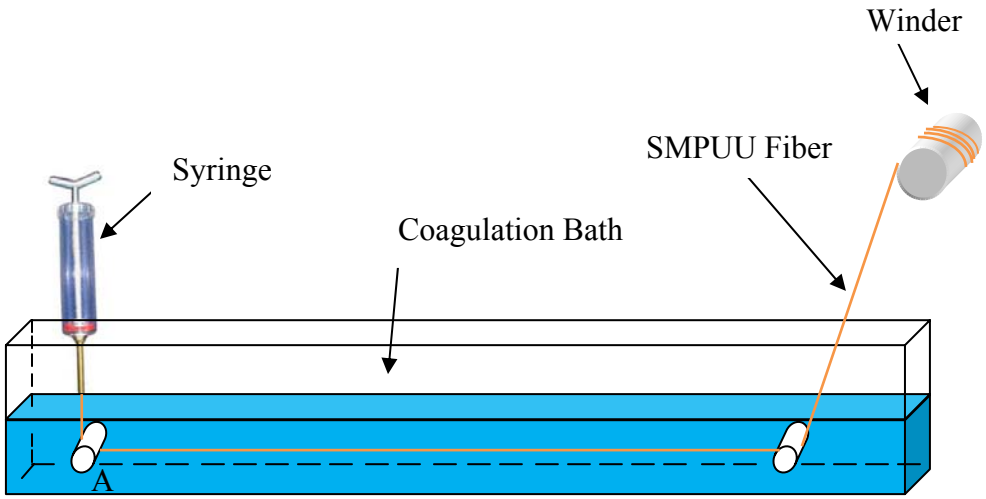

Figure 3.10. Schematic of Wet Spinning Line

The SMPUU fiber (PU-M-CL-4K-EDA-12%) was wet spun in tape water. The PU-M-CL-4K-EDA-12% solution was transferred into the barrel (with 16 mm internal diameter). The solution was extruded through a spinneret with an 18 G needle. Water was used as the coagulation bath at room temperature. The continuous fiber spinning was achieved by optimizing polymer extrusion rate through the spinneret and fiber take-up speeds. The fibers were dried in a vacuum oven at 50˚C for 7 days. The holding rod A in Figure 3.10 was removed during the wet spinning because of the good adhesive properties of the SMPUU solution; otherwise, the spun fibers stuck to the holding rod. Dry-jet wet spinning was also attempted but continuous fibers could not be produced.

Figure 3.11. SMPUU fibers produced by wet spinning

As shown in Figure 3.11, SMPUU continuous fibers produced by the wet spinning process demonstrated the spinnablity of SMPUU solution. The morphology and fiber geometry of SMPUU fibers were examined under a field emission scanning electron microscope (SEM) (LEO 1530 SEM). Samples were coated with gold palladium using EMS 350 sputter coating. SEM images were obtained using a 10 Kv accelerating voltage.

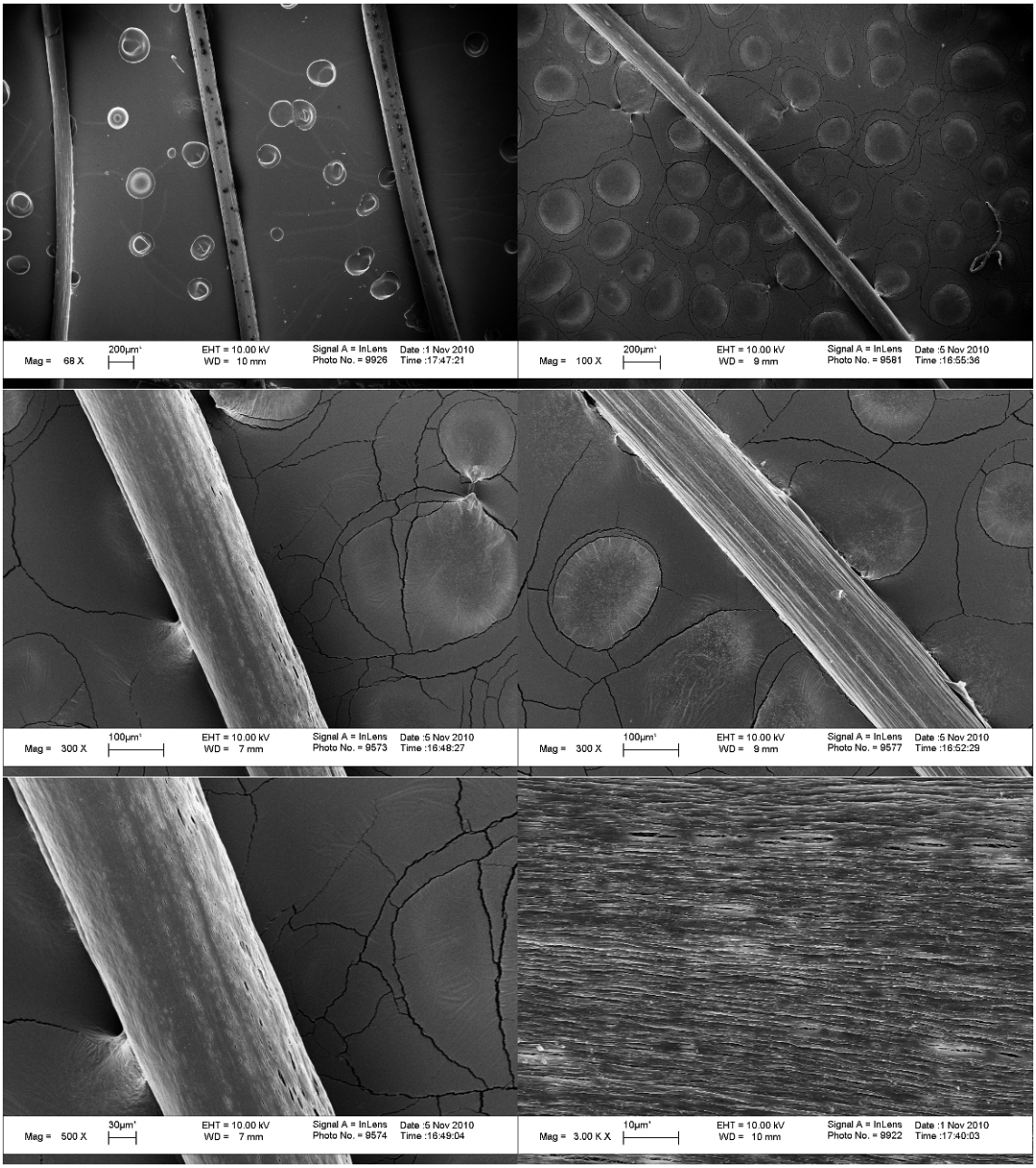

Figure 3.12. SEM images of wet spun SMPUU fibers

Figure 3.12 shows the SEM images of wet spun SMPUU fibers. All of the fibers present elongated voids on the surface. The grooves on the surface of the single filament were ascribed to the traces of the needle/spinneret where the solution was extruded.[66] The voids and defects reduced the mechanical properties of the spun SMPUU fiber

compared to its film and the mechanical properties cannot be measured in Insight 2 with 10 N load cell.

Small angle neutron scattering (SANS)

Although DSC results gave the melting point of the soft segment of SMPUUs which provides information on phase separation, no other important information such as phase morphology exists. Small Angel Neutron Scattering (the low-Q diffractometer) in the Lujan Neutron Scattering Center of Los Alamos National Laboratory was used to investigate the phase separation and phase morphology. Small angle neutron scattering is one of the most powerful tools for examining the conformation of polymer chains in the solid state. Selective labeling of polymer chains with deuterium allows determination of the single-chain dimensions of the deuterated polymer in a hydrogenous polymer matrix. This technique has been used successfully to characterize the chain dimensions of polyurethane[67] and polyurethane ionomers.[68, 69]

The low-Q diffractometer of the Lujan Neutron Scattering Center, LQD, is designed to study large-scale structures with dimensions from 10 Å to 1000 Å (1 nm – 100 nm). Examples of problems that LQD can help solve include phase separation, phase morphology and critical phenomena in hard and soft matter and in magnetic structures, colloid and polymer structures, biomolecular organization and bubble formation in metals. LQD accesses a broad range of Q (0.003 to 0.5 $Å^{-1}$) in a single measurement by using the time-of-flight (TOF) technique without any changes to the instrument's physical configuration. The relationship between the incident radiation wavelength, λ, the scattering angle, 2θ, and Q, given as $Q = (4\pi/\lambda) \sin\theta$. LQD uses an intense source of

long-wavelength ("cold") neutrons over a range from 2 to 15 Å. Figure 3.13 shows an overhead plan view of the SANS instrument:

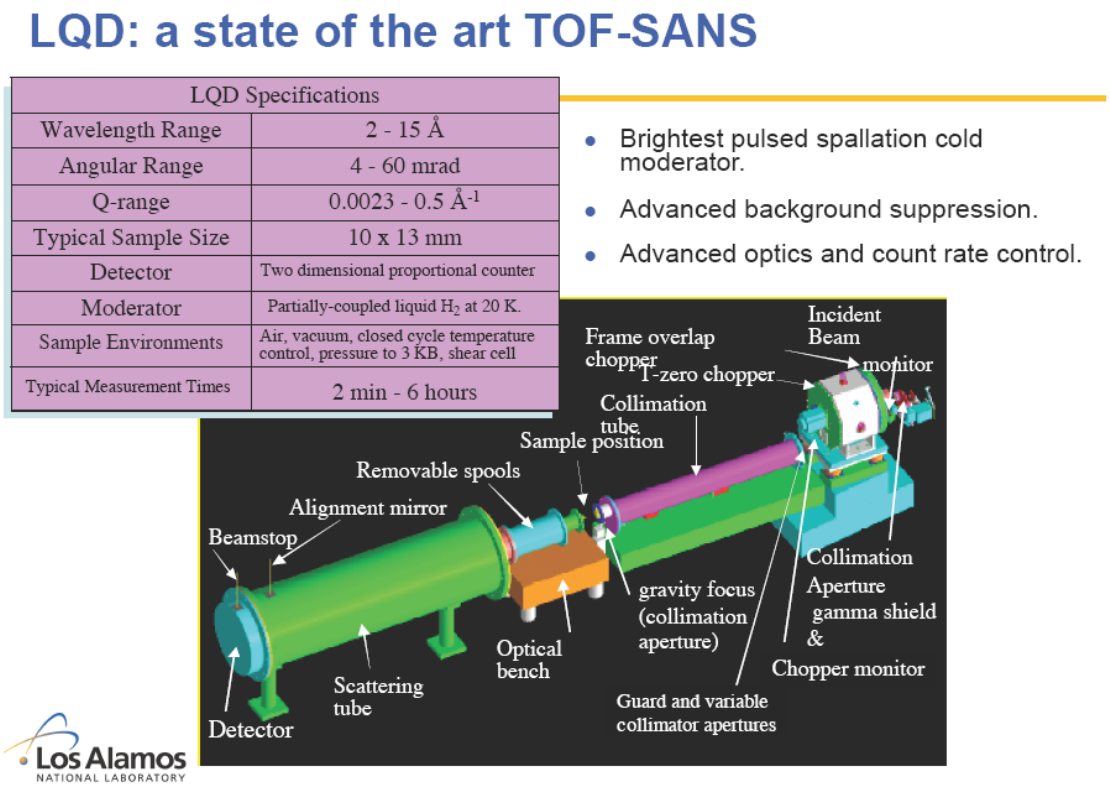

Figure 3.13. SANS instrument (LQD) at Los Alamos National Laboratory

The distance from source to detector is 12.72 m. LQD "looks" at a liquid hydrogen moderator that provides cold neutrons. Cold (=slow) neutrons have long wavelengths, and thus provide better spatial resolution for scattering applications where long length scales are probed. The liquid hydrogen moderator at the Lujan Center operates at ~ 20 K and ~ 220 psi pressure. The resulting spectrum is a Maxwellian distribution which has its maximum at 3.5 meV (40K). The cold neutron pulses are shaped by two choppers: the T-zero Chopper defines the start of the neutron pulse and cuts off most of the gamma rays and hot neutrons, the Frame Overlap Chopper prevents overlap of neutron pulses by eliminating the long wavelength neutrons. These two

choppers reduce the significant background caused by these neutrons from the previous frame.[70]

Samples used in the SANS measurements were SMPUUs synthesized from deuterated chain extender D-EDA by the prepolymer method. Two film samples with different hard segment contents were used to study the morphology of the hard segments labeled as PU-M-CL-4K-D-EDA-12% and PU-M-CL-4K-D-EDA-20%. Sample sheets were cut into strips with dimensions of approximately 10 mm×35 mm×0.15 mm to cover the incident beam and fit with the sample stretcher (Figure 3.14):

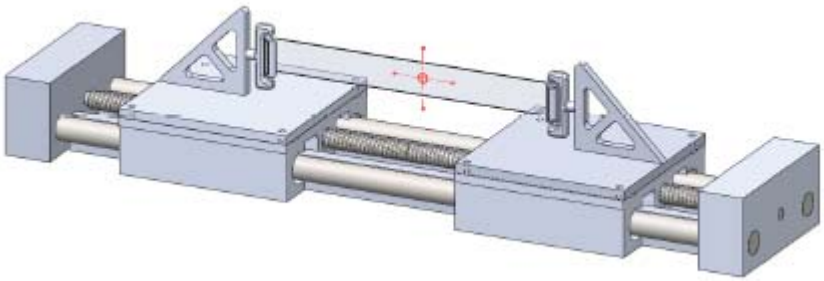

Figure 3.14. SANS sample load frame for polymer tensile response

Neutron scattering patterns were recorded and all the data for coherent scattering contribution was obtained by appropriate subtraction of background and incoherent scattering over whole Q range investigated. Scattered intensity $I(Q)$ of samples was measured as a function of Q. In the case of coherent elastic scattering, no energy transfer results only momentum transfer, as shown in Figure 3.15:

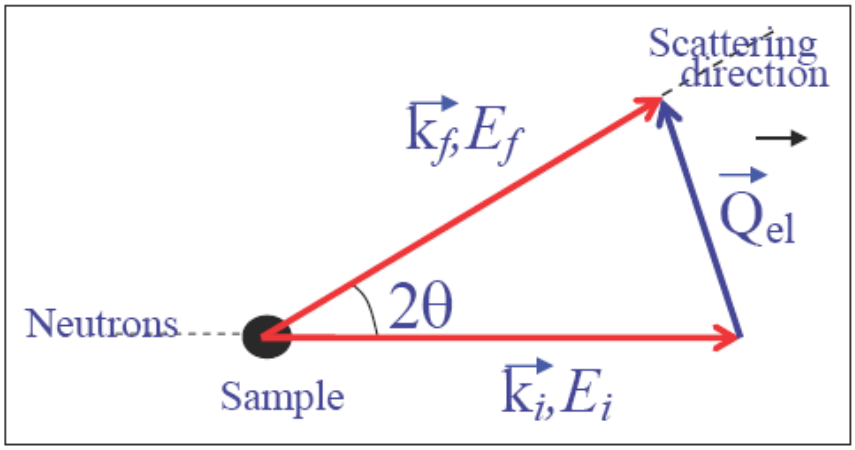

Figure 3.15. Schematic representation of the neutron scattering experiment

The scattering vector Q is defined as the difference between the incident wave vector and the scattered wave vector with a modulus of

$$Q = \frac{4\pi}{\lambda} \sin\theta$$

where λ is the wave length and 2θ is the angle between the incident and scattered wave vectors according to Bragg Equation. Data was analyzed using the Igor macros provided by NIST Center for Neutron Research.[71]

Isointensity patterns for PU-M-CL-4K-D-EDA-20% at four elongation levels (0%, 50%, 100% and 200%) at room temperature are shown in Figure 3.16:

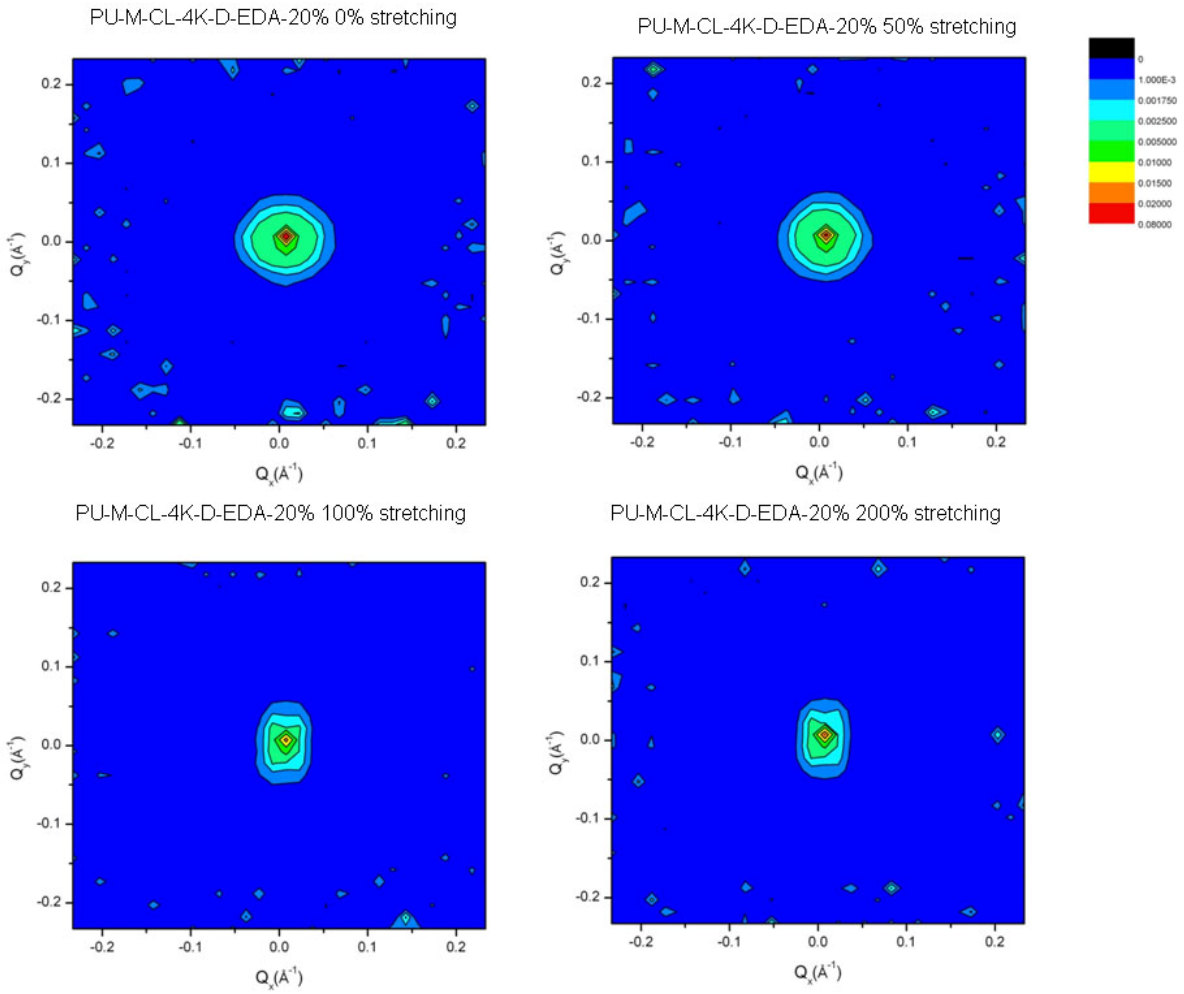

Figure 3.16. Isointensity patterns for PU-M-CL-4K-D-EDA-20% at four elongation levels: 0%, 50%, 100% and 200% at room temperature

The 2D pattern for 0% stretching was almost a circle which indicated isotropy of the sample. With increased stretching, the 2D pattern changed from circle to ellipse since only the chain extender was deuterated, the hard segment was the fixed phase, and the latter should not have moved as rapidly as the soft segment during the stretching. The ellipse 2D pattern at 100% and 200% stretching was observed because the SMPUU sample did not possess a 100% fixity rate, some of the hard segment chain slipped, and the hard segment domains also changed their relative positions during the stretching.

Figure 3.17 shows the isointensity patterns for PU-M-CL-4K-D-EDA-20% at four elongation levels: 0%, 50%, 100% and 200% at 65°C.

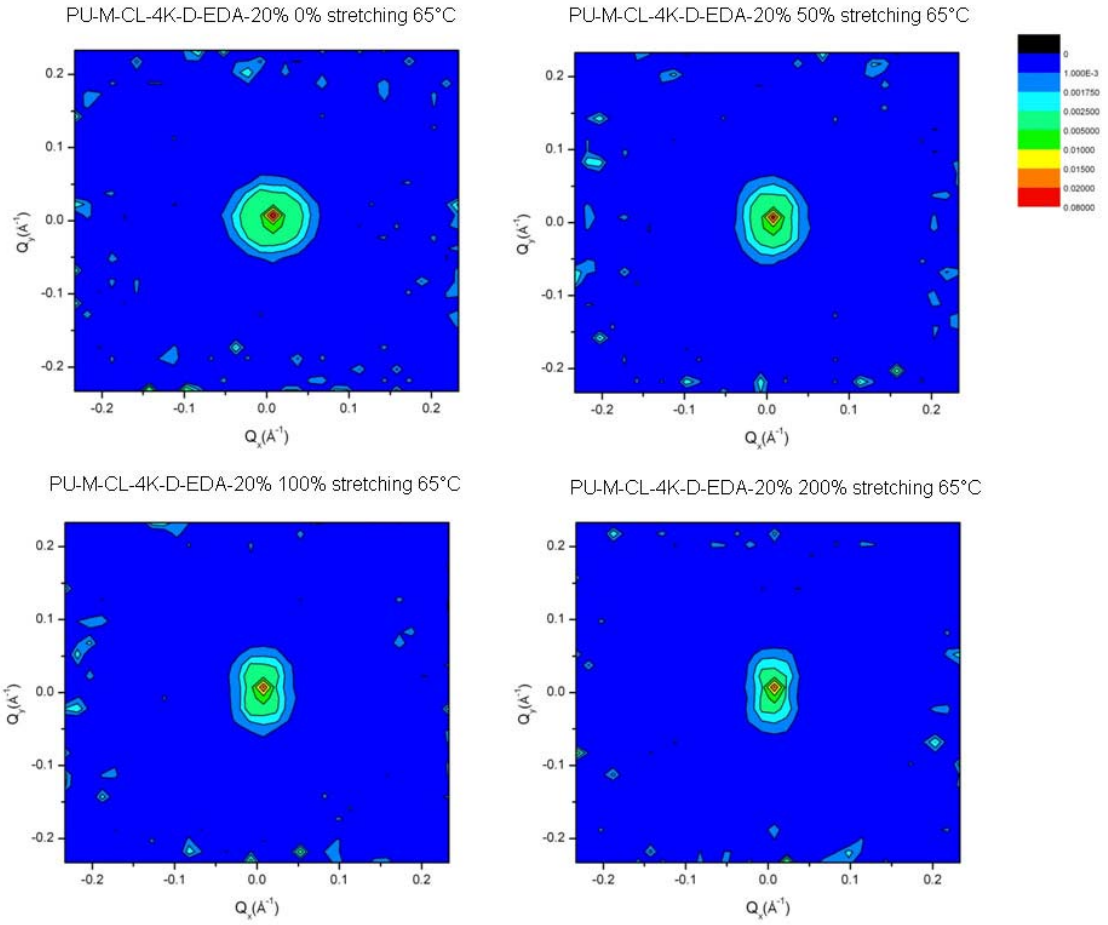

Figure 3.17. Isointensity patterns for PU-M-CL-4K-D-EDA-20% at four elongation levels: 0%, 50%, 100% and 200% at 65°C

The experiment resulted is almost the same patterns as the stretching at room temperature, with the hard segment operating as the fixed phase at both room temperature and 65°C.

For the sample with a low hard segment content PU-M-CL-4K-D-EDA-12%, the SANS 2D patterns are shown in Figures 3.18 and 3.19:

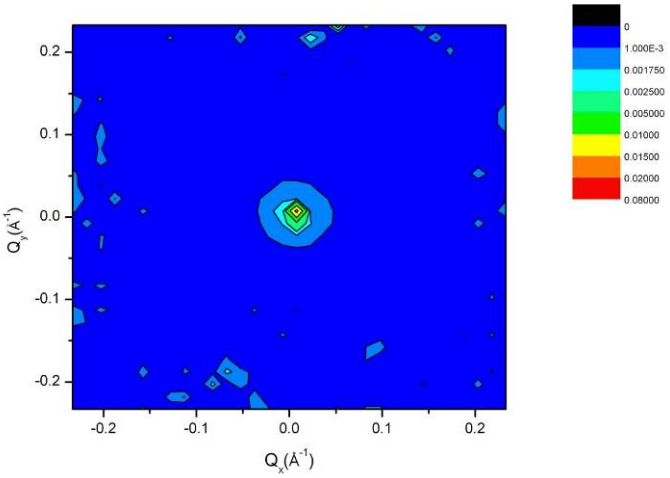

Figure 3.18. Isotropic patterns for PU-M-CL-4K-D-EDA-12% at room temperature

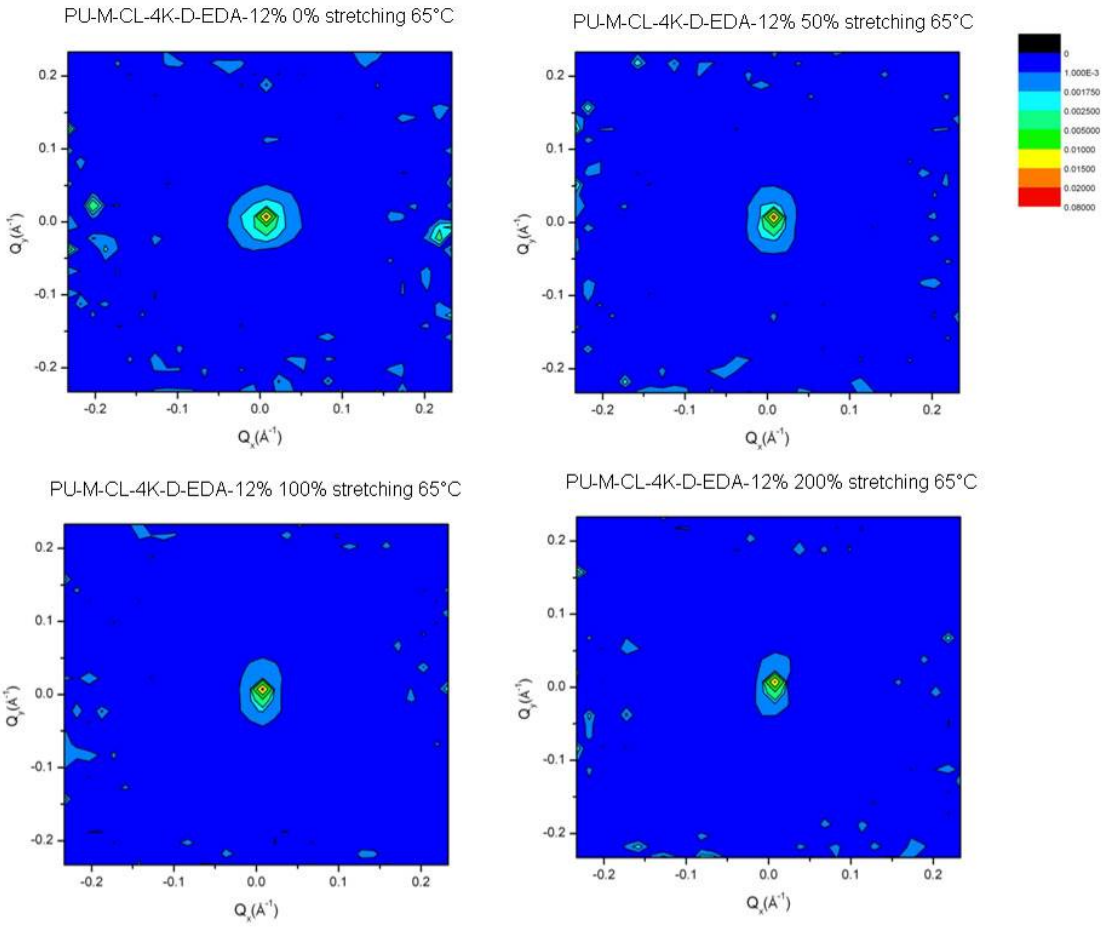

Figure 3.19. Isointensity patterns for PU-M-CL-4K-D-EDA-12% at four elongation levels: 0%, 50%, 100% and 200% at 65°C

The results were quite similar to the sample with higher hard segment (PU-M-CL-4K-D-EDA-20%).

The SANS 2D pattern was reduced to 1D data, which was then used to calculate the dimension of the hard segment by the models of Igor Macros (Figures 3.20 - 3.23):

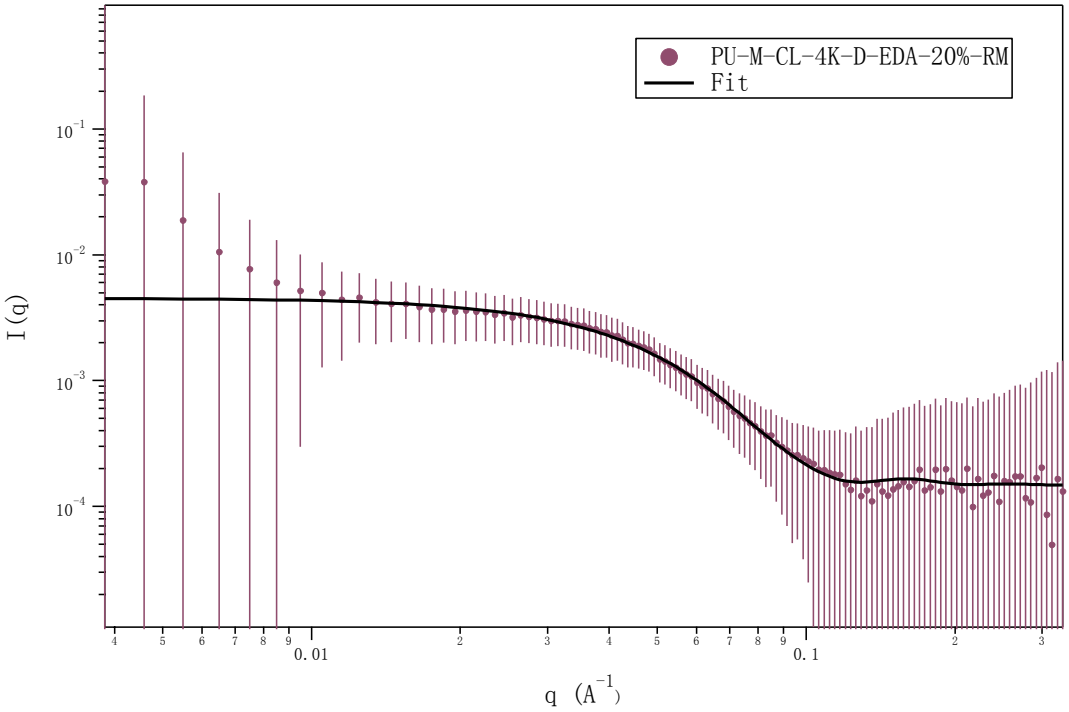

Figure 3.20. Model fit for PU-M-CL-4K-D-EDA-20% at room temperature

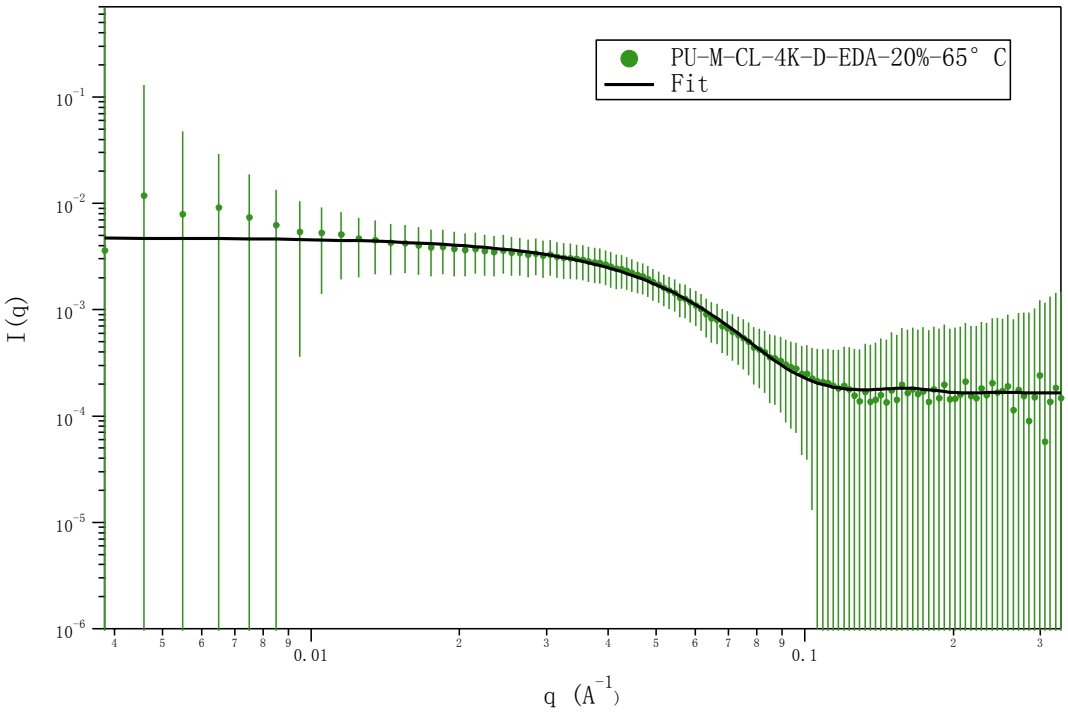

Figure 3.21. Model fit for PU-M-CL-4K-D-EDA-20% at 65°C

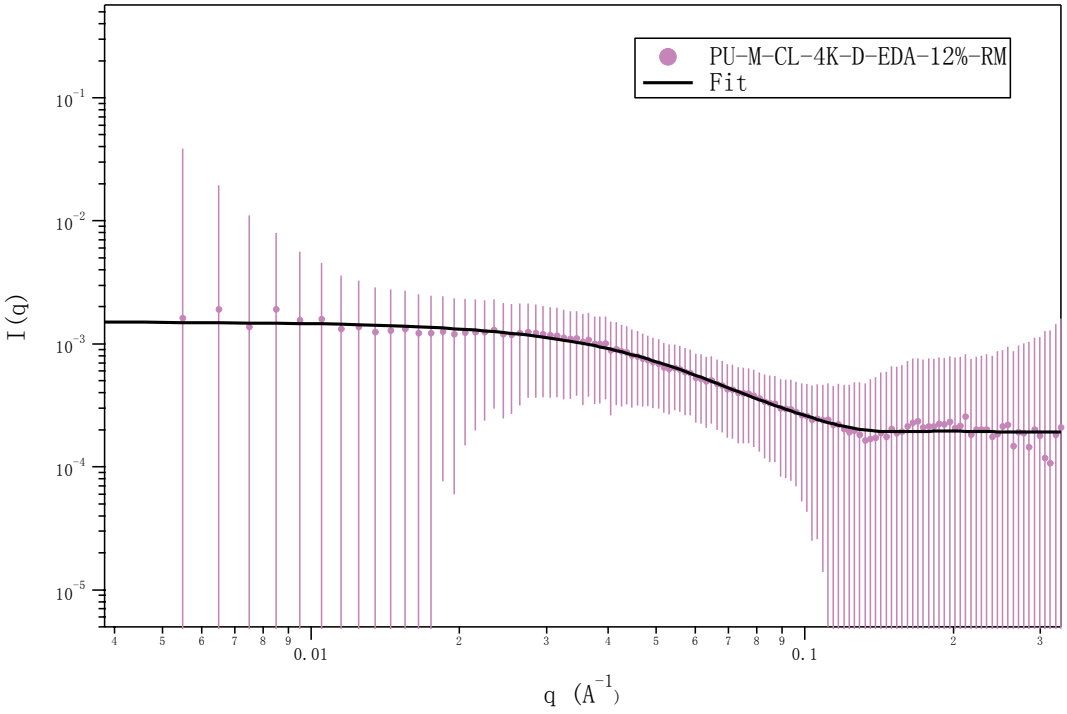

Figure 3.22. Model fit for PU-M-CL-4K-D-EDA-12% at room temperature

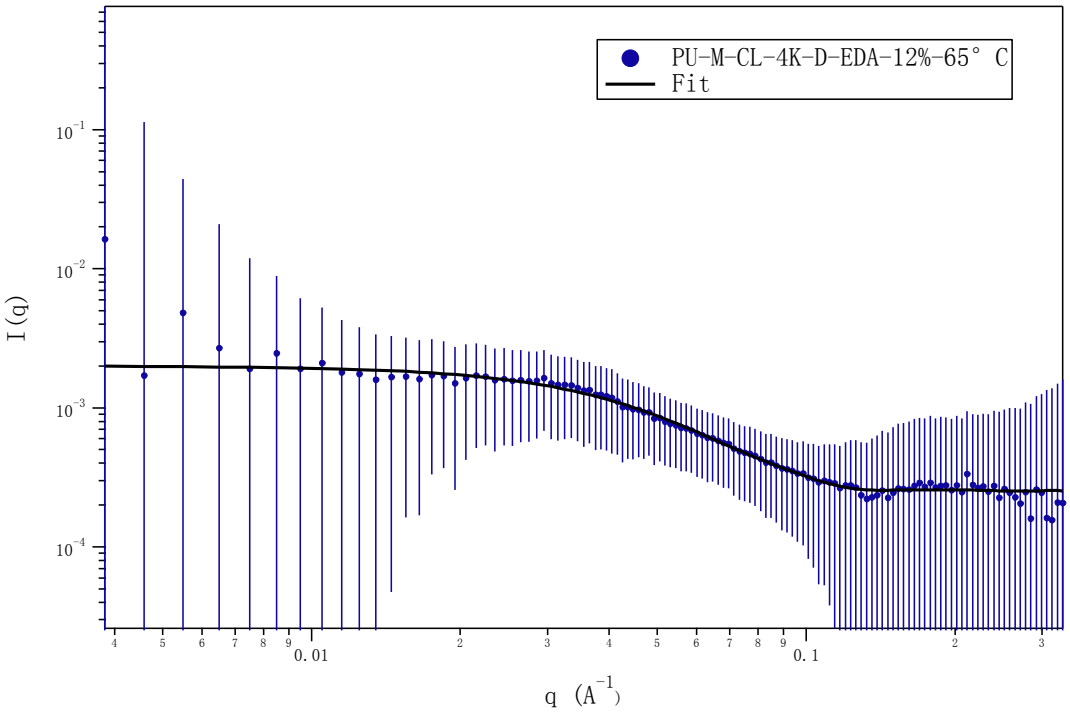

Figure 3.23. Model fit for PU-M-CL-4K-D-EDA-12% at 65°C

In this study, model function Cylinder.ipf, a SANS model developed by the NIST Center for Neutron Research to calculate the form factor for a monodisperse right circular cylinder with uniform scattering length density, was used to study the conformation of SMPUU chains.[71] The monodisperse rigid cylinder model fit the data quite well. Some deviation in the low Q region existed, and has arisen from inhomogeneities of the samples. The radius and length of the cylinder form model are listed in Table 3.3:

Table 3.3. Cylinder form model fit for SMPUUs

PCLUU with Hard Segment (wt %)	Test temperature	Radius(Å)	Length(Å)
PU-M-CL-4K-D-EDA-20%	RM[a]	32.3	99.6
	65°C	32.9	92.8
PU-M-CL-4K-D-EDA-12%	RM	25.5	100.0
	65°C	27.0	107.1

a: Room temperature.

The radius and length of cylinder did not depend on the temperature for both of the samples with different hard segment contents, reasonable because the deuterated chain extender was in the hard segment and did not change with the rising of temperature. The radius of the cylinder increased with increasing hard segment content. The SANS results revealed phase separation of hard and soft segments into nano scale domains.

CHAPTER 4

SHAPE MEMORY POLYURETHANE-UREAS WITH AROMATIC DIAMINE 4, 4'-METHYLENEDIANILINE AS CHAIN EXTENDER

To improve the recovery stress, many efforts have been made to increase the stiffness or elastic modulus of SMPs. Several methods such as increasing cross linking density[72], incorporating fillers[73, 74], and providing mesomorphic units[20, 24, 75] or ionic groups[25, 76] to SMPs have been investigated in the literature. For linear thermoplastic SMPs, incorporating mesomorphic units such as 4'4-Bis (2-hydroxyethoxy) biphenyl (BEBP) or 4'4-Bis (2-hydroxyhexoxy) biphenyl (BHBP) into the main chain is an effective way to improve the recovery stress comparing to traditional chain extenders such as Butanediol (BDO). With the same molecular weight and content of PCL soft segment, the MDI/PCL/BEBP system was able to improve the recovery stress from 2 MPa of the MDI/PCL/BDO to 3 MPa at 100% strain[20] which proved the effect of chain extender. The big disadvantage of mesomorphic units may be the higher cost and toxicity compared to aliphatic diols.[77] In the delineated research, aliphatic diamines were used as chain extenders to improve the recovery stress successfully because of the bidentate hydrogen bonding of urea linkage. In this chapter, aromatic Diamine-4, 4'-methylenedianiline (MDA) was incorporated into the main chain to increase the stiffness of SMPUUs. MDA is commercial available and wide used in industry as a hardener for making polyurethane foams, coating materials, epoxy resins, dyes, etc.

4.1. Synthesis of SMPUUs with MDA as chain extender

SMPUUs with 4, 4'-Methylenedianiline as chain extenders were synthesized with the prepolymer method described in the previous chapter. All flasks and utensils were thoroughly desiccated before use under high temperature (100°C) and N_2 purging. PCL diol having molecular weight of 8000 (Perstorp, CAPA2803) was dried under vacuum at 80°C for 12 hours before use. MDI (Alfa Aesar, 98%) was melted at 45°C and the supernatant liquid without MDI dimer or impurities was used to synthesize the polyurethane-ureas. N, N-Dimethylacetamide (DMAc, Sigma-Aldrich) was dried and distilled over calcium hydride (CaH_2, Sigma-Aldrich) at reduced pressure. 4, 4'-Methylenedianiline (MDA, Alfa Aesar,97%) was recrystallized in benzene twice, and Lithium chloride (LiCl, Alfa Aesar,98%) were used as received.

In a typical synthesis, PCLUUs were prepared by the prepolymer method: predetermined amounts of PCL with molecular weight of 8000 and MDI were added to a 250 mL round-bottom, three-necked separable flask under a nitrogen environment. The reactant mixture was then mechanically stirred at 90°C for three hours to prepare a prepolymer with terminal isocyanate groups. The prepolymer was then dissolved in dry DMAc and reacted with MDA for another three hours. The final polymer concentration was ~ 20 wt% and the molar ratio of MDI/ (PCL+MDA) was kept at 1.05 to yield a linear polymer. The polymer solution was poured onto a glass plate and dried at 80°C for 24 hours to prepare the test film. All samples were labeled according to the following method: "PU-M-CL-8K-MDA-20%", which indicated that the polyurethane-urea was prepared by using PCL with a molecular weight of 8000 as the soft segment and MDI/MDA of 20 wt% as the hard segment.

As shown in Figure 4.1, numbers of aromatic diamines are available on the market such as 4. 4'-Diaminodiphenyl sulfone (DDS), 4, 4'-Dianimodiphenyl ether (ODA), 4, 4'-Diaminodiphenylmethane (MDA) and 4, 4'-Diaminobiphenyl:

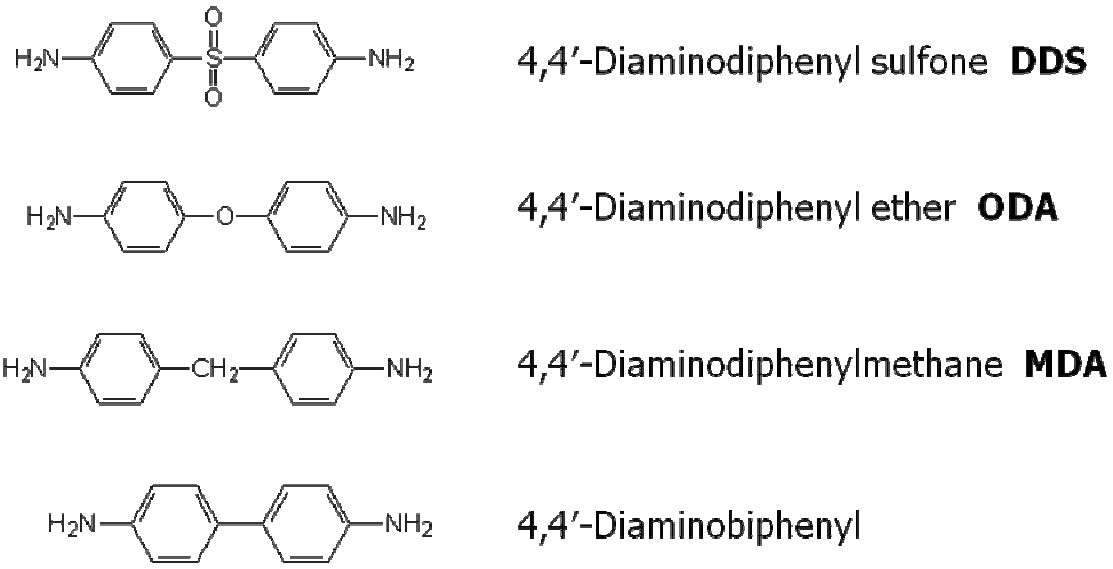

Figure 4.1. Aromatic diamines that can be used as chain extenders

Aromatic diamines usually have much lower reactivity compared to aliphatic diamines when reacted with diisocyanates.[54] From our experiment, SMPUUs with DDS and ODA as chain extenders did not have high enough molecular weight and exhibited poor mechanical properties because of the influence of the electron withdrawing group (sulfone and ether group). 4, 4'-Diaminobiphenyl was prospected to be the best candidate for chain extender based the reactivity and the rigidity of the aromatic molecular backbone. The planar structure should also help the hard segment to arrange, which may assist the formation of more bidentate hydrogen bonding of the urea linkage. No study on this system was conducted in this dissertation because of the high cost of 4, 4'-diaminobiphenyl, which inhibited future industrial production.

4.2. Characterization of SMPUUs with MDA as chain extender

4.2.1. Structure verification

Nuclear magnetic resonance (NMR)

The ^{1}H NMR spectra of shape memory PCLUUs with MDA as chain extender are presented in Figure 4.2.

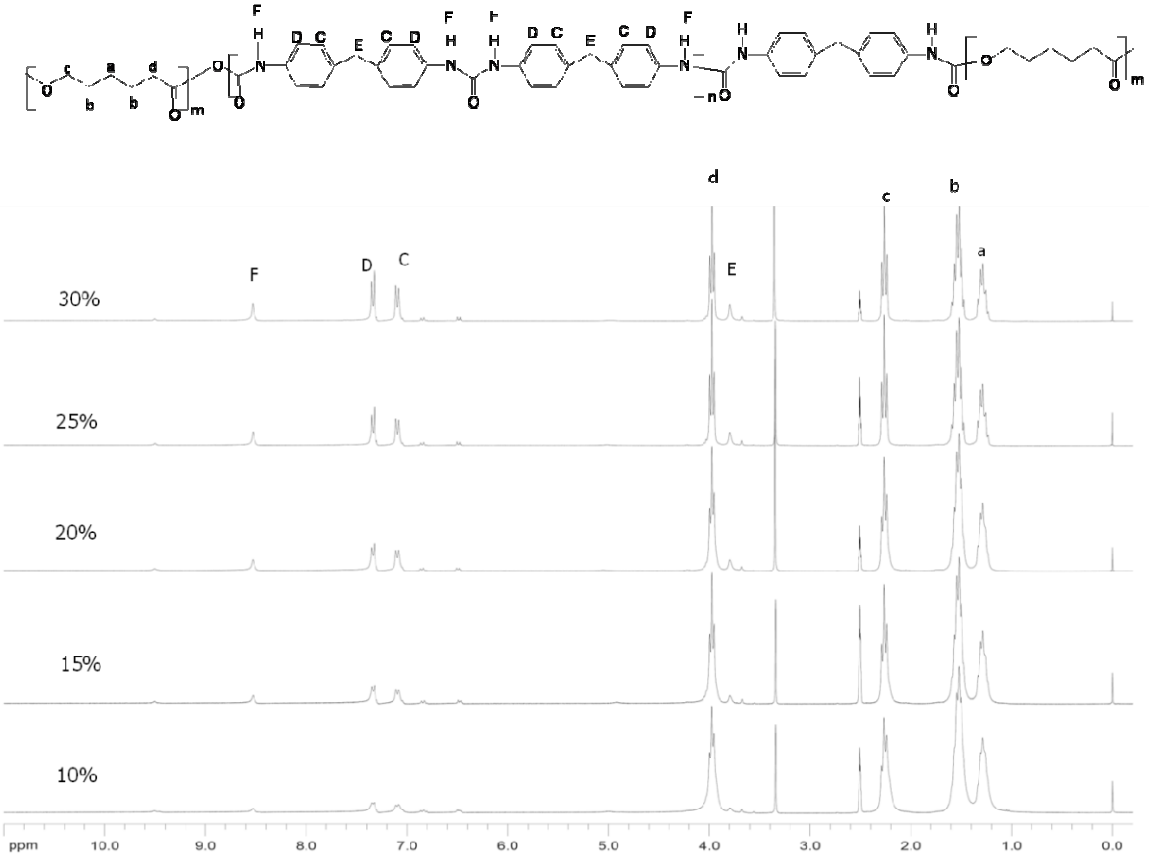

Figure 4.2. ^{1}H NMR spectra of PU-M-CL-8K with MDA as chain extender

The assignments of the NMR chemical shift peaks were: chemical shifts at ~1.3 ppm (a), ~1.5 ppm (b), ~2.2 ppm (c), and ~4.0 ppm (d) were assigned to the protons of soft segment PCL; peaks at ~7.0 ppm (C), ~7.3 ppm (D), and ~3.8 ppm (E) were from the protons of MDI or MDA; peak at ~ 8.6 ppm (F), was attributed to the NH group created by the condensation reaction.

With increasing hard segment (MDI+MDA), the peaks belonging to the protons of MDI and MDA, including C, D, and E, gradually increased in intensity and integral area when normalized to the peak intensity of the soft segment PCL. Small amounts of unreacted MDA were left in the SMPUUs as evidenced by the small peaks appearing at ~6.4 ppm, ~6.8 ppm and ~3.7ppm, reflecting lower reactivity of aromatic diamines compared to aliphatic ones.

Fourier transform infrared spectra (FT-IR)

Typical FT-IR absorption spectra of PCLUUs with different aliphatic chain extenders are presented in Figure 4.3:

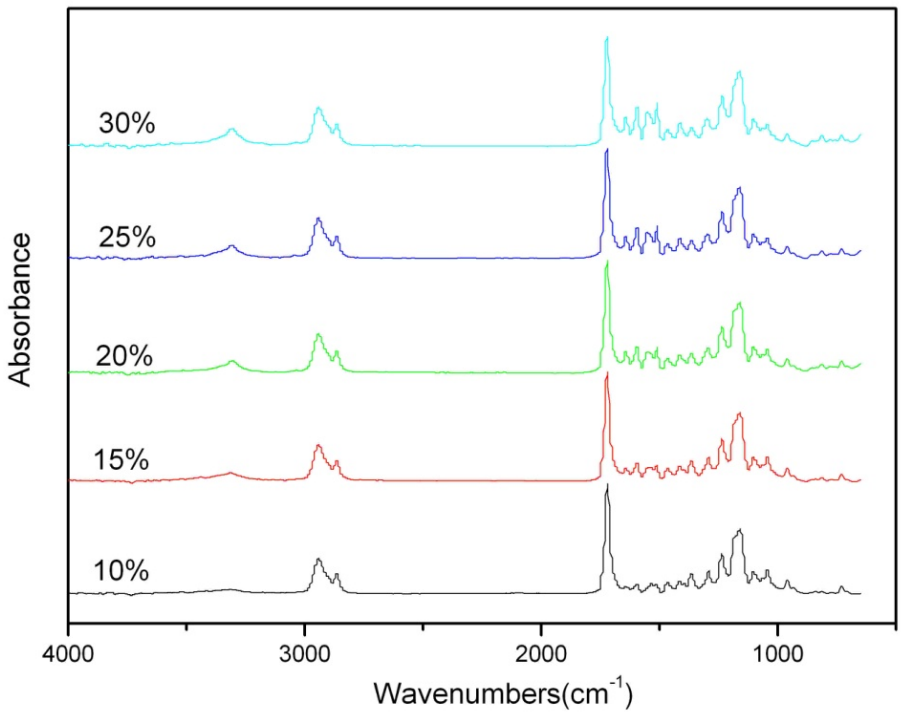

Figure 4.3. FT-IR spectra of PU-M-CL-8K with MDA as chain extender

No significant differences were observed in these spectra and the assignments of the main peaks in the FT-IR spectra were almost the same as in those of Chapter 2 (Table 2.1). The peak intensity around 3320 cm^{-1} for the bonded NH stretching increased with more hard segment content when normalized to the peak intensity of the carbonyl group at 1724 cm^{-1}, which indicated more hydrogen bonding was involved.[55] Based on the above analysis, the structures of the synthesized PCLUUs were confirmed as designed.

4.2.2. Properties of SMPUUs with MDA as chain extenders

Thermal properties

The thermal behavior of pure PCL and its copolymers were investigated by DSC. The peak melting temperature and heat of fusion determined directly from DSC thermographs are summarized in Table 4.1:

Table 4.1. DSC Results of PCL diols and SMPUUs with MDA as chain extenders

PCLUU with Hard Segment (wt %)	T_m(°C)	ΔH_m (J/g)	X_c (%)
PCL-8K	55.1	82.4	58.0
PU-M-CL-8K-MDA-10%	51.2	55.5	43.4
PU-M-CL-8K-MDA-15%	49.0	51.8	42.9
PU-M-CL-8K-MDA-20%	47.7	43.8	38.6
PU-M-CL-8K-MDA-25%	46.0	40.2	37.7
PU-M-CL-8K-MDA-30%	45.3	33.7	33.9

The crystallinities of the PCL prepolymer and the PCL phase of PCLUUs were calculated according to the melting peak area of the DSC curves by assuming the perfect PCL

crystal had a melting enthalpy of 142.0 J/g.[56, 57] The crystallization ability of PCL segments in segmented PCLUUs was significantly depressed compared to PCL-8K due to the influence of hard segments. For the PCLUUs with 8000 molecular weight of PCL, the crystallinity of PCL usually decreased with increasing hard segment content, the same result as in Chapter 2 (Page 27). The soft segments were only partially crystallized and all of the PCLUUs exhibited lower T_m than the corresponding PCLs.

Tensile properties

The tensile properties of all PCLUU films with MDA as chain extender are listed in Table 4.2:

Table 4.2. Tensile properties of PCLUUs with MDA as chain extender

PCLUU with Hard segment (Wt %)	Tensile modulus (MPa)	Yield strength (MPa)	Tensile strength at 200% (MPa)	Intrinsic viscotiy (dL/g)
PU-M-CL-8K-MDA-10%	418.3±13.3	20.6±0.8	14.7±0.6	0.54
PU-M-CL-8K-MDA-15%	424.7±6.1	20.6±0.5	16.7±0.5	0.52
PU-M-CL-8K-MDA-20%	489.9±14.7	21.8±0.7	18.1±0.7	0.53
PU-M-CL-8K-MDA-25%	504.6±41.9	21.6±0.8	18.8±0.9	0.55
PU-M-CL-8K-MDA-30%	516.8±52.8	21.6±0.1	18.7±0.4	0.53

Intrinsic viscosities were also measured to evaluate the influence of molecular weight. Because of the lower reactivity of aromatic diamines, the intrinsic viscosities of the samples synthesized were ~ 0.5dL/g, yielding films suitable for tensile and shape memory property tests, while the molecular weight was much lower than the samples

synthesized with aliphatic diamines as chain extenders. The tensile modulus was between 420 MPa to 520 MPa and the tensile stress at 200% strain was between 15 MPa to 18 MPa. The yield stress was around 21 MPa and did not change significantly with different hard segment contents. All of these three physical properties for PCLUUs were higher than those SMPUUs synthesized with aliphatic diamines as chain extender, even though the SMPUUs with MDA as chain extender had low molecular weights, showing the advantage of aromatic diamines over aliphatic diamines in improving the mechanical and recovery stress properties.

Shape memory properties

Figures 4.4 - 4.8 show the cyclic stress-strain behavior of SMPUU:

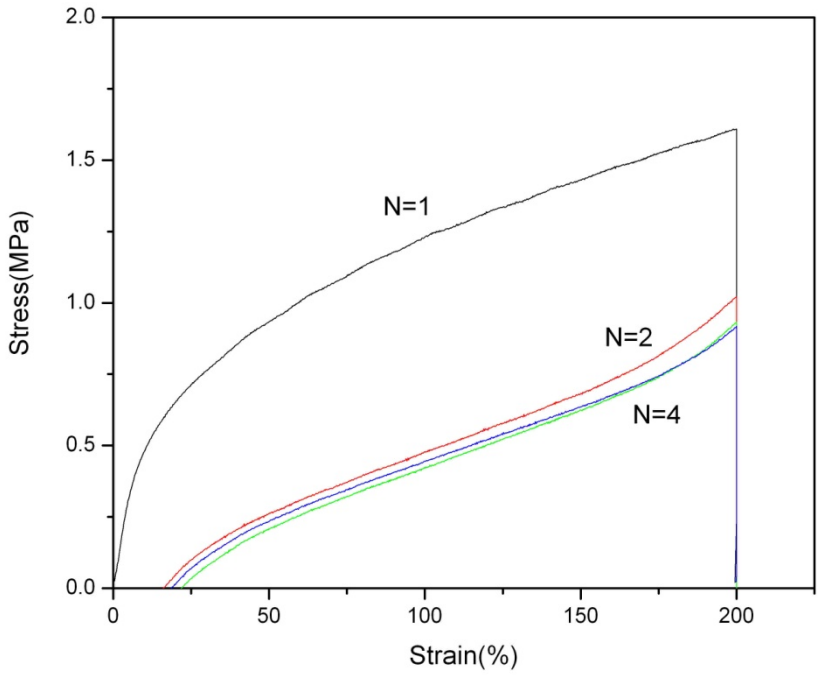

Figure 4.4. Cyclic tensile behavior of PU-M-CL-8K-MDA-10%

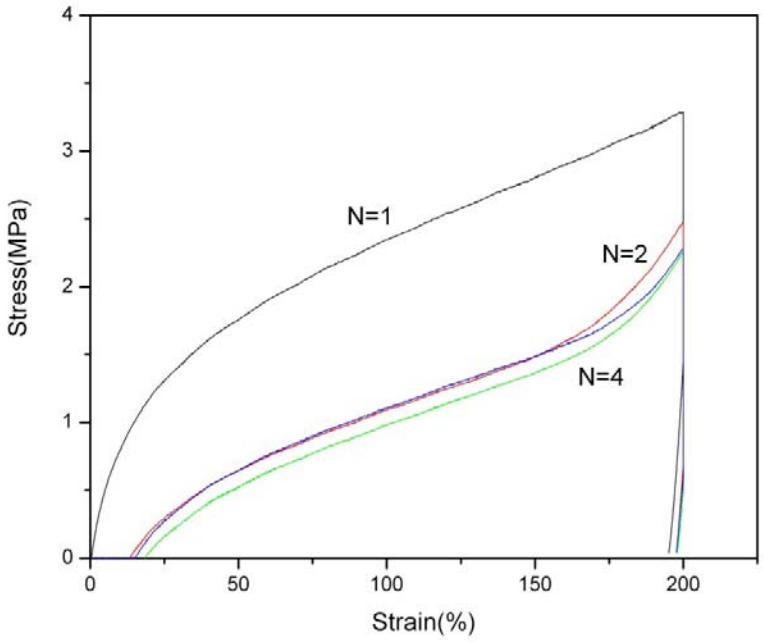

Figure 4.5. Cyclic tensile behavior of PU-M-CL-8K-MDA-15%

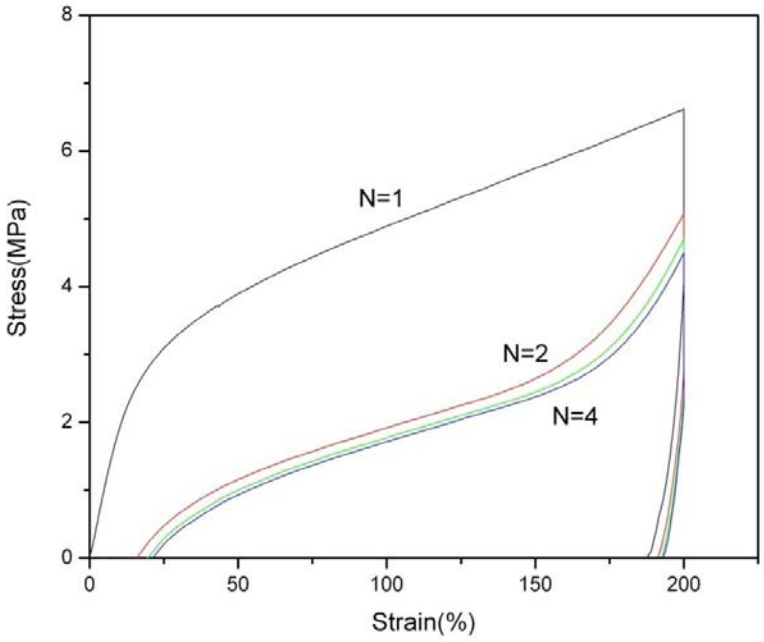

Figure 4.6. Cyclic tensile behavior of PU-M-CL-8K-MDA-20%

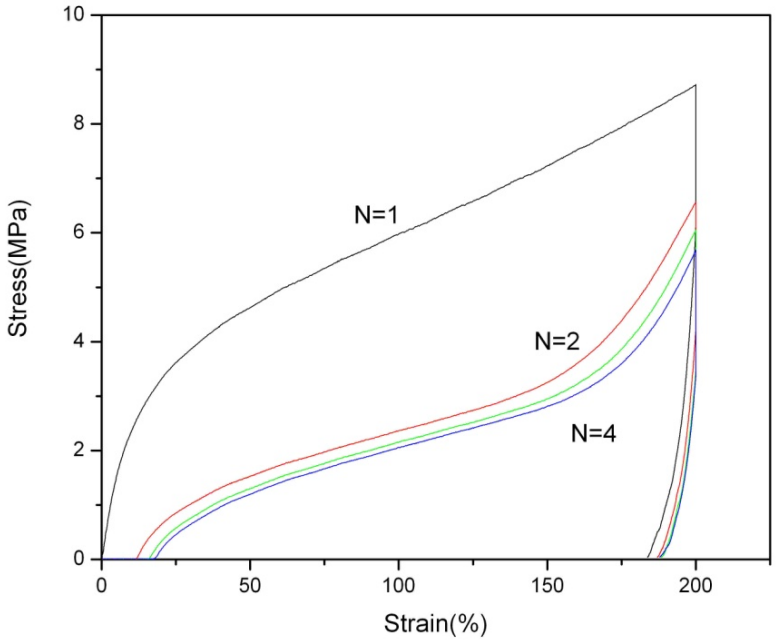

Figure 4.7. Cyclic tensile behavior of PU-M-CL-8K-MDA-25%

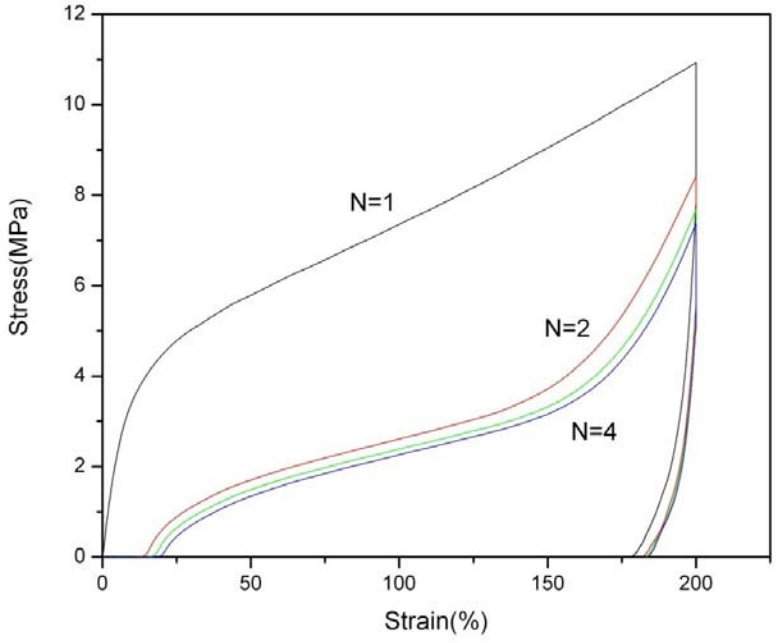

Figure 4.8. Cyclic tensile behavior of PU-M-CL-8K-MDA-30%

The shape recoveries and fixities of MDI/PCL/MDA SMPUUs were similar to the MDI/PCL/BDA copolymer system. Both of the properties for PU-M-CL-8K-MDA-20% were above 90% along with a small deviation which showed excellent shape memory properties after programming.

Figure 4.9 shows the recovery stress influenced by chain extender:

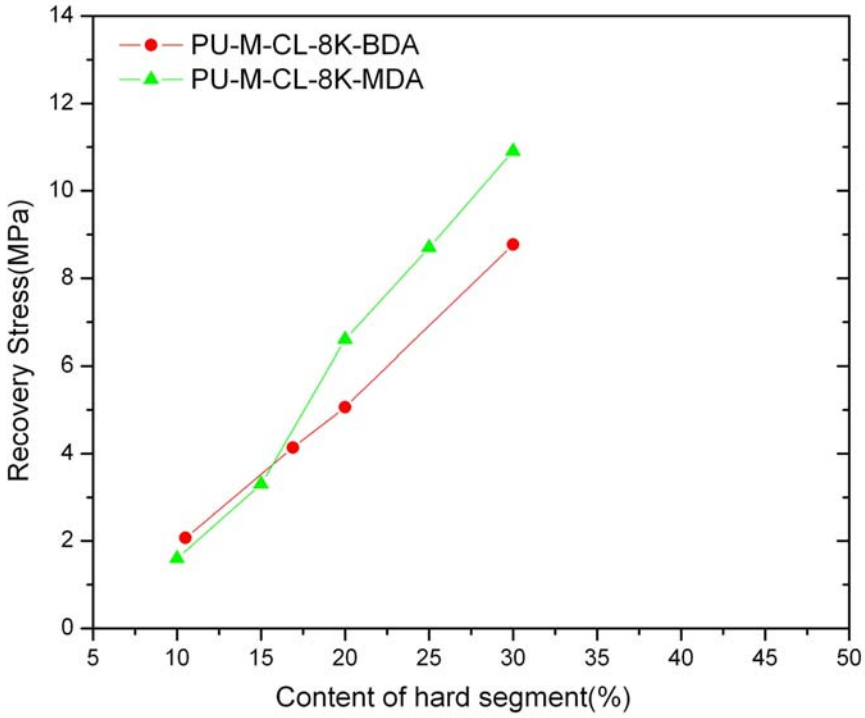

Figure 4.9. Influence of chain extender on the recovery stress

The recovery stresses of MDI/PCL/BDA and MDI/PCL/MDA with the same molecular weight of PCL at 200% strain were compared with different hard segment contents. Below 20% hard segment, the recovery stresses of the MDI/PCL/MDA system were quite similar to MDI/PCL/BDA, because the latter system usually has a much higher molecular weight and the effect of main chain rigidity with the aromatic diamines is

compensated. With the increasing of hard segment, the effect of rigidity of the main chain became more important and the recovery stress increased from 8.8 MPa of PU-M-CL-8K-BDA-30% to 10.9 MPa of PU-M-CL-8K-MDA-30%. With the help of bidentate hydrogen bonding interactions of urea linkages and the increasing of main chain rigidity, the recovery stress successfully increased to 287% comparing to PU-M-CL-8K-BDO-30%.

Figure 4.10 shows the shape recovery process triggered by heat gun:

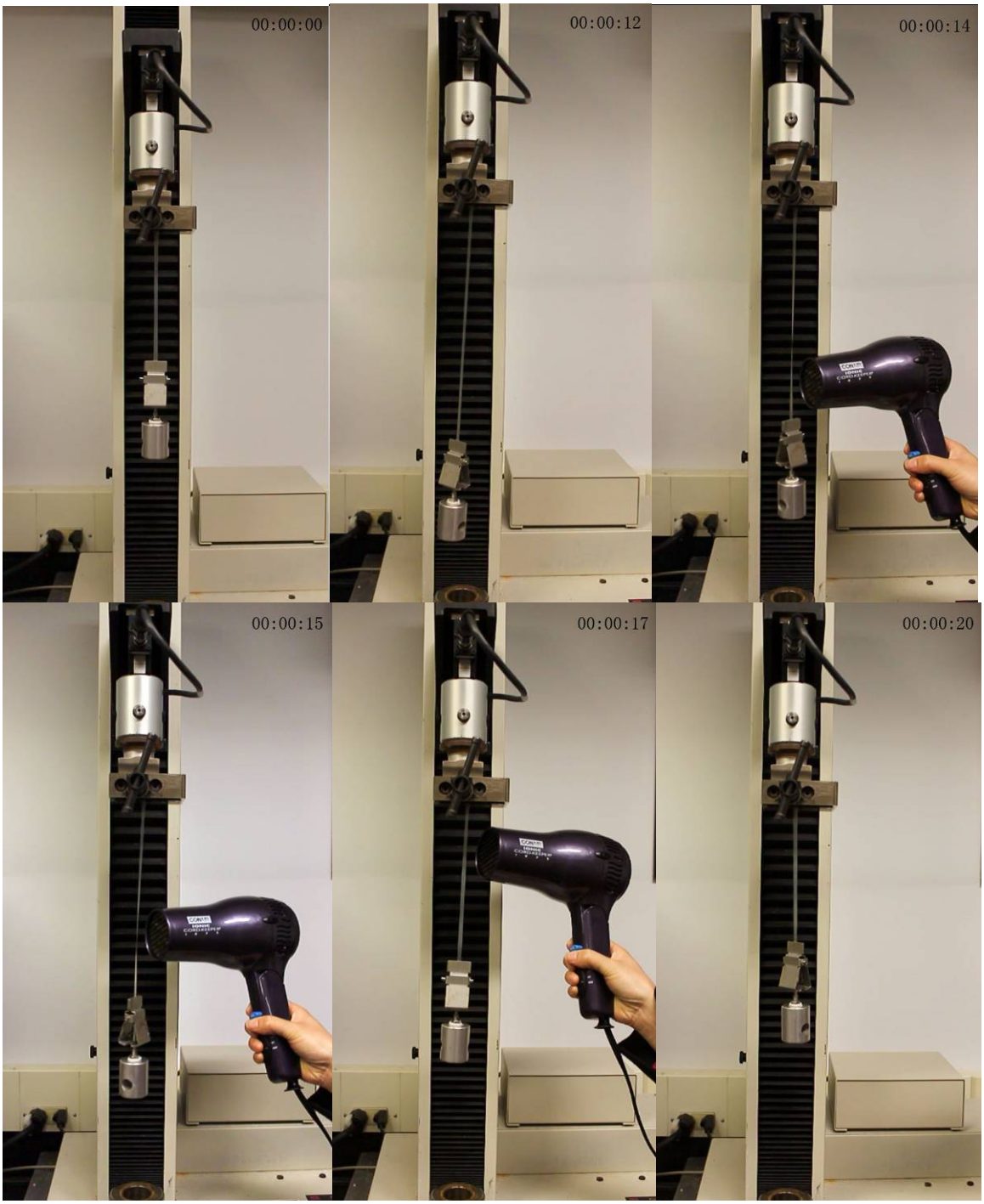

Figure 4.10. Shape recovery with load

The SMPUU (PU-M-CL-8K-MDA-30%) was stretched from the original shape (00:00:00) to temporary shape (00:00:12) at room temperature. Within several seconds of heating with heat gun, the small SMPUU sample (0.11 g) recovered its original shape

with 122.2 g of load. Figure 4.11 also shows the length of the sample with original and temporary shape.

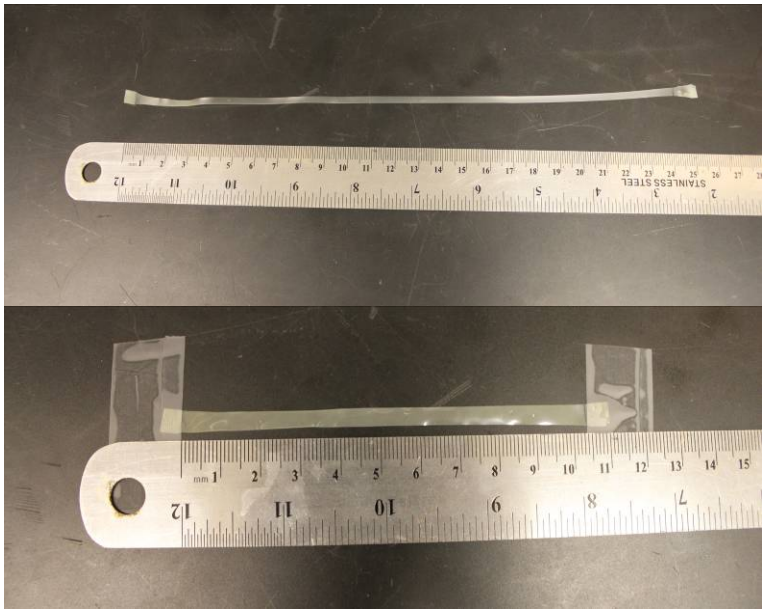

Figure 4.11. The length of the sample with original and temporary shape

Dynamic mechanical properties

The tensile storage modulus of PCLUUs with MDA as chain extender is shown in Figure 4.12:

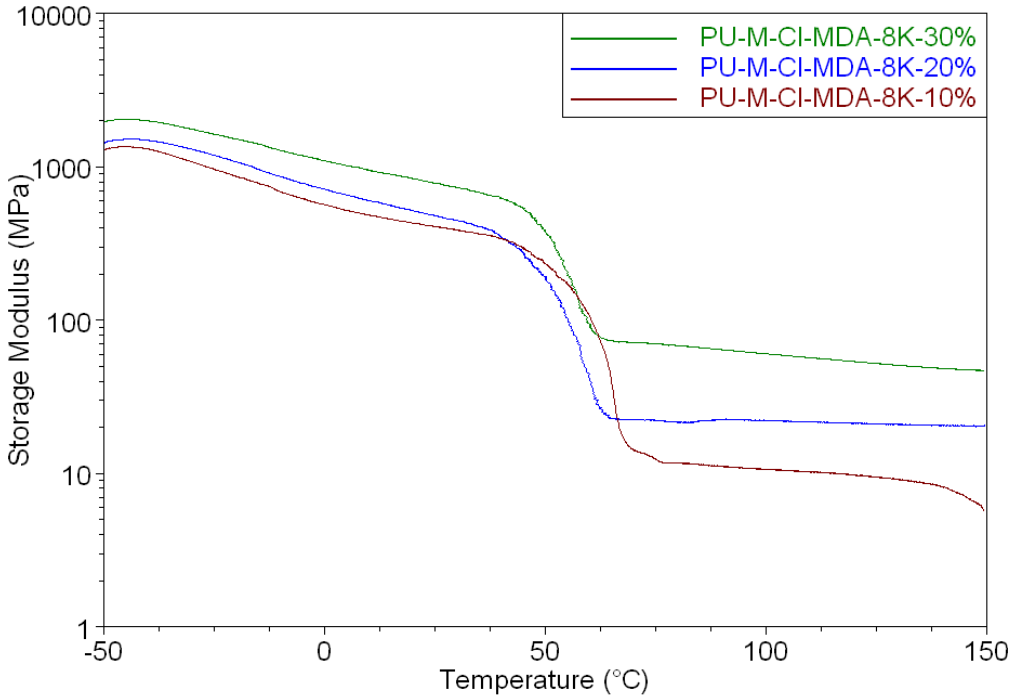

Figure 4.12. Tensile storage modulus of PU-M-CL-8K-MDA with different hard segment contents

The storage modulus slightly decreased below the melting temperature of PCL and a sharp drop was observed near the melting point. The storage modulus was significantly more stable above the melting point due to the bidentate hydrogen bonding of urea linkage which indicated a more constant recovery stress at different temperatures. With the increasing of hard segment, the storage modulus also increased because of the influence of bidentate hydrogen bonding interactions of the urea linkages and the main chain rigidity. For PU-M-CL-8K-MDA-10%, the storage modulus decreased slightly

which indicated not enough bidentate hydrogen bonding was present to maintain the inter molecule interactions, and some of linear molecules slipped with increased temperature.

CHAPTER 5

SHAPE MEMORY POLYURETHANE-UREAS WITH DIFFERENT DIISOCYANATES

The structure of chain extenders has great influence on the properties of SMPUUs, especially the recovery stress. Different diisocyanates were used to investigate the effect of diisocyanates in understanding structure-property relationships and provide an additional method to tailor the SMPUUs to fit different applications.

As shown in Figure 5.1, four different kinds of diisocyanates were used to synthesize SMPUUs:

5.1. Synthesis of SMPUUs with different diisocyanates

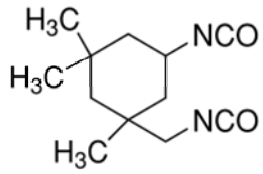

Isophorone diisocyanate IPDI

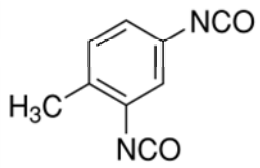

2,4-Diisocyanatotoluene TDI

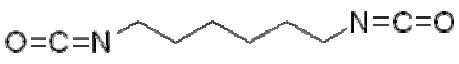

1,6-Diisocyanatohexane HDI

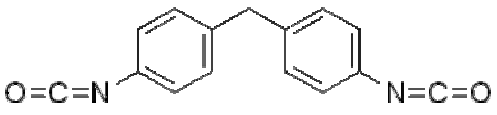

4,4′-Methylenebis(phenyl isocyanate) MDI

Figure 5.1. Different diisocyanates used to synthesize SMPUUs

The structures of the diisocyanates were unique, including two aliphatic diisocyanates (Isophorone diisocyanate (IPDI) and 1, 6-Diisocyanatohexane (HDI)) and two aromatic diisocyanates (2, 4-Diisocyanatotoluene (TDI) and 4, 4′-Methylenebis (phenyl isocyanate) (MDI)). IPDI and TDI also have side chains (methyl groups) which showed the effect of side chain as did MPDA (Chapter 3).

SMPUUs with different diisocyanates were synthesized with the prepolymer method described previously (Chapter 2). All flasks and utensils were thoroughly desiccated before use under high temperature (100°C) and N_2 purging. PCL diol having molecular weight of 8000 (Perstorp, CAPA2803) was dried under vacuum at 80°C for 12 hours before use. MDI (Alfa Aesar, 98%) was melted at 45°C and the supernatant liquid without MDI dimer or impurities was used to synthesize the polyurethane-ureas. N, N-Dimethylacetamide (DMAc, Sigma-Aldrich) was dried and distilled over calcium hydride (CaH_2, Sigma-Aldrich) at reduced pressure. 4, 4'-Methylenedianiline (MDA, Alfa Aesar, 97%) was recrystallized twice in benzene. Other materials such as IPDI (Alfa Aesar, 98%), TDI (TCI America, 95%), HDI (Acros Organics, 99%) and lithium chloride (LiCl, Alfa Aesar, 98%) were used as received.

In a typical case, PCLUUs were prepared by the prepolymer method: predetermined amounts of PCL with molecular weight of 8000 and diisocyanate were added to a 250 mL round-bottom, three-necked separable flask under a nitrogen environment. The reactant mixture was then mechanically stirred at 90°C for three hours to prepare a prepolymer with terminal isocyanate groups. The prepolymer was then dissolved in dry DMAc and reacted with MDA as chain extenders for another three hours. The final polymer concentration was about 20 wt% and the molar ratio of Diisocyanate/

(PCL+MDA) was kept at 1.05 to yield a linear polymer. The polymer solution was poured onto a glass plate and dried at 80°C for 24 hours to prepare the test film. All samples were labeled according to the following method: "PU-IP-CL-8 K-MDA-20%", which indicated the polyurethane-urea was prepared by using PCL with a molecular weight of 8000 as the soft segment and IPDI/MDA of 20 wt% as the hard segment.

5.2. Characterization of SMPUUs synthesized from different diisocyanates

5.2.1. Structure verification

Nuclear magnetic resonance (NMR)

The ^{1}H NMR spectra of shape memory PCLUUs with four different diisocyanates reacted with MDA as chain extender are presented in Figure 5.2:

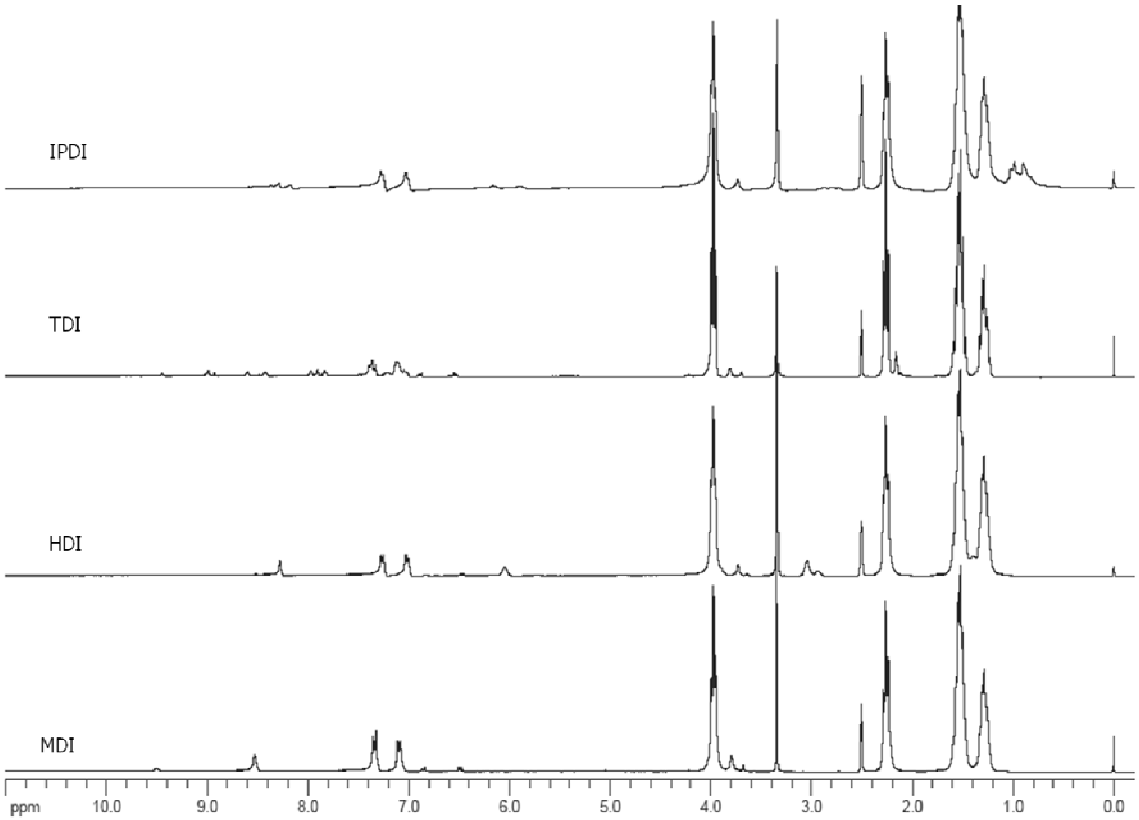

Figure 5.2. ^{1}H NMR spectra of PU-CL-8K-MDA-20% synthesized from different diisocyanates

The assignment of the NMR chemical shift peaks of PU-M-CL-8K-MDA-20% was showed in Chapter 4. Assignments for the rest of the samples were similar. Chemical shifts at ~1.3 ppm, ~1.5 ppm, ~2.2 ppm, and ~4.0 ppm were assigned to the protons of soft segment PCL; peaks at ~7.0 ppm, ~7.3 ppm, and ~3.8 ppm were from the protons of MDA. Because of complicated structure and small amounts of IPDI and TDI, proton peaks from diisocyanates were not identified.

Fourier transform infrared spectra (FT-IR)

Typical FT-IR absorption spectra of SMPUUs synthesized from different diisocyanates are presented in Figure 5.3:

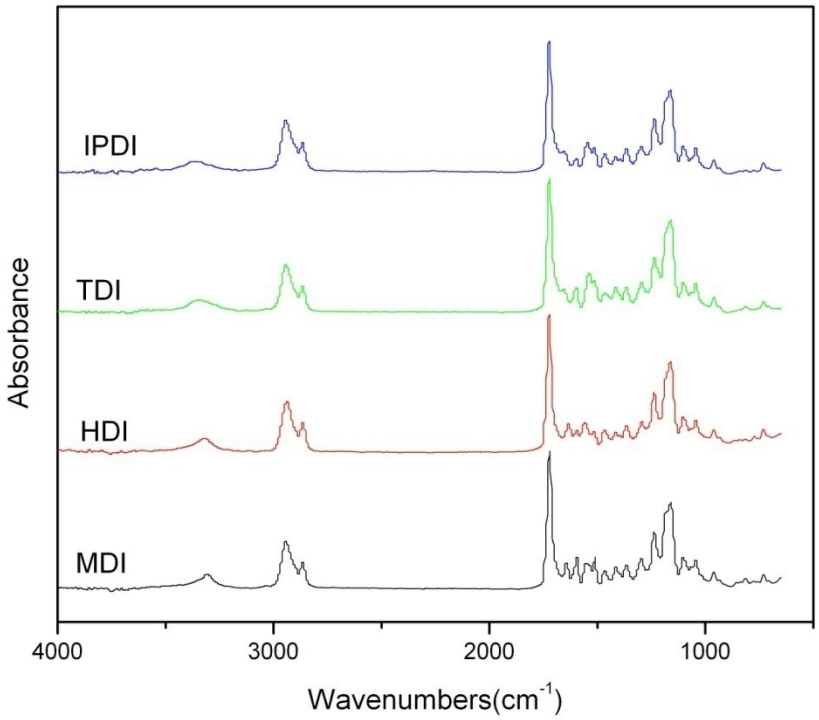

Figure 5.3. FT-IR spectra of PU-CL-8K-MDA-20% synthesized from different diisocyanates

All of these spectra were similar and the assignments of the main peaks in FT-IR spectra were almost the same as in those of Chapter 2 (Table 2.1). With different diisocyanates, the hydrogen bond interactions between urea and carbonyl groups were different which can clearly be seen from the N-H stretching listed in Table 5.1:

Table 5.1. Hydrogen bond interactions from FT-IR spectra

Samples	N-H stretching peak frequency(cm^{-1})
PU-IP-CL-8K-MDA-20%	3359
PU-T-CL-8K-MDA-20%	3336
PU-H-CL-8K-MDA-20%	3322
PU-M-CL-8K-MDA-20%	3305

SMPUUs synthesized from HDI and MDI, the N-H stretching peaks are sharper than the ones from IPDI and TDI whose side chains (methyl groups) interrupted the hydrogen bonding. At the same time, the peaks with weaker hydrogen bond interactions also shifted to higher frequency, but no free N-H stretching was observed around 3400 cm^{-1} indicating that the hydrogen bond interactions were quite strong.[55] Apparently, the rigidity of diisocyanates did not significantly affect the formation of hydrogen bonding. Based on the above analysis, the structures of PCLUUs were confirmed to be as designed and the hydrogen bond interactions were explained by the FT-IR data.

5.2.2. Properties of SMPUUs synthesized from different diisocyanates

Thermal properties

The thermal behavior of pure PCL and its copolymers synthesized from different diisocyanates were investigated using DSC and the results are shown in Figure 5.4:

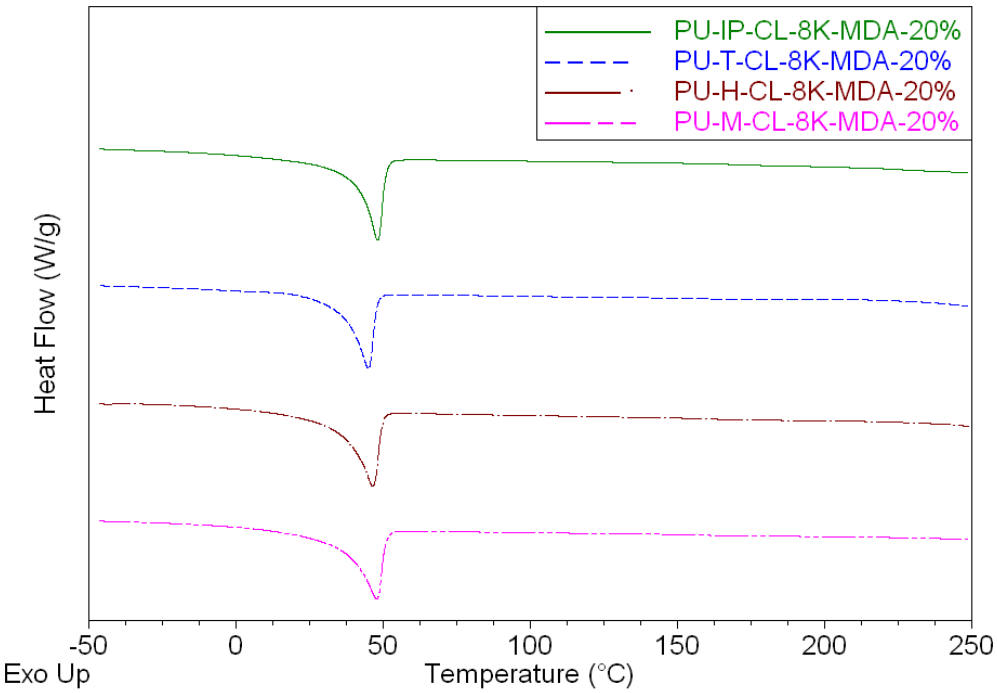

Figure 5.4. DSC curves of PU-CL-8K-MDA-20% synthesized from different diisocyanates

The peak melting temperature and heat of fusion determined directly from DSC thermographs are summarized in Table 5.2:

Table 5.2. DSC Results of SMPUUs synthesized from different diisocyanates

Samples	T_m(°C)	ΔH_m (J/g)	X_c (%)
PCL-8K	55.1	82.4	58.0
PU-IP-CL-8K-MDA-20%	48.1	40.9	36.0
PU-T-CL-8K-MDA-20%	45.0	36.0	31.7
PU-H-CL-8K-MDA-20%	46.6	44.2	38.9
PU-M-CL-8K-MDA-20%	47.7	43.8	38.6

The crystallinities of the PCL prepolymer and the PCL phase of PCLUUs were calculated according to the melting peak area of the DSC curves by assuming the perfect PCL crystal had a melting enthalpy of 142.0 J/g.[56, 57]

As shown in Table 5.2, different diisocyanates also influenced the crystallization ability of the PCL segment, the same as other parameters such as molecular weight, hard segment content and chain extender. For the PCLUUs with PCL of 8000 molecular weight, 20% of hard segment and MDA as chain extender, PU-M-CL-8K-MDA-20% and PU-H-CL-8K-MDA-20% exhibited high crystal content which may indicate excellent phase separation, although these two samples involved different mechanisms. PU-M-CL-8K-MDA-20% showed good phase separation because diisocyanates MDI and chain extender MDA had very similar structures which helped the main chain to neatly align. On the other hand, although the diisocyanate HDI and chain extender MDA of PU-H-CL-8K-MDA-20% had different structures, HDI was fairly flexible, which also helped the main chain to move more freely. PU-T-CL-8K-MDA-20% showed the lowest crystal content because of the interruption of side chain and the rigidity of benzene ring. The melting points of these samples followed the same pattern except for PU-IP-CL-8K-MDA-20%, which exhibited the highest melting point. The hydrogen bond interactions were apparently restrained because of the three side chains of IPDI, and as a result, the crystal grew larger.

Tensile properties

The tensile properties of all PCLUU films synthesized from different diisocyanates are listed in Table 5.3:

Table 5.3. Mechanical properties of PCLUUs synthesized from different diisocyanates

Samples	Tensile modulus (MPa)	Yield strength (MPa)	Tensile strength at 200% (MPa)	Intrinsic viscosity (dL/g)
PU-IP-CL-8K-MDA-20%	446.7±19.2	19.3±1.1	17.4±1.1	0.73
PU-T-CL-8K-MDA-20%	494.7±36.3	19.7±1.4	16.0±1.2	0.59
PU-H-CL-8K-MDA-20%	442.8±12.5	20.2±0.7	18.2±1.1	0.86
PU-M-CL-8K-MDA-20%	489.9±14.7	21.8±0.7	18.1±0.7	0.53

The mechanical properties of PCLUUs are not generally affected by the diisocyanates. The tensile moduli were between 440 MPa to 500 MPa and the tensile stresses at 200% strain were around 17 MPa. The mechanical properties were measured at room temperature, which is below the transition temperature of SMPUUs. Aromatic diisocyanates such as TDI and MDI showed higher tensile modulus than aliphatic diisocyanates although the intrinsic viscosity of the latter ones were much higher, which indicated high molecular weight since aliphatic diisocyanates usually exhibit much higher reactivity.

Shape memory properties

Figures 5.5 - 5.8 show the cyclic stress-strain behavior of SMPUUs synthesized from different diisocyanates:

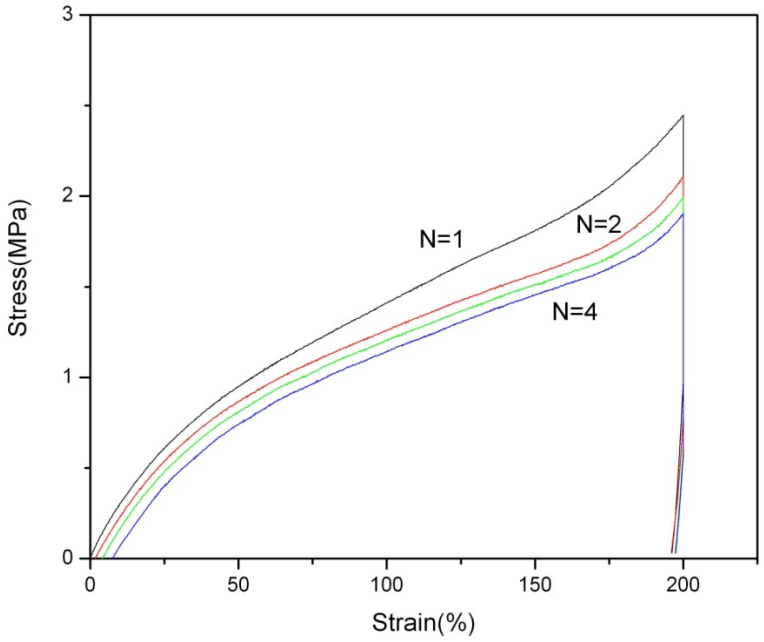

Figure 5.5. Cyclic tensile behavior of PU-IP-CL-8K-MDA-20%

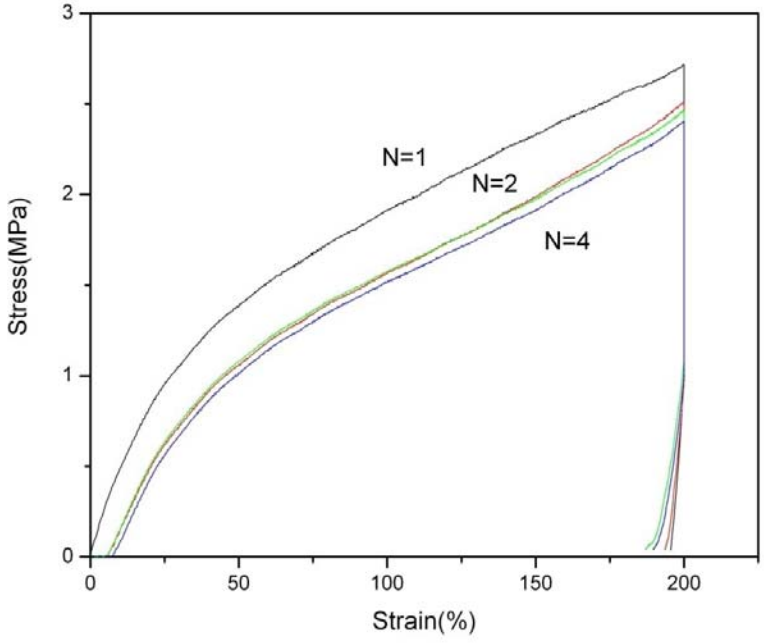

Figure 5.6. Cyclic tensile behavior of PU-T-CL-8K-MDA-20%

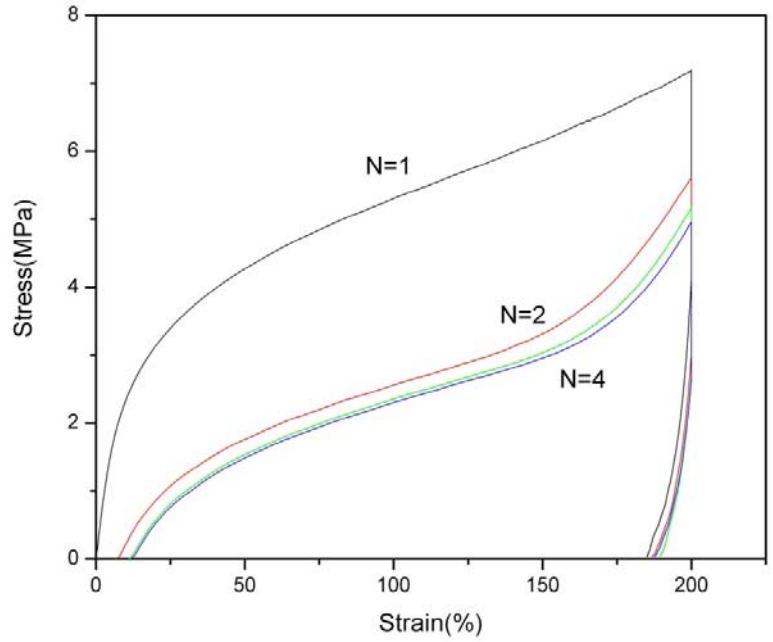

Figure 5.7. Cyclic tensile behavior of PU-H-CL-8K-MDA-20%

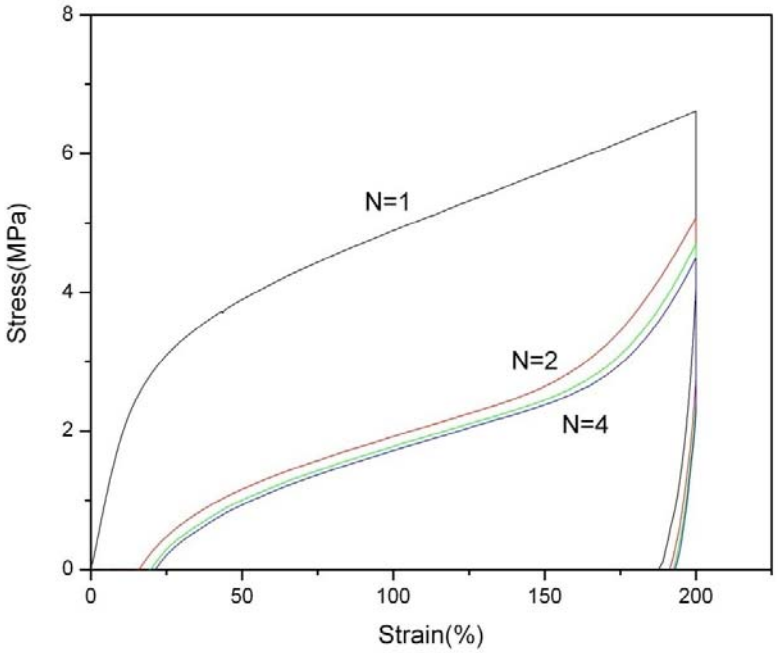

Figure 5.8. Cyclic tensile behavior of PU-M-CL-8K-MDA-20%

The shape memory properties including recovery stress, fixity and recovery rate at 200% strain of first circle are showed in Figure 5.9:

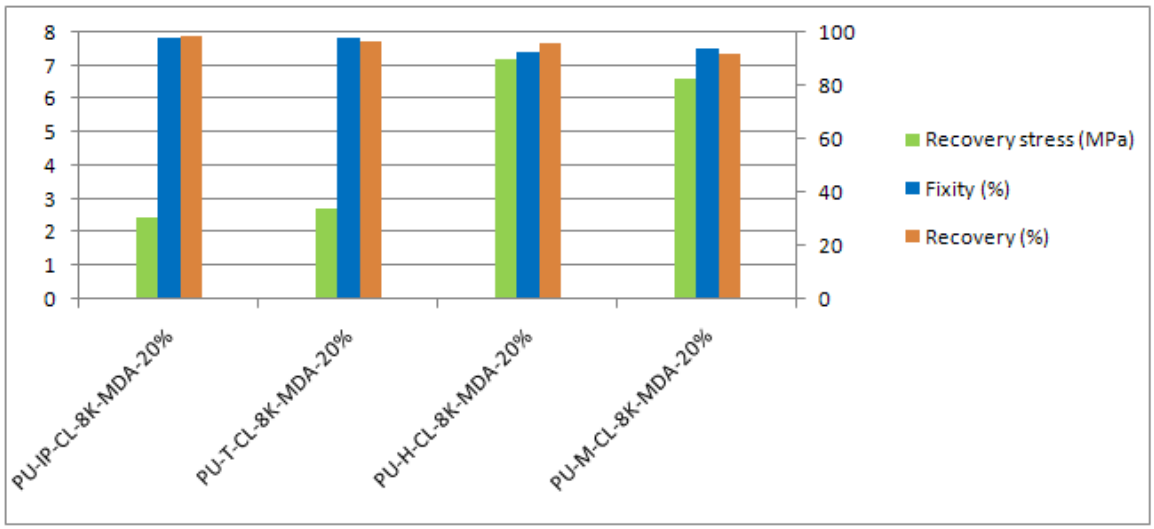

Figure 5.9. Shape memory properties of SMPUUs synthesized from different diisocyanates

PU-M-CL-8K-MDA-20% and PU-H-CL-8K-MDA-20% exhibited much higher recovery stress than PU-IP-CL-8K-MDA-20% and PU-T-CL-8K-MDA-20%, both having interruptions of side chain. The recovery stresses of PU-IP-CL-8K-MDA-20% and PU-T-CL-8K-MDA-20% were 2.5 MPa and 2.7 MPa respectively and less than 40% of the recovery stress of PU-M-CL-8K-MDA-20% (6.6 MPa)and PU-H-CL-8K-MDA-20% (7.2 MPa). The recovery stress of PU-H-CL-8K-MDA-20% was higher than that of PU-M-CL-8K-MDA-20% since the molecular weight of PU-H-CL-8K-MDA-20% was much higher, as evidenced by its higher intrinsic viscosity (Table 5.3).

The fixity and recovery rates of all these four samples were greater than 90%, indicating excellent shape memory properties. PU-IP-CL-8K-MDA-20% and PU-T-CL-8K-MDA-20% exhibited higher fixity and recovery rates than PU-M-CL-8K-MDA-20% and PU-H-CL-8K-MDA-20%, apparently because the stress applied was much less than

the latter ones so the polymer chains did not slip as much as the ones of PU-M-CL-8K-MDA-20% and PU-H-CL-8K-MDA-20%. The circle thermal test method influenced the fixity since only 20 minutes fixing time existed and the samples with less recovery stress fixed more efficiently because of the viscoelastic properties of the polymers.

From these results, some important conclusions can be drawn. The most important factor in increasing recovery stress was avoiding side chains, which interrupted the formation of hydrogen bonds. The molecular weight and the rigidity of the main chain also helped to increase the recovery stress, but not to the same level as the presence of side chains.

Dynamic mechanical properties

The tensile storage modulus of SMPUUS synthesized from different diisocyanates is shown in Figure 5.10.

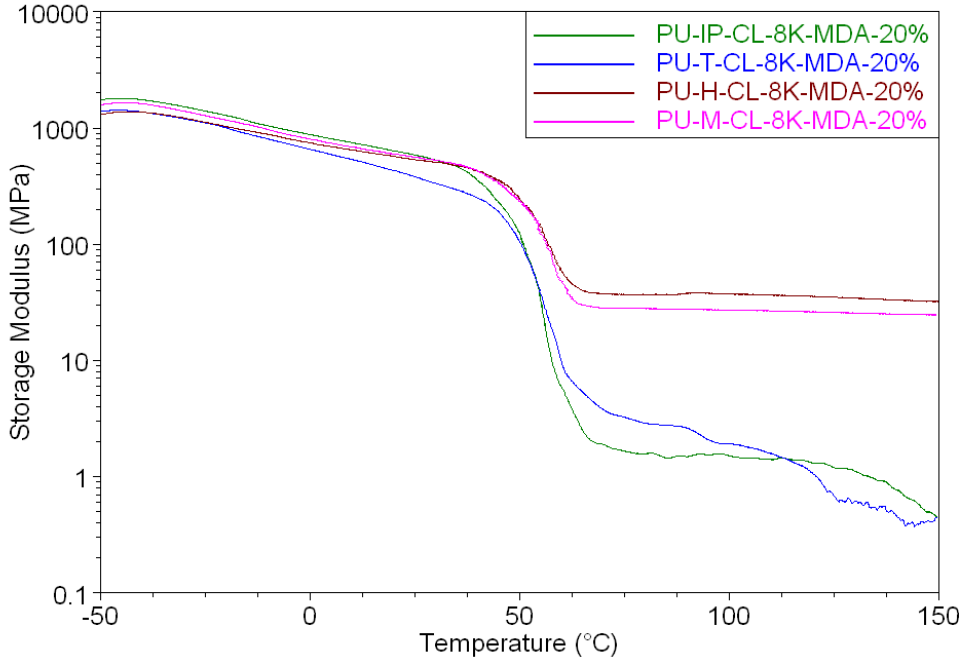

Figure 5.10. Tensile storage modulus of PU-CL-8K-MDA-20% synthesized from different diisocyanates

The storage modulus slightly decreased below the melting temperature of PCL and a sharp drop was observed near the melting point for all samples. The storage moduli were much more stable above the melting point due to the bidentate hydrogen bonding of the urea linkage for PU-M-CL-8K-MDA-20% and PU-H-CL-8K-MDA-20%. The storage moduli of PU-IP-CL-8K-MDA-20% and PU-T-CL-8K-MDA-20% decreased with the increasing temperature because the incorporation of the side chain interrupted the formation of hydrogen bond interactions. This result is consistent with other data such as FT-IR, DSC and cyclic thermo mechanical tests.

CHAPTER 6

BLOCK POLYESTER COPOLYMER WITH PET/POLY (OXY-1, 3-PROPYLENEOXYADIPATE

Additional shape memory polymer systems are discussed and investigated in Chapters 6 and 7 which were not fully developed either because of poor shape memory properties or unimproved recovery stress. Block polyester copolymers with PET/Poly (oxy 1, 3- propyleneoxyadipate) (POPA) were synthesized and evaluated for the shape memory properties.

The PET/POPA block polyester copolymer was described in National Textile Center (NTC) Project M05-GT14.[46] The PET/POPA system was chosen to make shape memory fibers for comfort wear because PET is the most widely used synthetic fiber in the world with low production costs and excellent properties. According to Martin in "Synthetic Methods in Step-Growth Polymers," POPA has a melting point of 45°C (Table 6.1), which may be lowered by copolymerization to form a random block system[78]. The transition temperature is slightly higher than ideal, which is the high end of standard room temperature (generally defined as 25°C).

Table 6.1. Glass transition temperature and melting point of some polyesters

Repeating Unit Formula	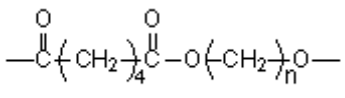		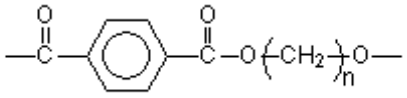	
n	Tg	Tm	Tg	Tm
1			101	269
2	**-63**	**50**	**69**	**265**
3	**-59**	**45**	**35**	**233**
4	**-74**	**55.8**	**17**	**232**
5	-	-	10	134
6	-73	61	-9	154
7	-	-	3	85
8	-	-	-	132
9	-	-	-3	95
10	-56	80	-5	125

6.1. Synthesis of PET/POPA copolymer

Two methods were proposed to synthesize of PET/POPA copolyester:

(1) Hydroxy-end capped PET blocks and POPA blocks coupled with adipoyl chloride:

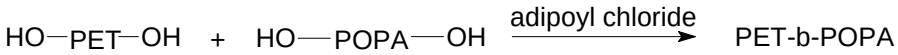

(2) Acyl chloride-end capped PET blocks reacted with hydroxyl-end capped POPA:

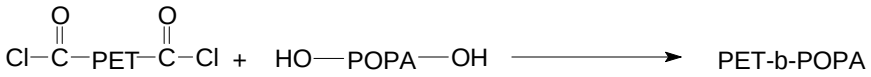

6.1.1. Preparation of hydroxyl-end capped PET

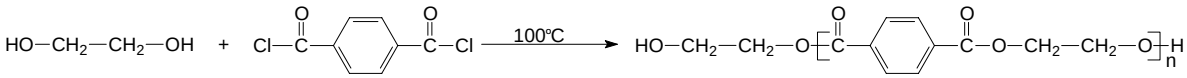

Synthesis of hydroxyl-end capped PET block was obtained by melt polymerization, starting form terephthaloyl dichloride and an appropriate excess of ethylene glycol. Terephthaloyl dichloride (10.15 g, 50 mmol) and ethylene glycol (4.65 g, 75 mmol) were placed in a three-necked flash and reacted at 100°C for eight hours, under

vigorous stirring. The solid residue was poured into 500 mL water, filtered, washed several times with water, and dried at 80°C in a vacuum oven, overnight.

The hydroxyl-end capped PET was not soluble in most common solvents such as THF, DMF, DMSO or 1,1,2,2- tetrachloroethane (TCE), and thus only FT-IR was used to verify the structure of PET (Figure 6.1):

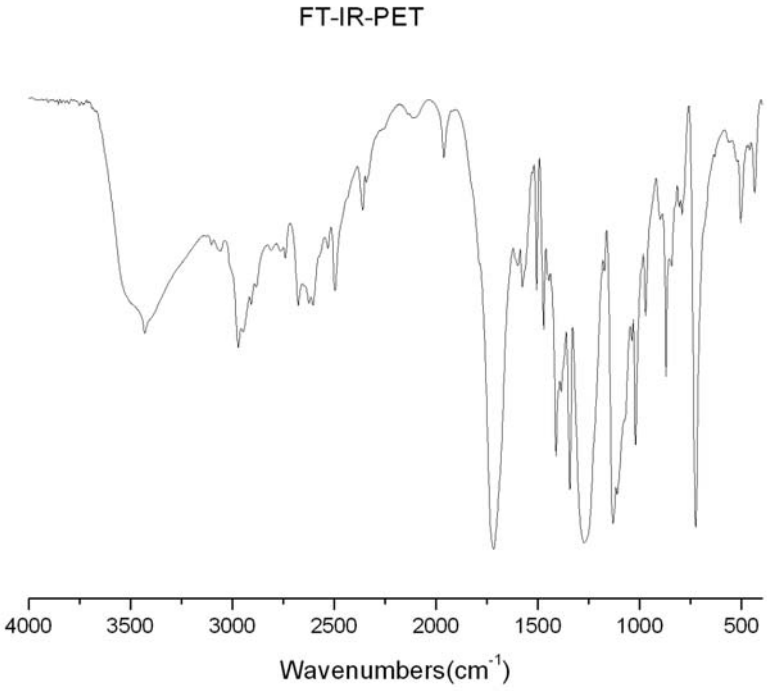

Figure 6.1. FT-IR spectrum of hydroxyl-end capped PET

6.1.2. Preparation of hydroxyl-end capped POPA

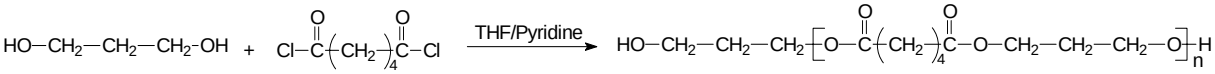

Synthesis of hydroxyl-end capped POPA block was obtained by solution polymerization. 1,3-Propanediol(1.522 g, 20 mmol), pyridine(3.164 g, 40 mmol) and 10 mL anhydrous tetrahydrofuran(THF) was mixed together, then adipoyl chloride(3.166 g,

20 mmol) solution in THF(10 mL) was added dropwise at 0°C. After four hours, additional 1, 3-propanediol (0.304 g, 4 mmol) was added and the mixture was stirred at room temperature for another four hours. The reaction mixture was then poured into 250 mL cold water, filtered, washed several times with water and dried. m.p.: 37°C; FT-IR (KBr, cm^{-1}):3600~3400 (O-H, m); 2940, 1470 (CH_2, m); 1722 (C=O, s);1260, 1177 (ester group, s). ^1H NMR ($CDCl_3$, δppm): 4.20~4.10 (m, 4H), 2.40~2.20 (m, 4H), 2.00~1.90 (m, 2H), 1.70~1.58 (m, 4H).

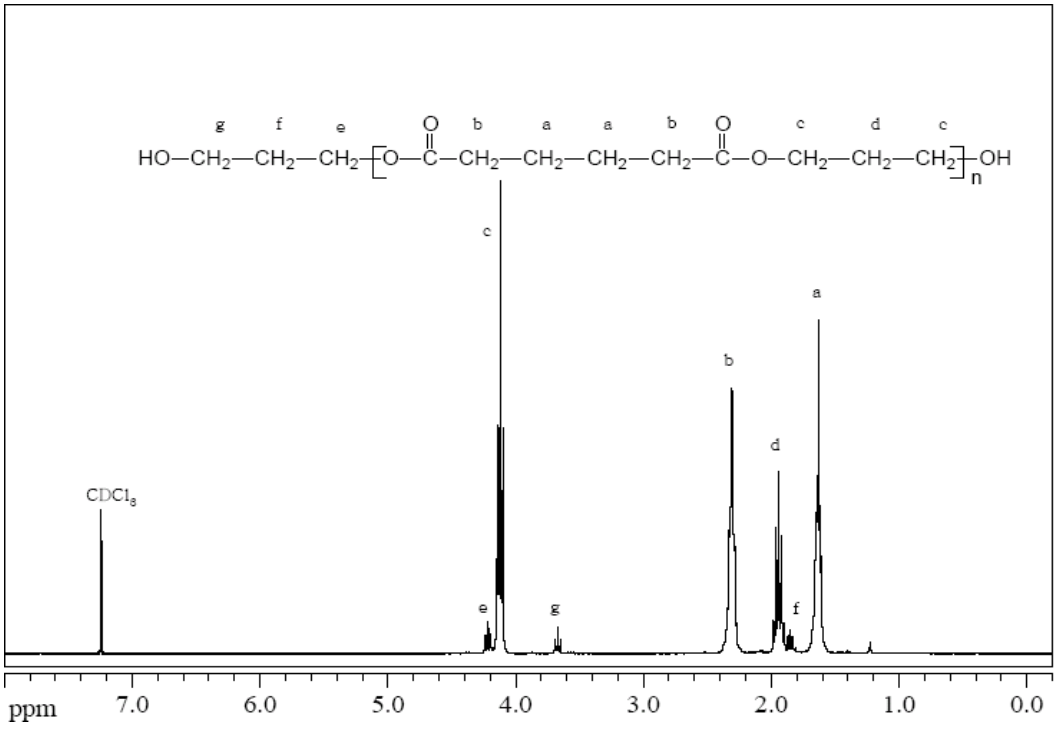

Figure 6.2. ^1H NMR spectrum of hydroxyl-end capped POPA

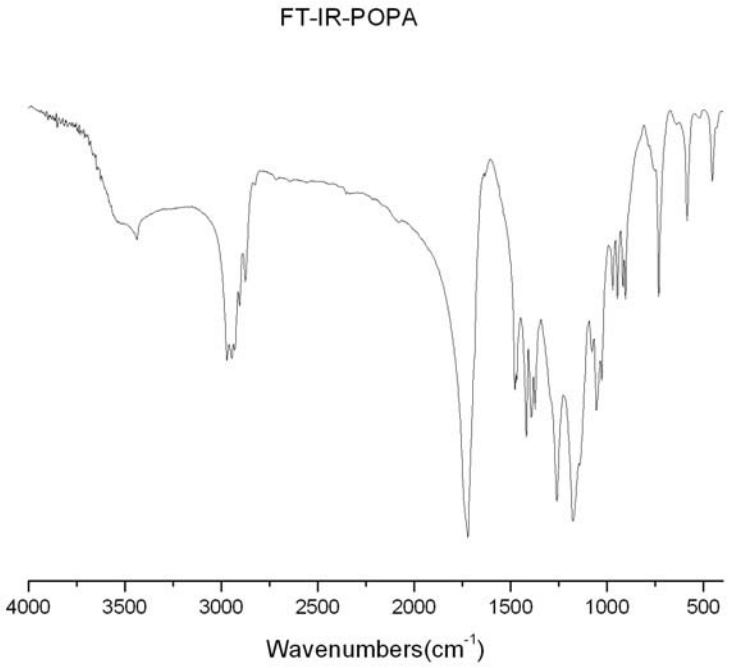

Figure 6.3. FT-IR spectrum of hydroxyl-end capped POPA

As Figure 6.4~ 6.5, thermal properties of POPA were measured with TGA and DSC.

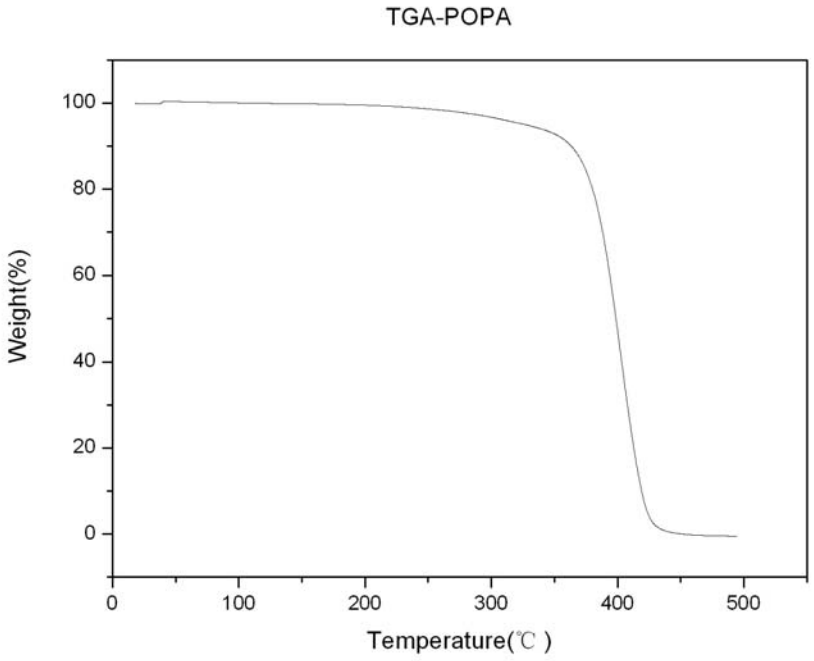

Figure 6.4. TGA curve of hydroxyl-end capped POPA

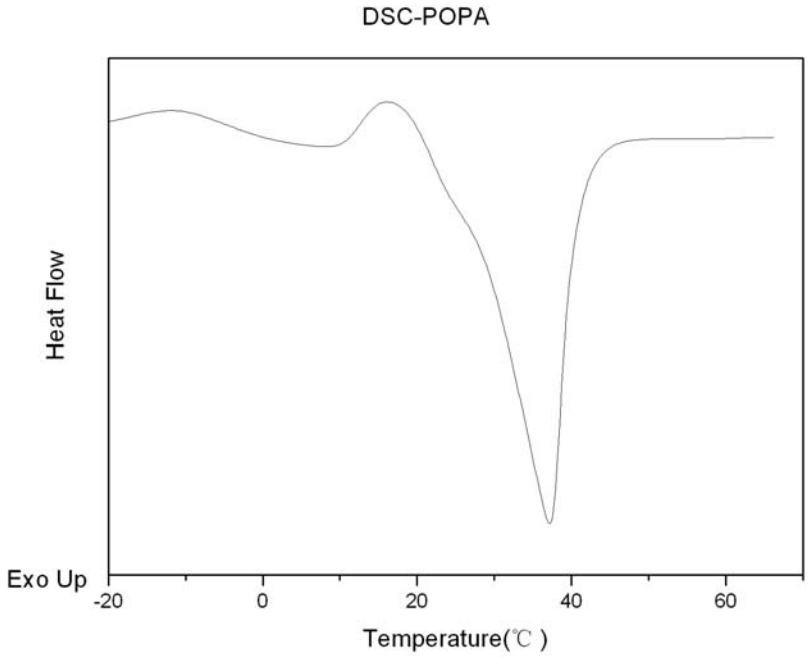

Figure 6.5. DSC curve of hydroxyl-end capped POPA

The melting point of POPA is ~ 37°C, almost the same as body temperature because the molecular weight of hydroxyl-end capped POPA is only 3800 with polydisperisty of 1.5 according to the GPC scan (Figure 6.6).

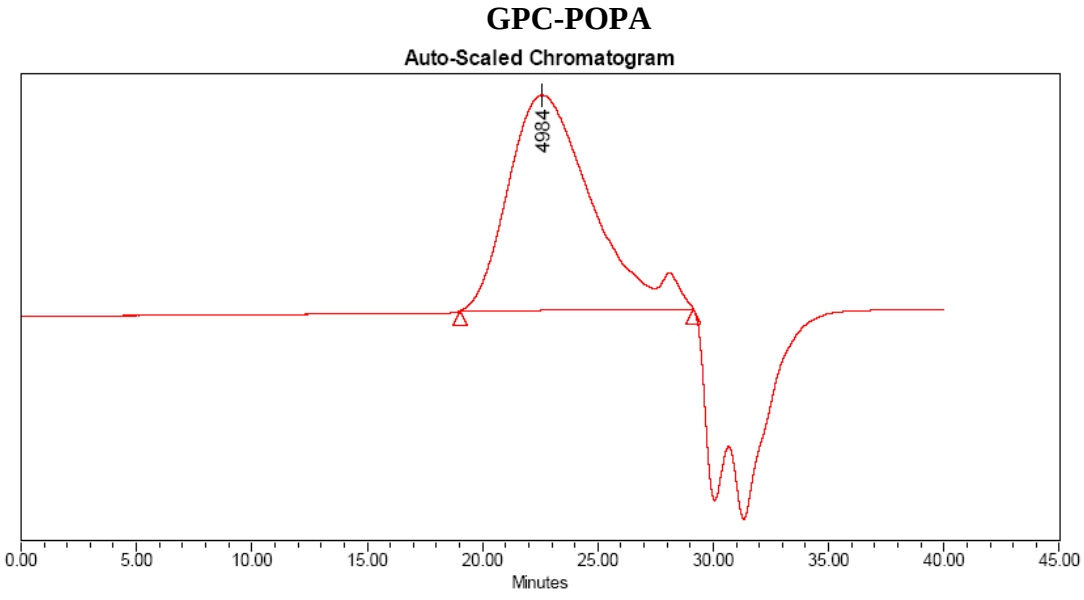

Figure 6.6. GPC result of hydroxyl-end capped POPA

Thermogravimetric analysis (TGA) showed the POPA to be quite stable before 350°C, which made the transesterification reaction between PET and POPA possible.

6.1.3. Preparation of PET/POPA copolymer

Although hydroxy-end capped PET blocks and POPA blocks were synthesized successfully, these two blocks cannot be coupled with adipoyl chloride because of the poor solubility of PET in common solvents. The TCE/phenol is used as the solvent to measure the viscosity of PET, but phenol cannot be used as a solvent during the reaction because the phenolic hydroxyl group will also react with adipoyl chloride.

PET/POPA copolyesters were synthesized by melt transesterification reaction between PET and POPA with two different catalysts: Sb_2O_3 and Ti (Obu) $_4$. These two catalysts are used in industry to synthesize PET and aliphatic polyesters, respectively. Transesterification reaction is widely used to synthesized copolyesters with different structure and properties.[79, 80]

PET/POPA copolyesters were synthesized by the following process. 10 g of commercial PET with intrinsic viscosity 0.65 dL/g was heated to 280°C in a 250 mL three neck flask to melt PET with N_2 purge to prevent degradation, then 10 g of POPA with molecular weight of 6554 was added followed by 0.5 g of catalyst. The reaction mixture was stirred mechanically and vacuum applied around 1mm Hg. After 30 min, the reaction was finished and the melt mixture was poured out from reaction flask.

As shown in Figure 6.7, PET/POPA copolyester was successfully synthesized according to ^{1}H NMR spectra. Compared with the homo polyesters, the copolyester spectra exhibited several additional peaks around 2.0 ppm and 4.6 ppm, which verified the transesterificaiton reaction.

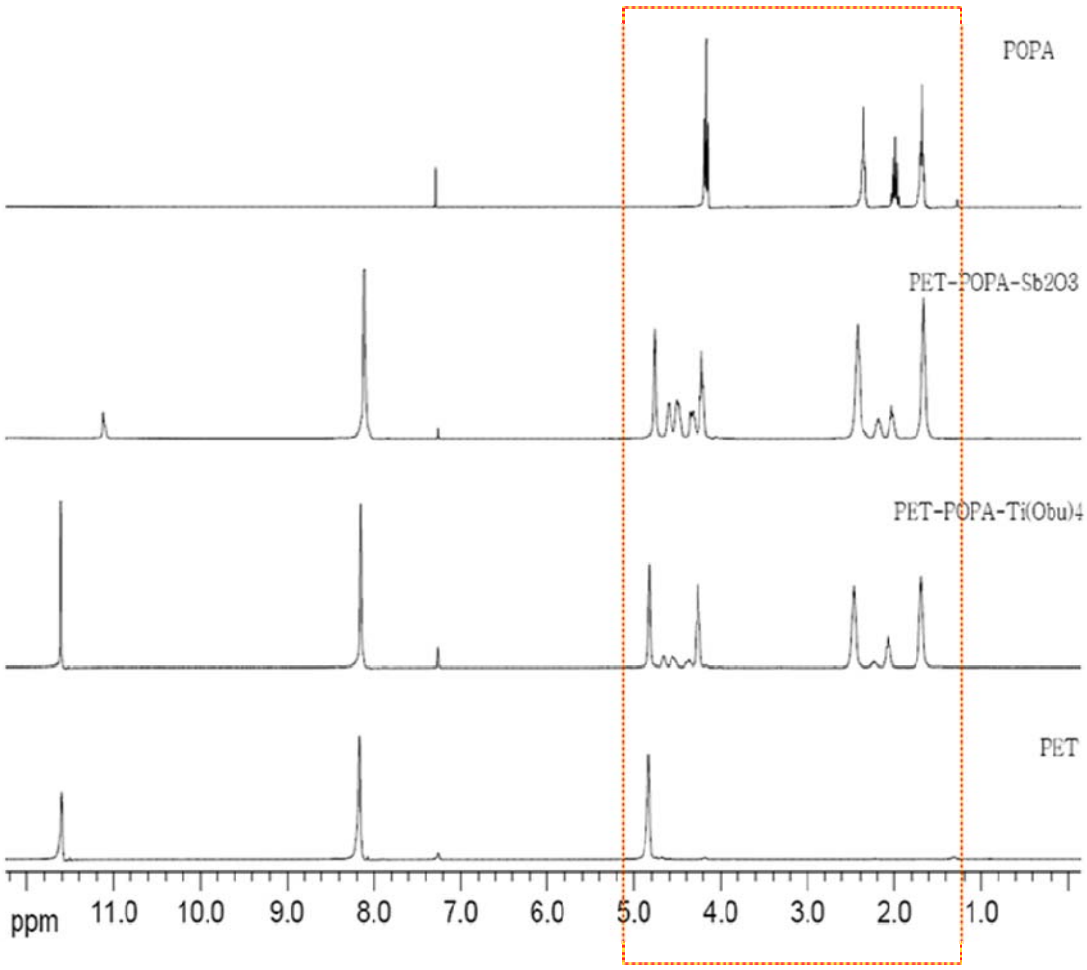

Figure 6.7. ^{1}H NMR spectra of PET/POPA copolyesters and homopolyesters

With the same amount of catalyst and the same reaction time, Sb_2O_3 worked more efficiently than Ti (Obu) $_4$ since the additional peaks from the copolyester with Sb_2O_3 as catalyst was stronger than the ones from the copolyester with $Ti(Obu)_4$ as catalyst. This same conclusion can also be drawn from the ^{13}C-NMR spectra of PET/POPA copolyester and homopolyesters mixture (Figure 6.8):

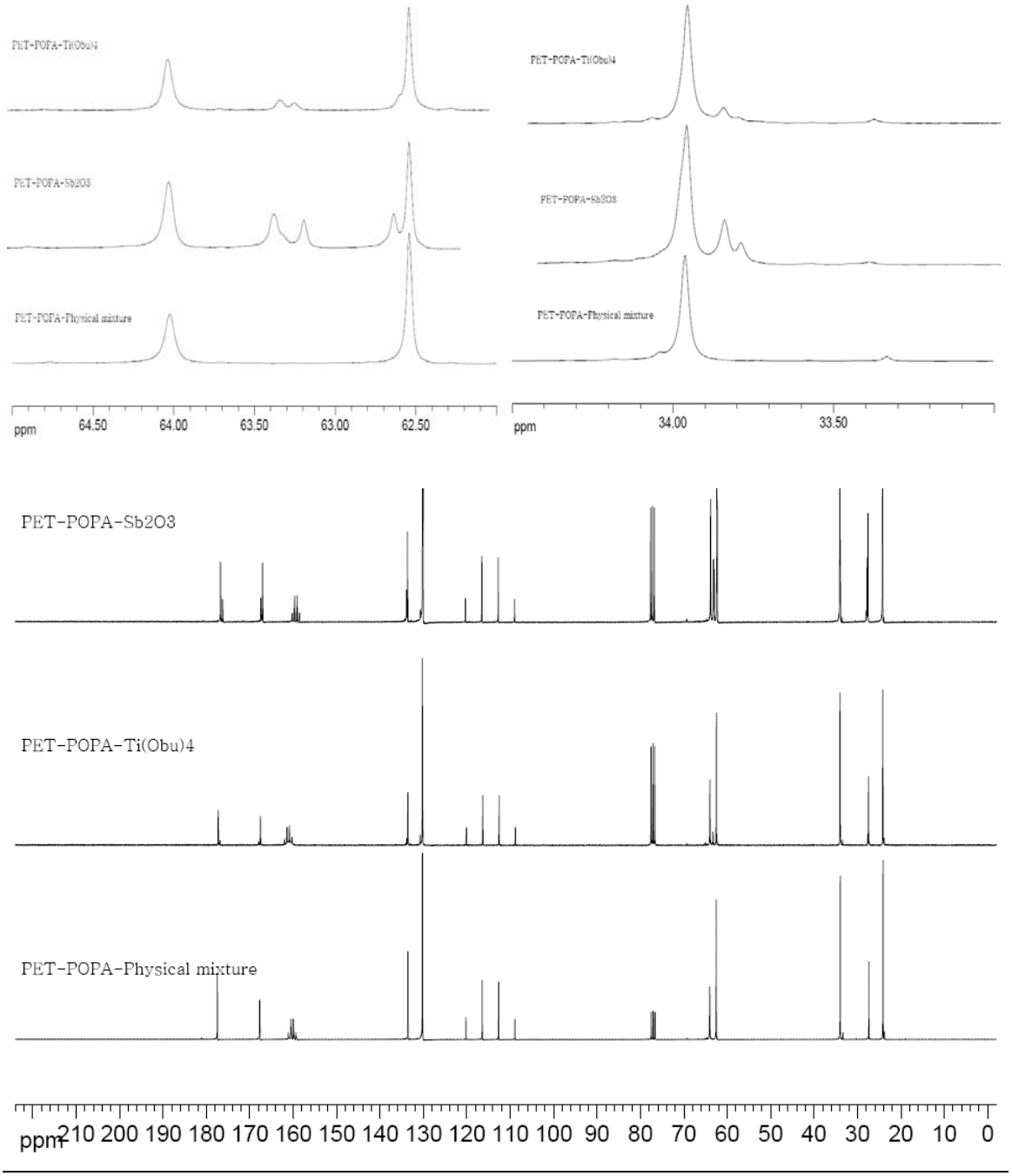

Figure 6.8. ^{13}C NMR spectra of PET/POPA copolyesters and homopolyesters

DSC was also used to verify the transesterification reaction between PET and POPA. As shown in Figure 6.9, the melting point of PET blocks from PET/POPA copolyesters synthesized with both catalysts decreased compared to pure PET. The more transesterification reaction happening, the greater the melting point decreased, which also confirmed the transesterification reaction between PET and POPA.

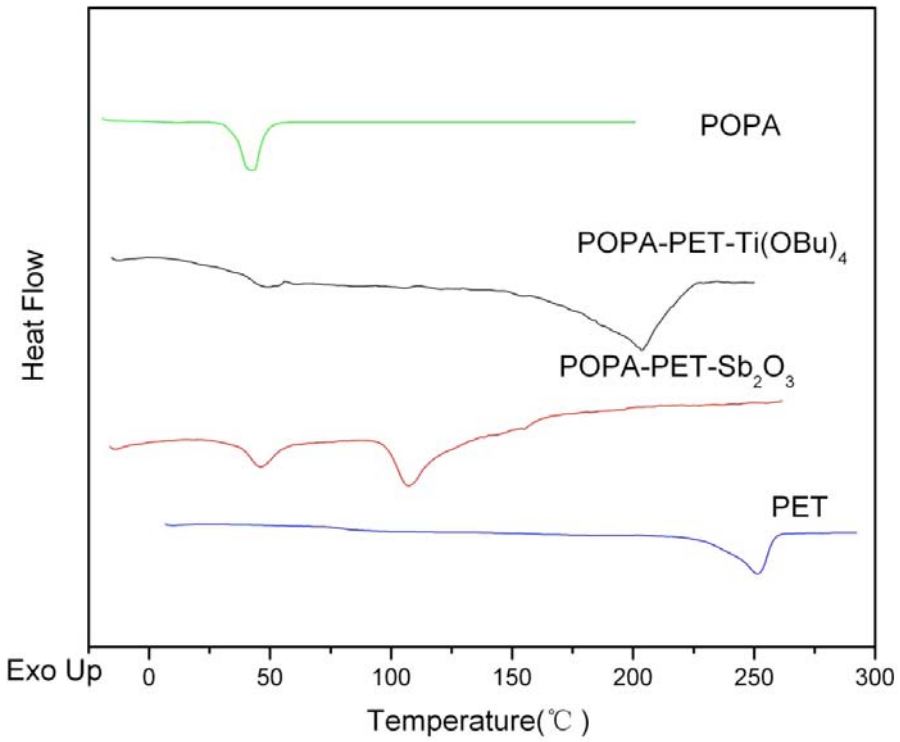

Figure 6.9. DSC curve of PET/POPA copolyesters and homopolyesters

All data from NMR spectra and DSC showed that the PET/POPA copolyester was synthesized successfully. No shape memory properties was observed for the copolyester, with several reasons proposed, the most important one was that the PET/POPA

copolyester should be a T_g type shape memory system, not a T_m type. All of the reported polyester diols such as PEA, PBA and PHA are T_g type shape memory polymers[34-37].

A method to understand the different types of shape memory soft segment was developed by the DSC data. As shown in Figures 6.10 and 6.11, PCL and PLA are two different types of soft segments that have been well studied in shape memory polymers. PCL is a T_m type soft segment and on the contrary, while PLA is a T_g type.

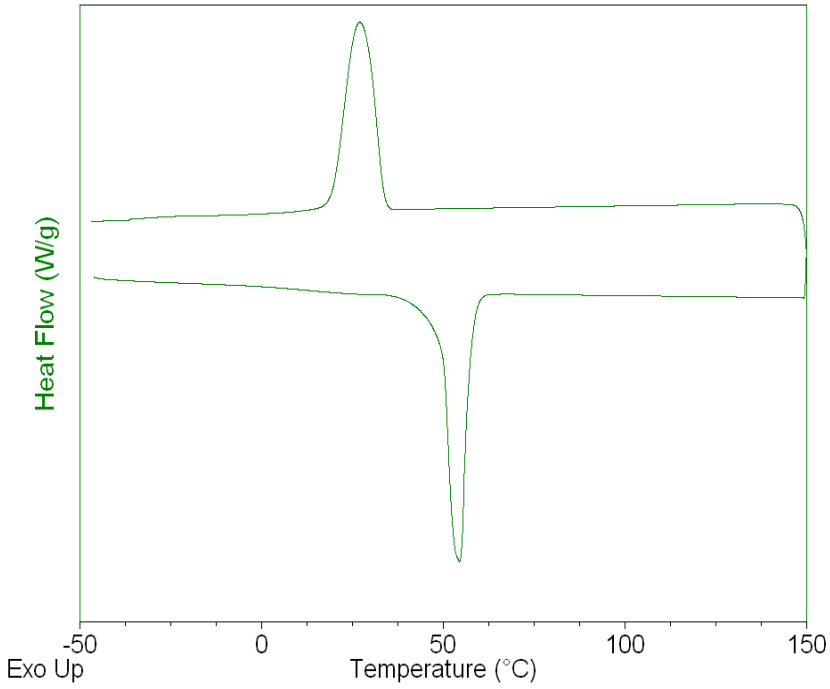

Figure 6.10. DSC curve of PCL

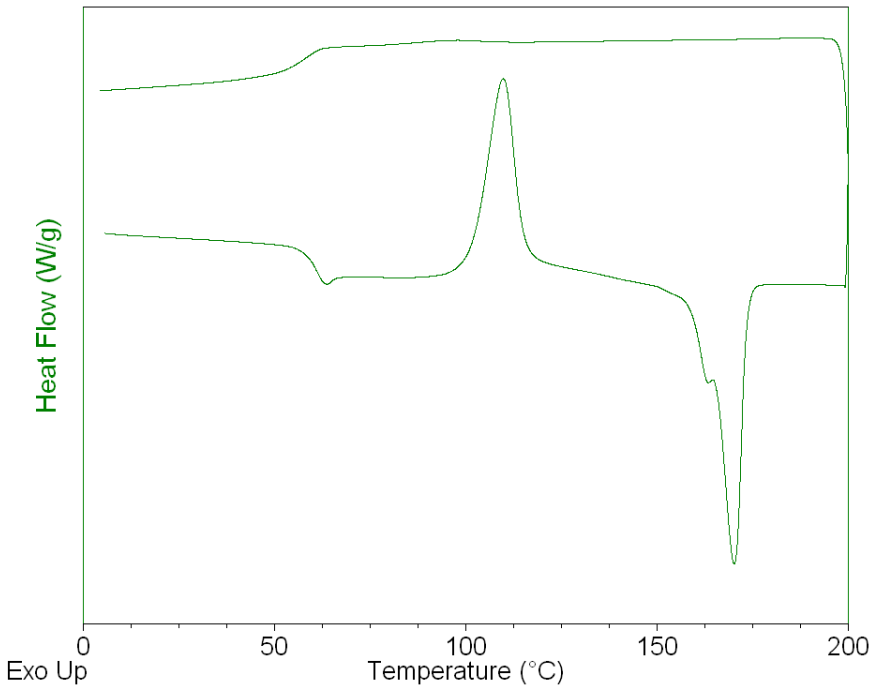

Figure 6.11. DSC curve of PLA

From Figure 6.11, the DSC curve of PLA also has a melting point around 170°C. The reason PLA is not a T_m type soft segment is that PLA crystallizes much slower than PCL. With 10°C/min cooling speed, PLA does not crystal at all as PCL does. Without crystallinity, PLA soft segment cannot hold the temporary shape and only below T_g, the soft segment will hold the temporary shape because the chains are frozen. As a result, PLA is a T_g type shape memory soft segment.

Figure 6.12 shows the DSC curve of POPA. As PLA, POPA will not crystallize with a cooling speed of 10°C/min, which indicates that POPA is also a T_g type soft segment. Glass transition temperature is not observed in Figure 6.12 because T_g of POPA is below -59°C (Table 6.1).

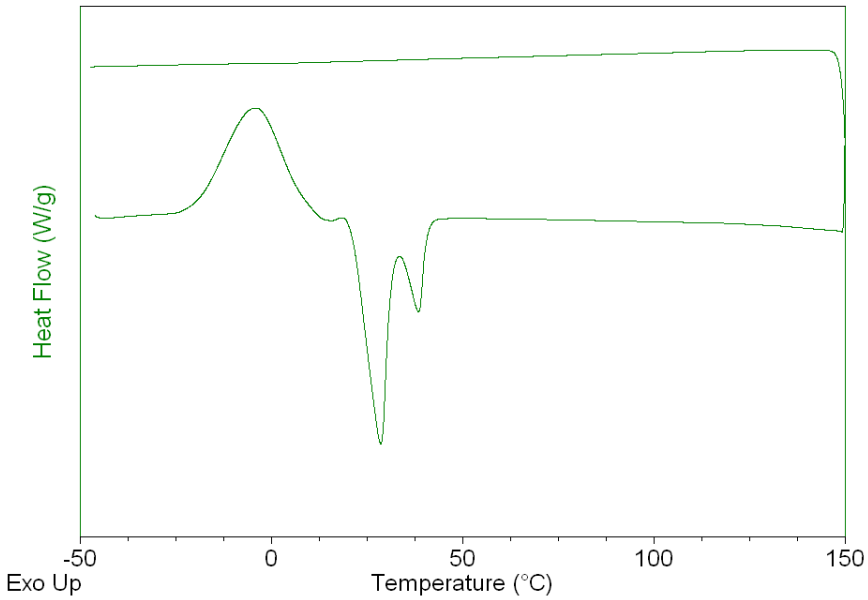

Figure 6.12. DSC curve of POPA

CHAPTER 7

LIQUID CRYSTALLINE SHAPE MEMORY POLYURETHANES

For linear thermo plastic SMPs, incorporating mesomorphic units such as 4'4-bis (2-hydroxyethoxy) biphenyl (BEBP) or 4'4-bis (2-hydroxyhexoxy) biphenyl (BHBP) into the main chain is an effective way to improve the recovery stress comparing to traditional chain extenders such as butanediol (BDO). Some advantages also exist in incorporating liquid crystal (LC) units into the main chain since the orientational order of the LC phase can be retained in the polymer after processing, with performance properties undergoing increases in values close to those of theoretical predictions (extremely high modulus, high strength and high heat resistance, etc). On the other hand, the LC phase can be trapped or stabilized in the glassy phase of the polymer so that the electro-optical and magnetic properties can be conveniently manipulated for applications in areas such as imaging technology, nonlinear optics, telecommunications, etc. Moreover, LC polymers have excellent dimensional stability, thermal stability, and flame resistance, coupled with the absence of creep and shrinkage; these properties make them ideal candidates for high-performance Applications.[81, 82] The biggest disadvantage for LC polymers is the high cost, e.g., the raw material to synthesize BHBP and BEBP, 4, 4′-Biphenol, is very expensive which limits the application of LC polymers.

7.1. Synthesis of LC units as chain extender

LC units with different flexible chain were synthesized with commercial chemicals with low cost as shown in Figure 7.1[83]:

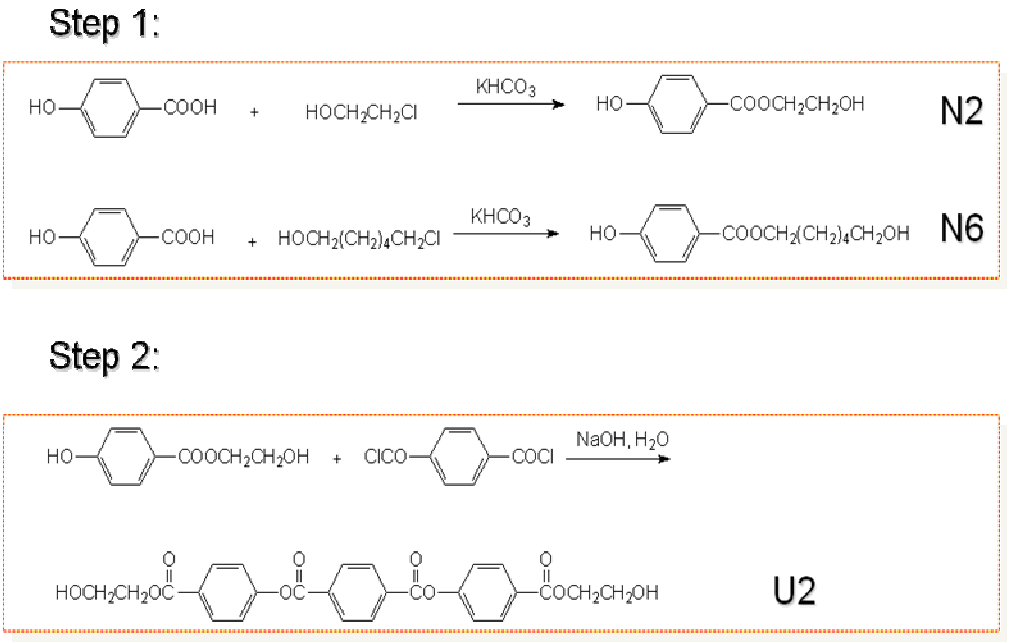

Figure 7.1. Scheme to synthesize liquid crystal units

As confirmed in Figures 7.2 - 7.5, liquid crystal units U2 and U6 were synthesized step by step and the structure of the products for each step were confirmed with NMR. The final products were recrystallized in diacetyl three times to attain high purity.

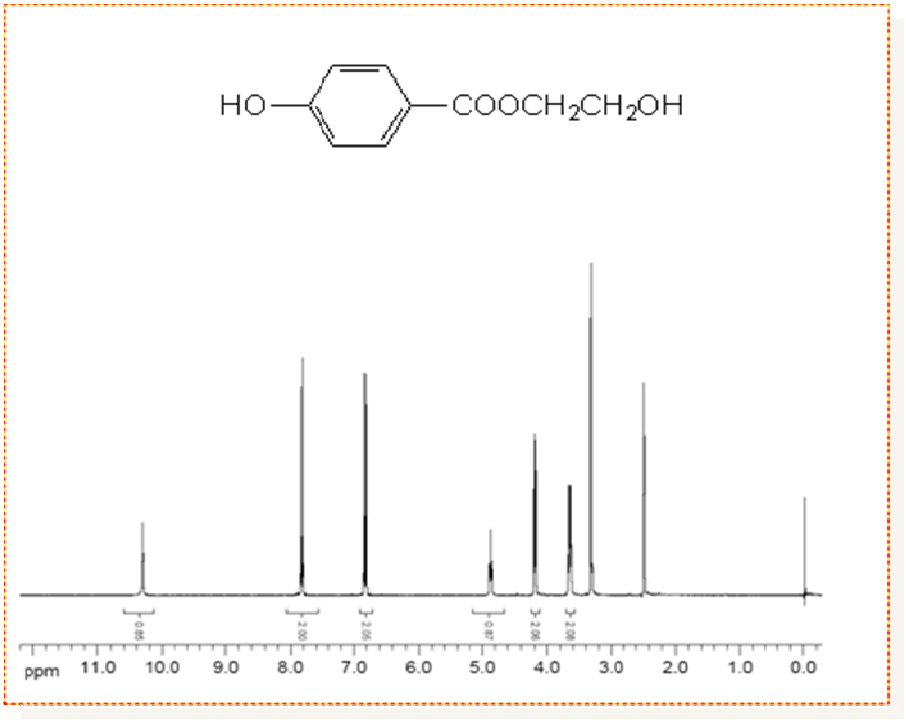

Figure 7.2. ^{1}H NMR spectrum of N2

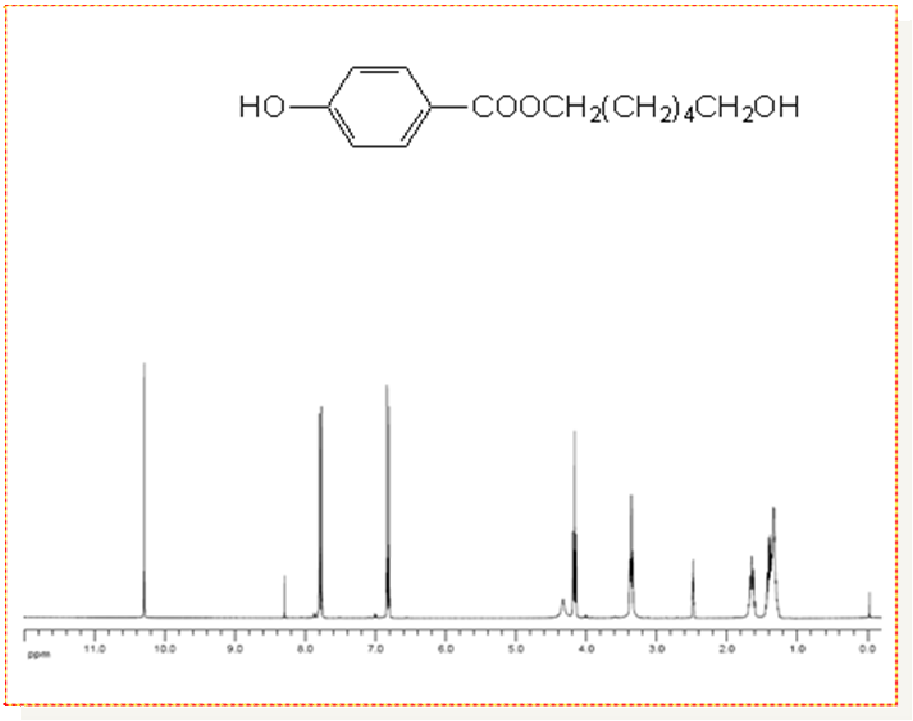

Figure 7.3. ^{1}H NMR spectrum of N6

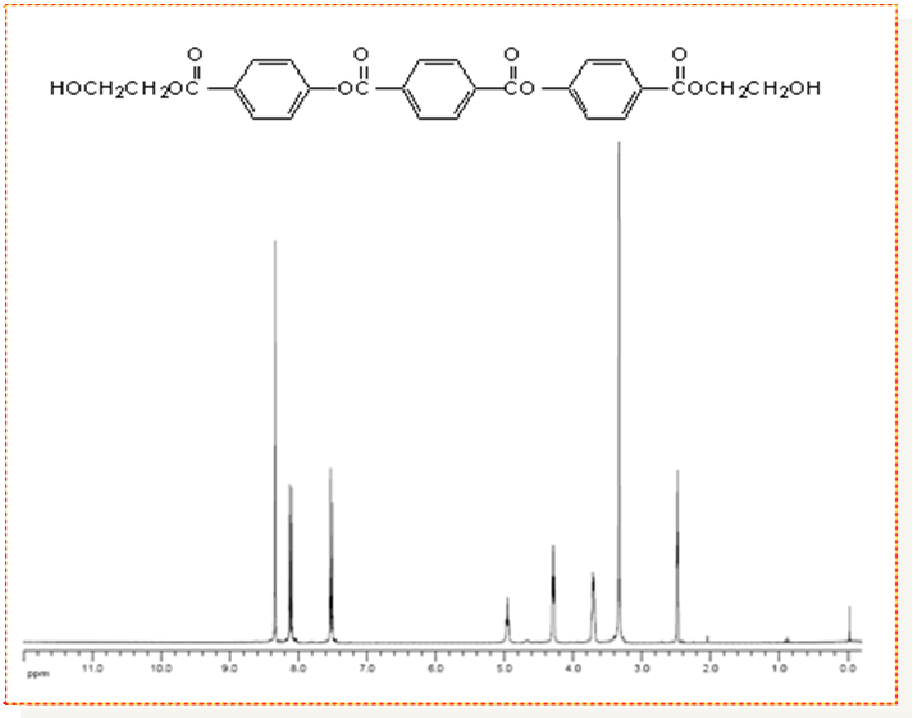

Figure 7.4. ^{1}H NMR spectrum of U2

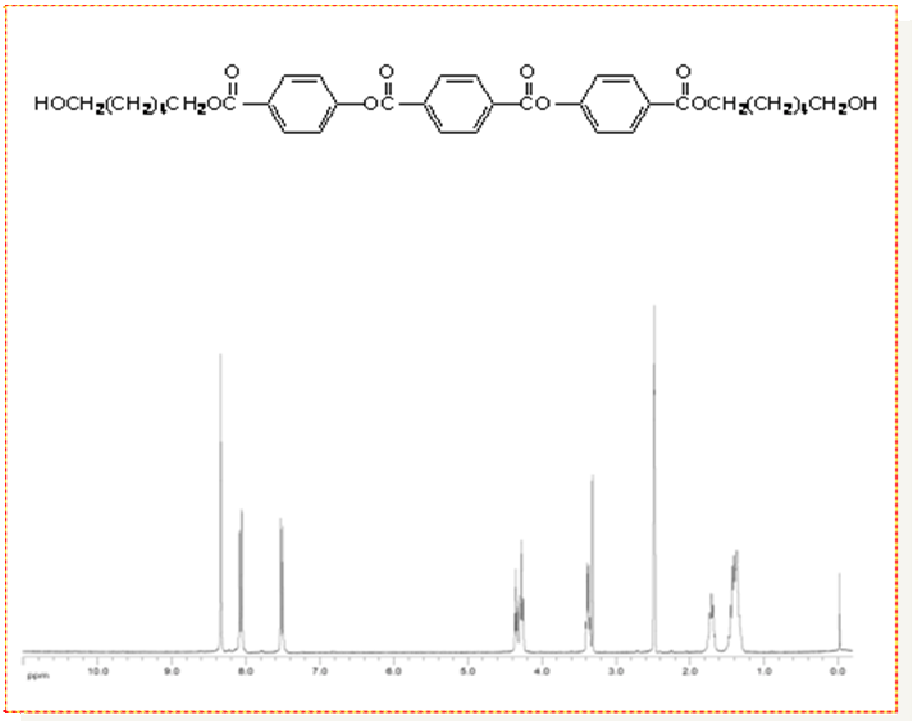

Figure 7.5. ^{1}H NMR spectrum of U6

DSC result also showed high purity of the synthesized LC units (Figures 7.6 - Figure 7.7):

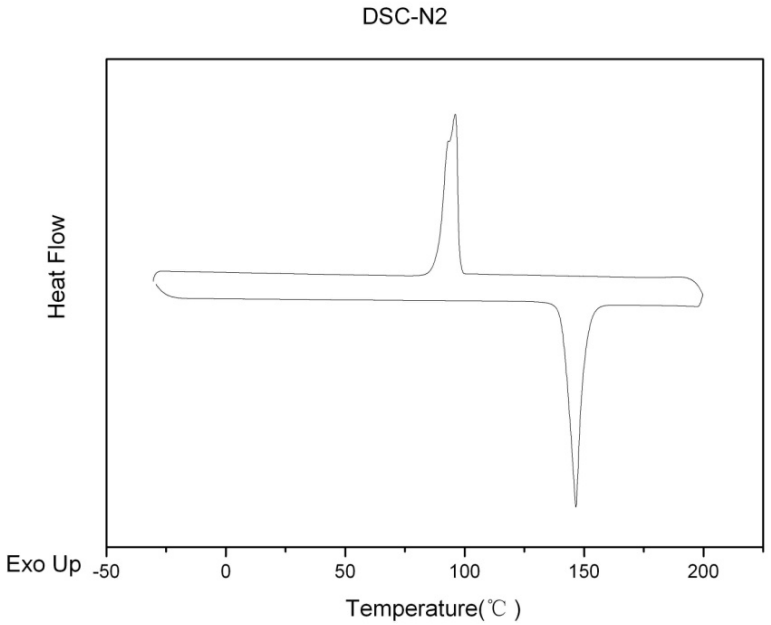

Figure B.6. DSC curve of N2

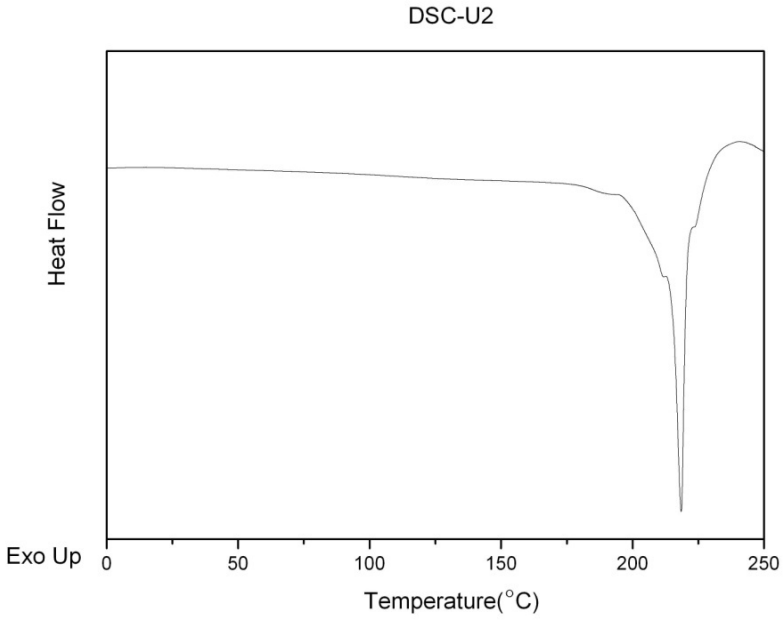

Figure B.7. DSC curve of U2

7.2. Synthesis of LC SMPUs

LC SMPUs were synthesized with the prepolymer method as detailed in previous chapters with LC units U2 and U6 as chain extenders. Figure 7.8 shows the NMR spectrum of PU-M-CL-5K with U2 as chain extender, the molar ratio between PCL diol and chain extender U2 is 1 to 2. The DSC result of the product is showed in Figure 7.9:

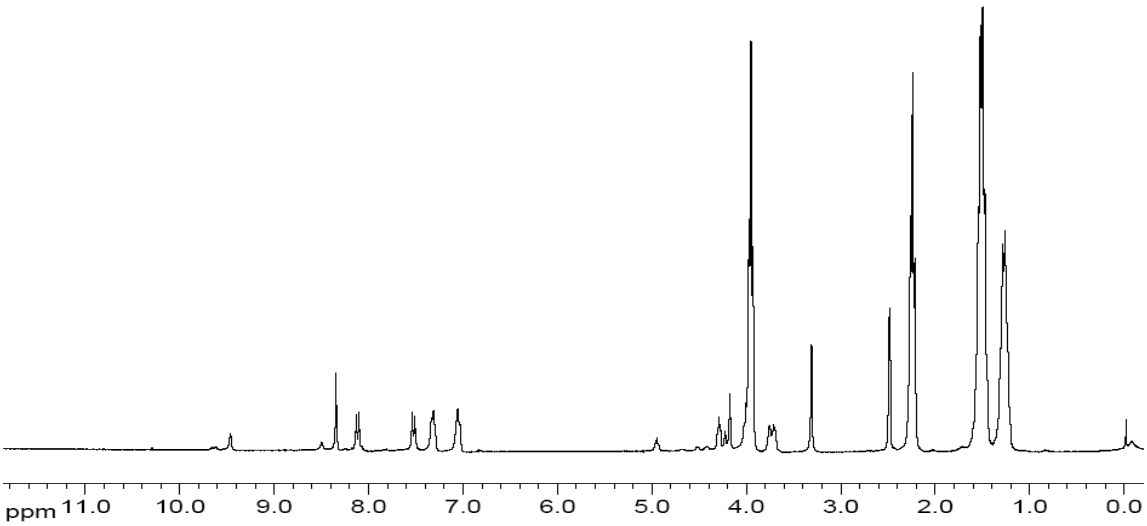

Figure 7.8. ^{1}H NMR spectrum of PU-M-CL-5K with U2 as chain extender

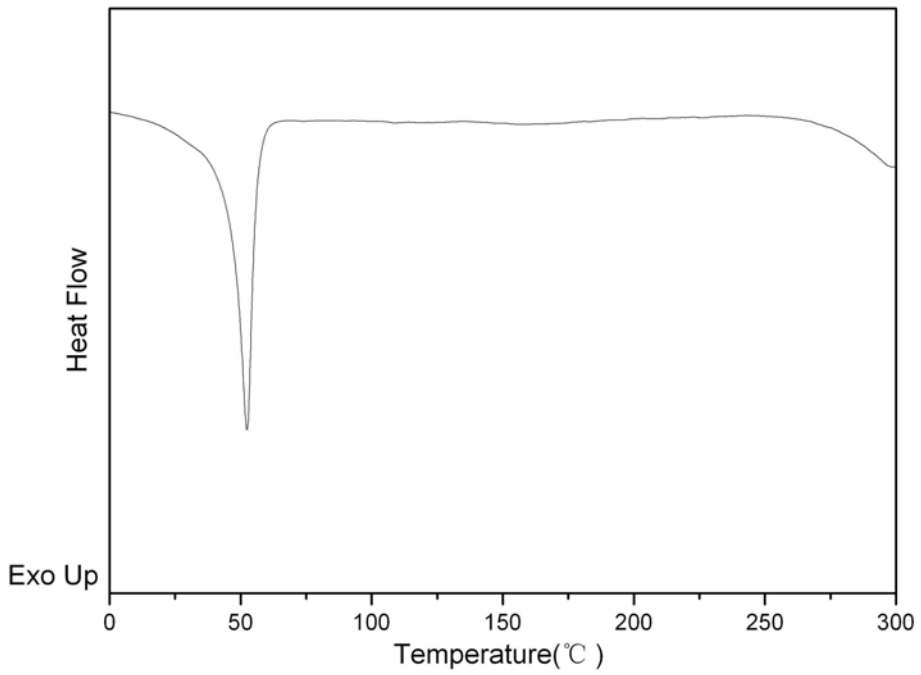

Figure 7.9. DCS curve of PU-M-CL-10K-U2-14.8%

7.3. Shape memory properties of LC SMPUs

Figured 7.10 - 7.13 show the cyclic thermal mechanic test of PU-M-CL-10K-U2 with different hard segment contents:

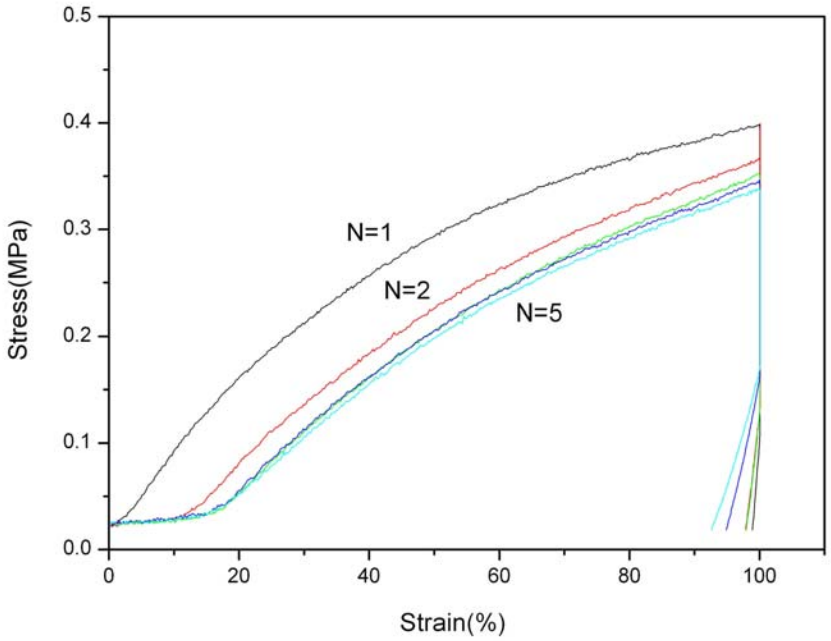

Figure 7.10. Cyclic tensile behavior of PU-M-CL-10K-U2-14.8%

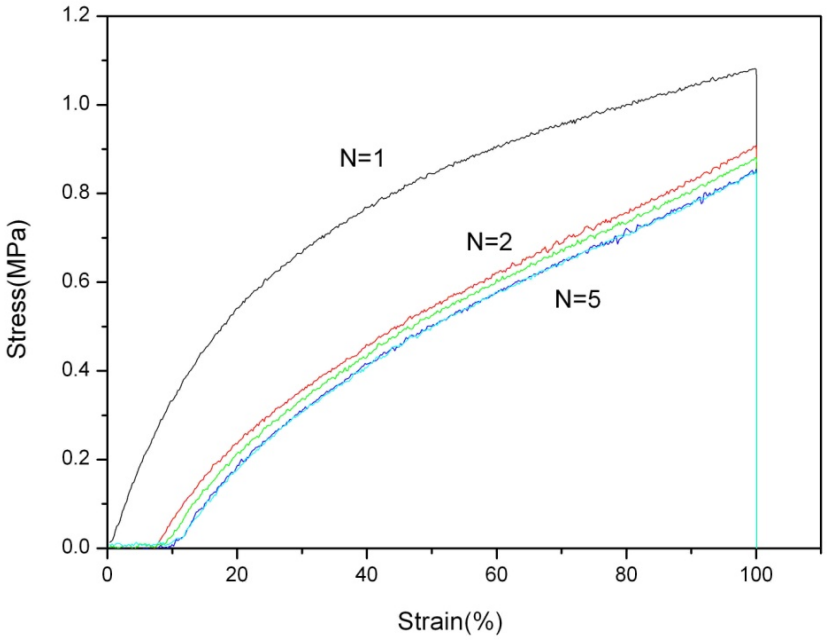

Figure 7.11. Cyclic tensile behavior of PU-M-CL-10K-U2-20%

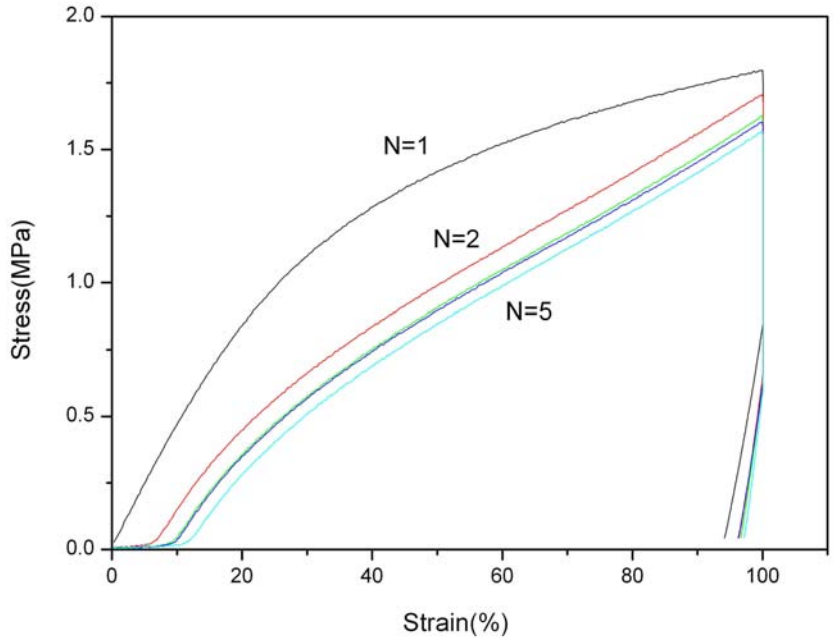

Figure 7.12. Cyclic tensile behavior of PU-M-CL-10K-U2-26.8%

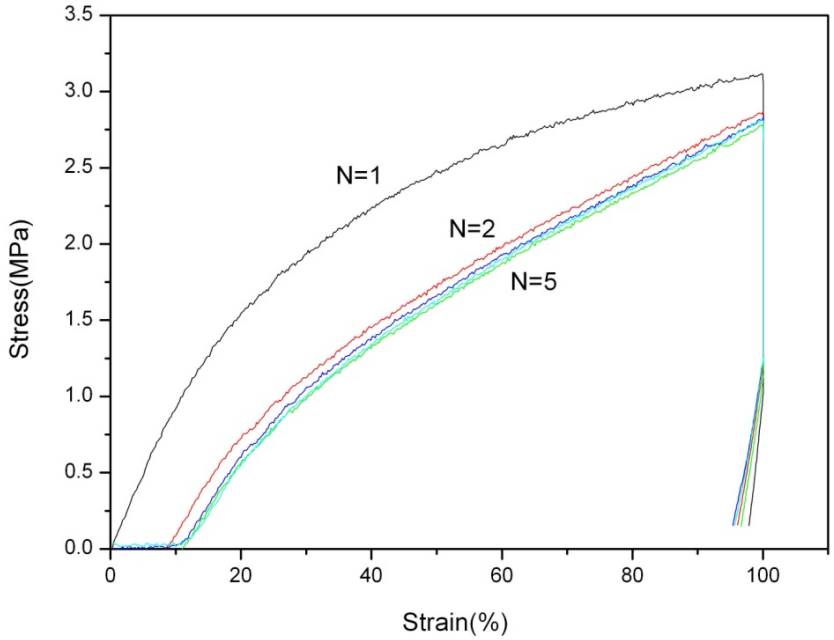

Figure 7.13. Cyclic tensile behavior of PU-M-CL-10K-U2-32.1%

Although the recovery stress increased with increasing hard segment content, the value was not improved as expected and almost similar to the MDI/PCL/BDO system. One of the reasons that the recovery stress was not improved in this system was that the molecular weights of the LC SMPUs were not high enough.

Although LC SMPUs were synthesized as designed, the recovery stress was not improved compared with the MDI/PCL/BDO system since the molecular weights of LC SMPUs were low. The result showed the reactivity of chain extender was quite critical to get high molecular weight SMPUs via solution polymerization. Most of industrial PUs are synthesized by bulk polymerization with small molecular weight diols as chain extenders. U2 and U6 are not suitable for chain extenders because of the high melting pointds (~ 200°C). At that temperature, side reactions will take place as shown in Figure 7.14.

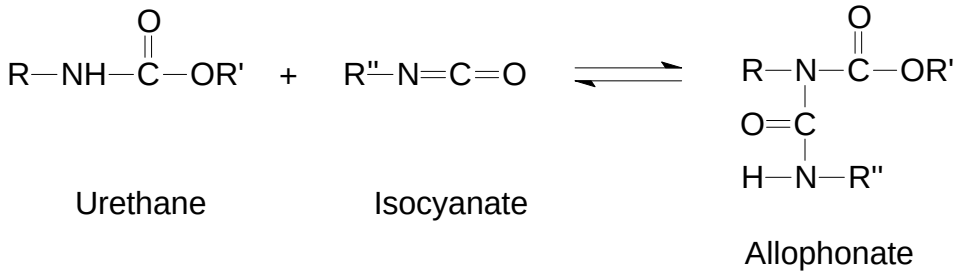

Figure 7.14. Side reaction between Urethane and Isocyanate above 120°C

As a result, SMPUs will be cross linked and may not dissolve in solvents and thus cannot be spun into fibers. The synthesis of MDI/PCL/BDO system was also attempted via solution polymerization. Lower molecular weight was achieved compared to bulk polymerization which indicated diols do not have high enough reactivity to achieve high molecular weight polymers in solution polymerization.

CHAPTER 8

CONCLUSIONS AND RECOMMENDATIONS

8.1. Conclusions

The objective of this study was to develop linear shape memory polymers with improved recovery stress to fulfill the requirement in different applications such as comfort wear and biomedical devices. SMPUUs were synthesized with different molecular weights of PCL, chain extenders, hard segment content and diisocyanates, and the structures of the designed SMPUUs were verified with NMR and FT-IR analyses. The SMPUU films were characterized to evaluate their structure-property relationships and tested for their tensile properties, dynamic mechanical properties, thermal properties, and shape memory properties.

8.1.1. Shape memory polyurethane-ureas with aliphatic amine 1, 4-butanediamine as chain extender

Segmented poly (epsilon-caprolactone) polyurethane-ureas (PCLUUs) were synthesized with significantly improved recovery stress by changing the chain extender from BDO to BDA. The mechanism of improvement was studied by NMR and DSC which showed that the bidentate hydrogen bonding of the urea linkage gave more effective physical crosslinks. This system showed similar shape memory properties as the MDI/PCL/BDO system with above 200% recovery stress, which may be important in some medical applications. The rubbery moduli of PCLUUs were quite stable above the

melting point of PCL, which provided another advantage in comparison to shape memory polyurethanes using diols as chain extenders.

8.1.2. Shape memory polyurethane-ureas with different aliphatic amines as chain extenders

Segmented poly (epsilon-caprolactone) polyurethane-ureas (PCLUUs) were synthesized by using different aliphatic chain extenders. The recovery stress was significantly influenced by chain extenders. PCLUU prepared with linear chain extenders such as EDA, BDA and HDA showed similar shape memory recovery stresses, while for the non-linear chain extenders, incorporation of side chains such as MDPA hindered the formation of the bidentate hydrogen bonding between urea linkages, resulting in a 50% decrease of the recovery stress.

Wet spinning was used to produce the SMPUU fibers from the reaction solution. Production of continuous filaments proved that the SMPUUs were indeed fiber-formers, although the physical properties of the spun fibers were poor.

The morphology of the hard segment of PU-M-CL-4K-D-EDA was investigated by SANS at the Los Alamos National Laboratory. SANS results revealed that the hard segments fit the cylinder model quite well and consisted of nano scale domains. The hard segments were almost fixed during stretching from the 2D patterns of two samples below or above the transition temperature.

8.1.3. Shape memory polyurethane-ureas with aromatic diamine 4, 4'-methylenedianiline as chain extender

Segmented poly (epsilon-caprolactone) polyurethane-ureas (PCLUUs) were synthesized by using MDA as the chain extender. The recovery stress of PU-M-CL-8K-

MDA-30% film was successfully improved to 287% with the help of bidentate hydrogen bonding interactions of the urea linkages and increased main chain rigidity compared to PU-M-CL-8K-BDO-30%. The rubbery moduli of PCLUUs were quite stable above the melting point of PCL, which was another advantage compared with shape memory polyurethanes using diols as chain extenders.

8.1.4. Shape memory polyurethane-ureas with different diisocyanates

Segmented poly (epsilon-caprolactone) polyurethane-ureas (PCLUUs) were synthesized by reacting different diisocyanates with PCL and chain extender MDA. The recovery stresses were greatly influenced by diisocyanates. The side chain of diisocyanates restrained the hydrogen bond interactions in the hard segment phase and rapidly reduced the recovery stress. From the cyclic thermo mechanic tests, the recovery stresses of PU-IP-CL-8K-MDA-20% and PU-T-CL-8K-MDA-20% were 2.5 MPa and 2.7 MPa respectively and less than 40% of the recovery stresses of PU-M-CL-8K-MDA-20% (6.6 MPa)and PU-H-CL-8K-MDA-20% (7.2 MPa).

8.1.5. Block polyester copolymer with PET/Poly (oxy-1, 3-propyleneoxyadipate)

PET/POPA copolyesters were synthesized with different methods. Because of poor solubility of the PET block, PET and POPA blocks could not be coupled with adipoyl chloride. Transesterification reactions between PET and POPA created PET/POPA block copolyesters which could be verified with NMR and DSC. Two catalysts were studied during the reaction, and Sb_2O_3 worked more efficiently than $Ti(OBu)_4$ with the same amount and reaction time. PET/POPA did not show shape memory properties around room temperature, which was because POPA is a T_g type soft segment. Finally, DSC is a very useful tool to determine the soft segment type.

8.1.6 Liquid crystalline shape memory polyurethanes

LC units with low cost were synthesized with high purity and used as chain extenders to increase the rigidity of main chain. The LC SMPUs were successfully synthesized but the recovery stress was not improved from cyclic thermal mechanic test because of the low attained molecular weight. SMPUs are not suitable to synthesize in solution polymerization with low reactivity diols.

8.2. Recommendations

Although SMPUUs were synthesized and characterized with different molecular weights of PCL, chain extenders, hard segment content and diisocyanates, the soft segment was limited to PCL which produced T_m type SMPs. T_g type SMPs constitute another interesting system to investigate, and PLA is a quite good candidate and will improve the recovery stress and lower the transition temperature to body temperature[27]. The biggest disadvantage of T_g type SMPs compared with T_m type SMPs is the slow recovery speed.

Another recommendation is to increase the hard segment content, which is quite critical to improve the recovery stress. Currently, the highest hard segment content is 30% and the reaction solution is difficult to dissolve with more than 30% hard segment because too much hydrogen bonding is involved. Salts such as LiCl and $CaCl_2$ are used to cleave the hydrogen bonds to synthesize high molecule Kevlar[84-87]. This idea has already been tried to solve the problem, but another problem was created. The LiCl salt cannot be removed during the process and the SMPUU films absorb moisture from the

atmosphere. As a result, more research should be done to investigate the effect of salt addition.

Wet spinning was used to verify the spinnability of SMPUUs and continuous fibers can be manufactured by this technology. However, the properties of the SMPUU fibers were not good compared with the SMPUU films and the parameters of wet spinning were not optimized in this study. Dry spinning is highly recommended to overcome the voids and defects introduced during the wet spinning process.

SANS experiments showed the morphology of the hard segment, aiding in the understanding of the mechanism of shape memory. Only two samples were SANS studied in this research and more data should be collected to clearly understand the behavior of SMPUUs at different temperatures and stretch rates.

REFERENCES

1. Lendlein, A.; Kelch, S., Shape-memory polymers. *Angewandte Chemie-International Edition* **2002,** 41, (12), 2034-2057.

2. Hu, J., *Shape memory polymers and textiles*. Woodhead in association with The Textile Institute: Cambridge :, 2007.

3. *Shape memory alloys : modeling and engineering applications*. Springer: New York ;, 2008.

4. Buehler, W. J.; Wiley, R. C.; Gilfrich, J. V., Effect of low temperature phase changes on mechanical properties of alloys near composition TiNi. *Journal of Applied Physics* **1963,** 34, (5), 1475-1477.

5. Ratna, D.; Karger-Kocsis, J., Recent advances in shape memory polymers and composites: a review. *Journal of Materials Science* **2008,** 43, (1), 254-269.

6. Liu, C.; Qin, H.; Mather, P. T., Review of progress in shape-memory polymers. *Journal of Materials Chemistry* **2007,** 17, (16), 1543-1558.

7. Lendlein, A.; Jiang, H. Y.; Junger, O.; Langer, R., Light-induced shape-memory polymers. *Nature* **2005,** 434, (7035), 879-882.

8. Yoo, H. J.; Jung, Y. C.; Sahoo, N. G.; Cho, J. W., Polyurethane-carbon nanotube nanocomposites prepared by in-situ polymerization with electroactive shape memory. *Journal of Macromolecular Science Part B-Physics* **2006,** 45, (4), 441-451.

9. Zhu, Y.; Hu, J.; Yeung, K., Effect of soft segment crystallization and hard segment physical crosslink on shape memory function in antibacterial segmented polyurethane ionomers. *Acta Biomaterialia* **2009,** 5, (9), 3346-3357.

10. Oprea, S., Effect of structure on the thermal stability of crosslinked poly(ester-urethane). *Polimery* **2009,** 54, (2), 120-125.

11. Chang, Y. W.; Mishra, J. K.; Cheong, J. H.; Kim, D. K., Thermomechanical properties and shape memory effect of epoxidized natural rubber crosslinked by 3-amino-1,2,4-triazole. *Polymer International* **2007,** 56, (5), 694-698.

12. Zhu, G. M.; Xu, S. G.; Wang, J. H.; Zhang, L. B., Shape memory behaviour of radiation-crosslinked PCL/PMVS blends. *Radiation Physics And Chemistry* **2006,** 75, (3), 443-448.

13. Lee, S. H.; Kim, J. W.; Kim, B. K., Shape memory polyurethanes having crosslinks in soft and hard segments. *Smart Materials & Structures* **2004,** 13, (6), 1345-1350.

14. Chun, B. C.; Cha, S. H.; Chung, Y. C.; Cho, J. W., Enhanced dynamic mechanical and shape-memory properties of a poly(ethylene terephthalate)-poly(ethylene glycol) copolymer crosslinked by maleic anhydride. *Journal Of Applied Polymer Science* **2002,** 83, (1), 27-37.

15. Xu, M.; Li, F. K., Thermally stimulated shape memory behavior of polymers with physical crosslinks. *Chinese Journal of Polymer Science* **1999,** 17, (3), 203-213.

16. Kagami, Y.; Gong, J. P.; Osada, Y., Shape memory behaviors of crosslinked copolymers containing stearyl acrylate. *Macromolecular Rapid Communications* **1996,** 17, (8), 539-543.

17. Kim, B. K.; Lee, S. Y.; Xu, M., Polyurethanes having shape memory effects. *Polymer* **1996,** 37, (26), 5781-5793.

18. Li, F. K.; Hou, J. N.; Zhu, W.; Zhang, X.; Xu, M.; Luo, X. L.; Ma, D. Z.; Kim, B. K., Crystallinity and morphology of segmented polyurethanes with different soft-segment length. *Journal of Applied Polymer Science* **1996,** 62, (4), 631-638.

19. Li, F. K.; Zhang, X.; Hou, J. N.; Xu, M.; Lu, X. L.; Ma, D. Z.; Kim, B. K., Studies on thermally stimulated shape memory effect of segmented polyurethanes. *Journal of Applied Polymer Science* **1997,** 64, (8), 1511-1516.

20. Jeong, H. M.; Lee, J. B.; Lee, S. Y.; Kim, B. K., Shape memory polyurethane containing mesogenic moiety. *Journal of Materials Science* **2000,** 35, (2), 279-283.

21. Ping, P.; Wang, W. S.; Chen, X. S.; Jing, X. B., Poly(epsilon-caprolactone) polyurethane and its shape-memory property. *Biomacromolecules* **2005,** 6, (2), 587-592.

22. Kim, B. K.; Lee, S. Y.; Lee, J. S.; Baek, S. H.; Choi, Y. J.; Lee, J. O.; Xu, M., Polyurethane ionomers having shape memory effects. *Polymer* **1998,** 39, (13), 2803-2808.

23. Zhu, Y.; Hu, J. L.; Yeung, K. W.; Liu, Y. Q.; Liem, H. M., Influence of ionic groups on the crystallization and melting behavior of segmented polyurethane ionomers. *Journal of Applied Polymer Science* **2006,** 100, (6), 4603-4613.

24. Jeong, H. M.; Kim, B. K.; Choi, Y. J., Synthesis and properties of thermotropic liquid crystalline polyurethane elastomers. *Polymer* **2000,** 41, (5), 1849-1855.

25. Zhu, Y.; Hu, J.; Yeung, K. W.; Choi, K. F.; Liu, Y. Q.; Liem, H. M., Effect of cationic group content on shape memory effect in segmented polyurethane cationomer. *Journal of Applied Polymer Science* **2007,** 103, (1), 545-556.

26. Wang, W. S.; Ping, P.; Chen, X. S.; Jing, X. B., Polylactide-based polyurethane and its shape-memory behavior. *European Polymer Journal* **2006,** 42, (6), 1240-1249.

27. Wang, Y. L.; Li, Y. G.; Luo, Y. F.; Huang, M. N.; Liang, Z. Q., Synthesis and characterization of a novel biodegradable thermoplastic shape memory polymer. *Materials Letters* **2009,** 63, (3-4), 347-349.

28. Lin, J. R.; Chen, L. W., Study on shape-memory behavior of polyether-based polyurethanes. II. Influence of soft-segment molecular weight. *Journal Of Applied Polymer Science* **1998,** 69, (8), 1575-1586.

29. Lin, J. R.; Chen, L. W., Study on shape-memory behavior of polyether-based polyurethanes. I. Influence of the hard-segment content. *Journal Of Applied Polymer Science* **1998,** 69, (8), 1563-1574.

30. Lee, B. S.; Chun, B. C.; Chung, Y. C.; Sul, K. I.; Cho, J. W., Structure and thermomechanical properties of polyurethane block copolymers with shape memory effect. *Macromolecules* **2001,** 34, (18), 6431-6437.

31. Chun, B. C.; Cho, T. K.; Chung, Y. C., Blocking of soft segments with different chain lengths and its impact on the shape memory property of polyurethane copolymer. *Journal of Applied Polymer Science* **2007,** 103, (3), 1435-1441.

32. Wang, H. H.; Yuen, U. E., Synthesis of thermoplastic polyurethane and its physical and shape memory properties. *Journal Of Applied Polymer Science* **2006,** 102, (1), 607-615.

33. Yang, J. H.; Chun, B. C.; Chung, Y. C.; Cho, J. H., Comparison of thermal/mechanical properties and shape memory effect of polyurethane block-copolymers with planar or bent shape of hard segment. *Polymer* **2003,** 44, (11), 3251-3258.

34. Takahashi, T.; Hayashi, N.; Hayashi, S., Structure and properties of shape-memory polyurethane block copolymers. *Journal of Applied Polymer Science* **1996,** 60, (7), 1061-1069.

35. Tobushi, H.; Hayashi, S.; Ikai, A.; Hara, H., Thermomechanical properties of shape memory polymers of polyurethane series and their applications. *Journal De Physique Iv* **1996,** 6, (C1), 377-384.

36. Chen, S. J.; Hu, J. L.; Liu, Y. Q.; Liem, H. M.; Zhu, Y.; Meng, Q. H., Effect of molecular weight on shape memory behavior in polyurethane films. *Polymer International* **2007,** 56, (9), 1128-1134.

37. Chen, S. J.; Hu, J. L.; Liu, Y. Q.; Liem, H. M.; Zhu, Y.; Liu, Y. J., Effect of SSL and HSC on morphology and properties of PHA based SMPU synthesized by bulk polymerization method. *Journal of Polymer Science Part B-Polymer Physics* **2007,** 45, (4), 444-454.

38. Li, F. K.; Chen, Y.; Zhu, W.; Zhang, X.; Xu, M., Shape memory effect of polyethylene nylon 6 graft copolymers. *Polymer* **1998,** 39, (26), 6929-6934.

39. Wang, M. T.; Luo, X. L.; Zhang, X. Y.; Ma, D. Z., Shape memory properties in poly(ethylene oxide)-poly(ethylene terephthalate) copolymers. *Polymers for Advanced Technologies* **1997,** 8, (3), 136-139.

40. Luo, X. L.; Zhang, X. Y.; Wang, M. T.; Ma, D. H.; Xu, M.; Li, F. K., Thermally stimulated shape-memory behavior of ethylene oxide ethylene terephthalate segmented copolymer. *Journal of Applied Polymer Science* **1997,** 64, (12), 2433-2440.

41. Lendlein, A.; Schmidt, A. M.; Langer, R., AB-polymer networks based on oligo(epsilon-caprolactone) segments showing shape-memory properties. *Proceedings of the National Academy of Sciences of the United States of America* **2001,** 98, (3), 842-847.

42. Rousseau, I. A., Challenges of Shape Memory Polymers: A Review of the Progress Toward Overcoming SMP's Limitations. *Polymer Engineering and Science* **2008,** 48, (11), 2075-2089.

43. Tobushi, H.; Hara, H.; Yamada, E.; Hayashi, S., Thermomechanical properties in a thin film of shape memory polymer of polyurethane series. *Smart Materials & Structures* **1996,** 5, (4), 483-491.

44. Liu, C. D.; Chun, S. B.; Mather, P. T.; Zheng, L.; Haley, E. H.; Coughlin, E. B., Chemically cross-linked polycyclooctene: Synthesis, characterization, and shape memory behavior. *Macromolecules* **2002,** 35, (27), 9868-9874.

45. http://www.diaplex.ocm.

46. Cook, F. L.; Jacob, K. I.; Polk, M.; Pourdeyhimi, B., Shape Memory Polymer Fibers for Comfort Wear. *NTC Project: M05-GT14* **2005**.

47. Lendlein, A.; Langer, R., Biodegradable, elastic shape-memory polymers for potential biomedical applications. *Science* **2002,** 296, (5573), 1673-1676.

48. Yakacki, C. M.; Shandas, R.; Lanning, C.; Rech, B.; Eckstein, A.; Gall, K., Unconstrained recovery characterization of shape-memory polymer networks for cardiovascular applications. *Biomaterials* **2007,** 28, (14), 2255-2263.

49. Baer, G. M.; Wilson, T. S.; Small, W.; Hartman, J.; Benett, W. J.; Matthews, D. L.; Maitland, D. J., Thermomechanical Properties, Collapse Pressure, and Expansion of Shape Memory Polymer Neurovascular Stent Prototypes. *Journal of Biomedical Materials Research Part B-Applied Biomaterials* **2009,** 90B, (1), 421-429.

50. Wache, H. M.; Tartakowska, D. J.; Hentrich, A.; Wagner, M. H., Development of a polymer stent with shape memory effect as a drug delivery system. *Journal of Materials Science-Materials in Medicine* **2003,** 14, (2), 109-112.

51. Meng, Q. H.; Liu, J. L.; Shen, L. M.; Hu, Y.; Han, J. P., A Smart Hollow Filament with Thermal Sensitive Internal Diameter. *Journal of Applied Polymer Science* **2009,** 113, (4), 2440-2449.

52. Yang, F.; Wornyo, E.; Gall, K.; King, W. P., Nanoscale indent formation in shape memory polymers using a heated probe tip. *Nanotechnology* **2007,** 18, (28), -.

53. Hampikian, J. M.; Heaton, B. C.; Tong, F. C.; Zhang, Z. Q.; Wong, C. P., Mechanical and radiographic properties of a shape memory polymer composite for intracranial aneurysm coils. *Materials Science & Engineering C-Biomimetic And Supramolecular Systems* **2006,** 26, (8), 1373-1379.

54. *The polyurethanes book*. Huntsman Polyurethanes] ;: [Everberg, Belgium :, 2002.

55. Yen, F. S.; Lin, L. L.; Hong, J. L., Hydrogen-bond interactions between urethane-urethane and urethane-ester linkages in a liquid crystalline poly(ester-urethane). *Macromolecules* **1999,** 32, (9), 3068-3079.

56. Fukushima, K.; Tabuani, D.; Camino, G., Nanocomposites of PLA and PCL based on montmorillonite and sepiolite. *Materials Science & Engineering C-Biomimetic and Supramolecular Systems* **2009,** 29, (4), 1433-1441.

57. Crescenz.V; Manzini, G.; Calzolar.G; Borri, C., Thermodynamics of fusion of poly-beta-propiolactone and poly-epsilon-caprolactone - comparative analysis of melting of aliphatic polylactone and polyester chains. *European Polymer Journal* **1972,** 8, (3), 449-463.

58. Schriemer, D. C.; Li, L., Mass discrimination in the analysis of polydisperse polymers by MALDI time-of-flight mass spectrometry .1. Sample preparation and desorption/ionization issues. *Analytical Chemistry* **1997,** 69, (20), 4169-4175.

59. Wu, K. J.; Odom, R. W., Characterizing synthetic polymers by MALDI MS. *Analytical Chemistry* **1998,** 70, (13), 456A-461A.

60. Byrd, H. C. M.; McEwen, C. N., The limitations of MALDI-TOF mass spectrometry in the analysis of wide polydisperse polymers. *Analytical Chemistry* **2000,** 72, (19), 4568-4576.

61. Das, S.; Yilgor, I.; Yilgor, E.; Wilkes, G. L., Probing the urea hard domain connectivity in segmented, non-chain extended polyureas using hydrogen-bond screening agents. *Polymer* **2008,** 49, (1), 174-179.

62. Zhou, Q. X.; Wang, X. G.; Liu, D. S.; Fan, K. C.; Wang, H. F., Study on solubilization mechanism in the synthesis of high molecular weight poly(p-Phenylene Terephthalamide). *Chinese Journal of Polymer Science* **1987,** 5, (2), 95-100.

63. Luo, N.; Wang, D. N.; Ying, S. K., Hydrogen-bonding properties of segmented polyether poly(urethane urea) copolymer. *Macromolecules* **1997,** 30, (15), 4405-4409.

64. Bretches, D.; Pardini, S. P., Fiber from polyether-based spandex. *US patent 4973647* **1990**.

65. Jerde, J., *Encyclopedia of textiles*. Facts on File: New York :, 1992.

66. Ji, F. L.; Zhu, Y.; Hu, J. L.; Liu, Y.; Yeung, L. Y.; Ye, G. D., Smart polymer fibers with shape memory effect. *Smart Materials & Structures* **2006,** 15, (6), 1547-1554.

67. Mang, J. T.; Hjeim, R. P.; Orler, E. B.; Wrobleski, D. A., Distribution and polymer domain composition of a solvent-swollen segmented polyurethane by small-angle neutron scattering. *Abstracts Of Papers Of The American Chemical Society* **2005,** 230, 190-PMSE.

68. Visser, S. A.; Pruckmayr, G.; Cooper, S. L., Small-angel neutron-scattering invesigation of the response of medel polyurethane ionomers to uniaxial deformation. *Polymer* **1992,** 33, (20), 4280-4287.

69. Visser, S. A.; Pruckmayr, G.; Cooper, S. L., Small-Angle neutron-scattering analysis of model polyurethane ionomers. *Macromolecules* **1991,** 24, (25), 6769-6775.

70. Hartl, M.; Hjelm, R., 2010 Lansce Neutron School. **2010**.

71. Kline, S. R., Reduction and analysis of SANS and USANS data using IGOR Pro. *Journal of Applied Crystallography* **2006,** 39, 895-900.

72. Xu, J. W.; Shi, W. F.; Pang, W. M., Synthesis and shape memory effects of Si-O-Si cross-linked hybrid polyurethanes. *Polymer* **2006,** 47, (1), 457-465.

73. Auad, M. L.; Contos, V. S.; Nutt, S.; Aranguren, M. I.; Marcovich, N. E., Characterization of nanocellulose-reinforced shape memory polyurethanes. *Polymer International* **2008,** 57, (4), 651-659.

74. Koerner, H.; Price, G.; Pearce, N. A.; Alexander, M.; Vaia, R. A., Remotely actuated polymer nanocomposites - stress-recovery of carbon-nanotube-filled thermoplastic elastomers. *Nature Materials* **2004,** 3, (2), 115-120.

75. Jeong, H. M.; Lee, S. Y.; Kim, B. K., Shape memory polyurethane containing amorphous reversible phase. *Journal of Materials Science* **2000,** 35, (7), 1579-1583.

76. Zhu, Y.; Hu, J. L.; Yeung, K. W.; Fan, H. J.; Liu, Y. Q., Shape memory effect of PU ionomers with ionic groups on hard-segments. *Chinese Journal of Polymer Science* **2006,** 24, (2), 173-186.

77. Acetti, D.; D'Arrigo, P.; Giordano, C.; Macchi, P.; Servi, S.; Tessaro, D., New aliphatic glycerophosphoryl-containing polyurethanes: Synthesis, platelet adhesion and elution cytotoxicity studies. *International Journal of Artificial Organs* **2009,** 32, (4), 204-212.

78. Rogers, M. E., Long, Timothy E, Synthetic methods in step-growth polymers. **2003**.

79. Zhang, Z. P.; Luo, X. L.; Lu, Y. C.; Ma, D. Z., Transesterification of poly(ethylene terephthalate) with poly(epsilon-caprolactone). *Chinese Journal of Polymer Science* **2000,** 18, (5), 405-412.

80. Zhang, Z. P.; Luo, X. L.; Lu, Y. C.; Ma, D. Z., Transesterifications of poly(bisphenol A carbonate) with aromatic and aliphatic segments in ethylene terephthalate-caprolactone copolyester. *Journal of Applied Polymer Science* **2001,** 80, (9), 1558-1565.

81. Srinivasan, K. S. V.; Padmavathy, T., Liquid crystalline properties of unsegmented and segmented polyurethanes synthesised from high aspect ratio mesogenic diols. *Macromolecular Symposia* **2003,** 199, 277-292.

82. Padmavathy, T.; Srinivasan, K. S. V., Liquid crystalline polyurethanes - A review. *Journal of Macromolecular Science-Polymer Reviews* **2003,** C43, (1), 45-85.

83. Lian, Y. Q.; Li, M. Q.; Zhan, J.; Zhou, Q. X.; Liu, D. S., Synthesis and liquid crystalline properties of new thermotropic polyurethanes. *Polymer Journal* **1999,** 31, (12), 1189-1193.

84. Kwoleck, S. L., Wholly aromatic carbocyclic polycarbonamide fiber having orientation angle of less than about 45º. *US patent 3819587* **1971**.

85. Bao, J. S.; You, A. J.; Zhang, S. Q.; Zhang, S. A.; Hu, C., Studies on the semirigid chain polyamide-poly(1,4-phenyleneterphthalamide). *Journal of Applied Polymer Science* **1981,** 26, (4), 1211-1220.

86. Polk, M. B.; Bota, K. B.; Akubuiro, E. C., Block copolyamides .1. Preparation and properites of block copolyamides containing cyclohexane and benzene rings. *Industrial & Engineering Chemistry Product Research and Development* **1984,** 23, (2), 230-233.

87. Russo, S.; Mariani, A.; Ignatov, V. N.; Ponomarev, II, High molecular weight aromatic polyamides by direct polycondensation. *Macromolecules* **1993,** 26, (18), 4984-4985.